Open-File Report 82-312

United States
Department of the Interior
Geological Survey

CONTRACT REPORT ON A REMOTE-REFERENCE MAGNETOTELLURIC SURVEY IN THE SOUTHERN APPALACHIAN OVERTHRUST BELT, NORTH CAROLINA

by

Argonaut Enterprises

with an introduction
by
Jeffrey C. Wynn

1982

BACKGROUND

In the Fall of 1979, a meeting was held at the U.S. Geological Survey National Center, under the auspices of the Geological Framework Program. This meeting met to consider what steps should be taken to augment seismic information on the southern Appalachian overthrust belt that indicated that there might possibly be sediments beneath a thrust sheet made up largely of igneous and metamorphic rocks. Two seismic surveys had been conducted (See Figure 1) where data was released to the public domain. One survey was carried out by the Consortium for Continental Reflection Profiling (labeled "COCORP" in Figure 1) in northeastern Georgia (Cook and others, 1979); the other survey was done under contract by the U.S. Geological Survey (labeled "USGS" in Figure 1) in eastern Tennessee and northwestern North Carolina (Harris and others, 1981). Both surveys showed strong evidence of thin-skinned tectonic movement, with steep faults at the surface becoming flat-lying at depth, implying an extensive overthrust of largely metamorphic rock that covers the Blue Ridge and Piedmont geologic provinces (See Figure 2). This possibility has enormous economic implications, even suggesting the possibility of a new hydrocarbon province. The problem then faced was how to test the underlying rocks: were they sediments, and if so, were they indurated? Since the thrust sheet was typically 5 - 10 kilometers thick, an exploratory drill hole was prohibitively expensive without further information to be able to locate it. Magnetotellurics was suggested as a less expensive alternative to drilling that could possibly test for conductive rocks beneath the overthrust.

The recommendation of the meeting was to suppport a limited experiment into whether magnetotellurics could provide the relevant information about possible underlying sediments. Some initial modelling was carried out (Figures 3, 4, and 5) and these results appeared to justify a test survey, which was ultimately specified to be coincidental with the U.S.G.S. seismic profile in North Carolina. This report is the ultimate product of that magnetotelluric survey.

REFERENCES

Cook, Frederick, A., Albaugh, Dennis A., Brown, Larry D., Kaufman, Sidney, and Oliver, Jack E., 1979, Thin-skinned tectonics in the crystalline southern Appalachians; COCORP seismic reflection profiling of the Blue Ridge and Piedmont: Geology, Vol. 7, p. 563-567.

Harris, Leonard D., Harris, Anita G., deWitt, Wallace, and Bayer, Kenneth C., 1981, Evaluation of the southern eastern overthrust belt beneath the Blue Ridge-Piedmont thrust: A.A.P.G. Bulletin, Vol. 65, no. 12.

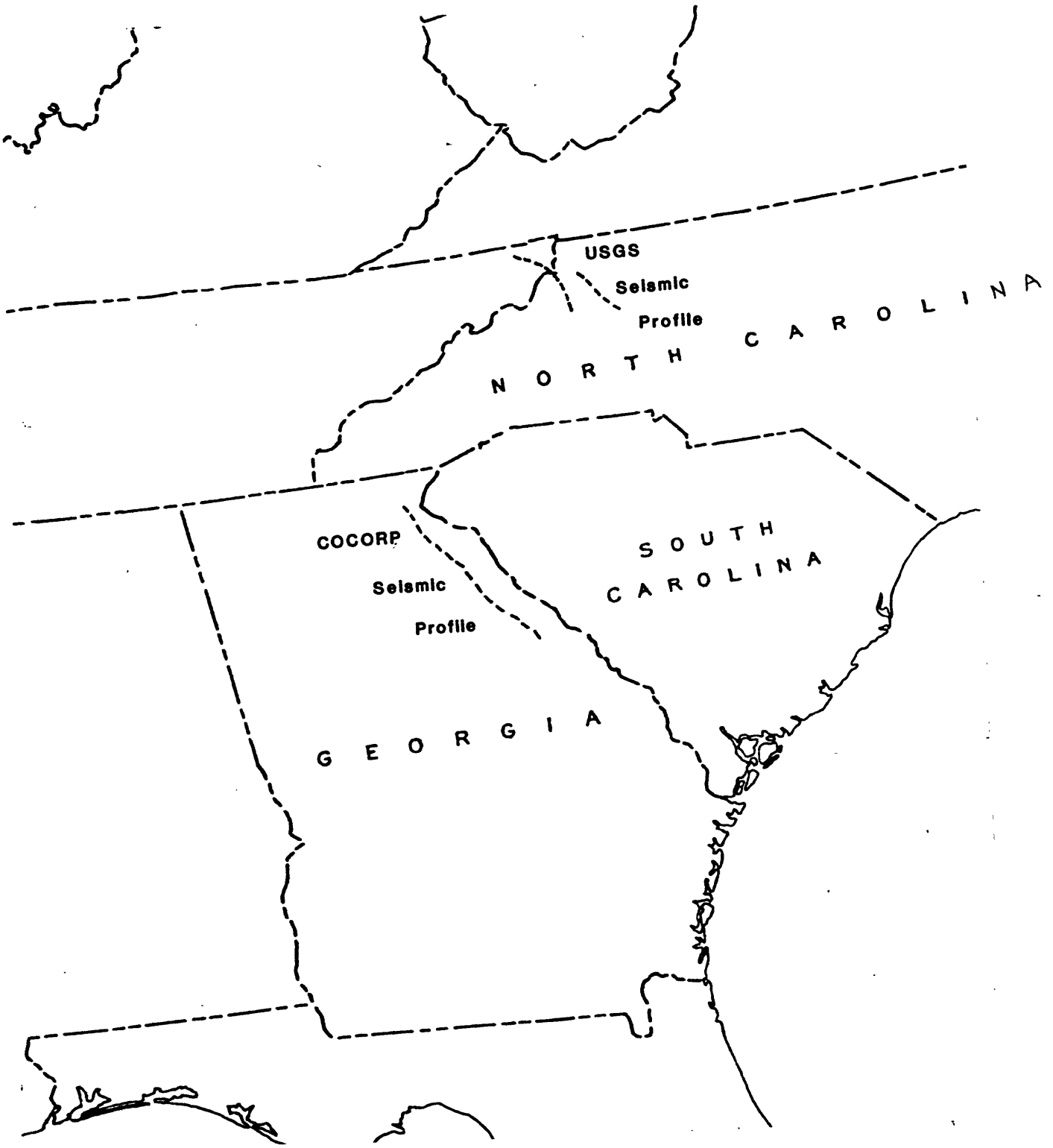

Figure 1. Location of USGS and COCORP Seismic Profiles.

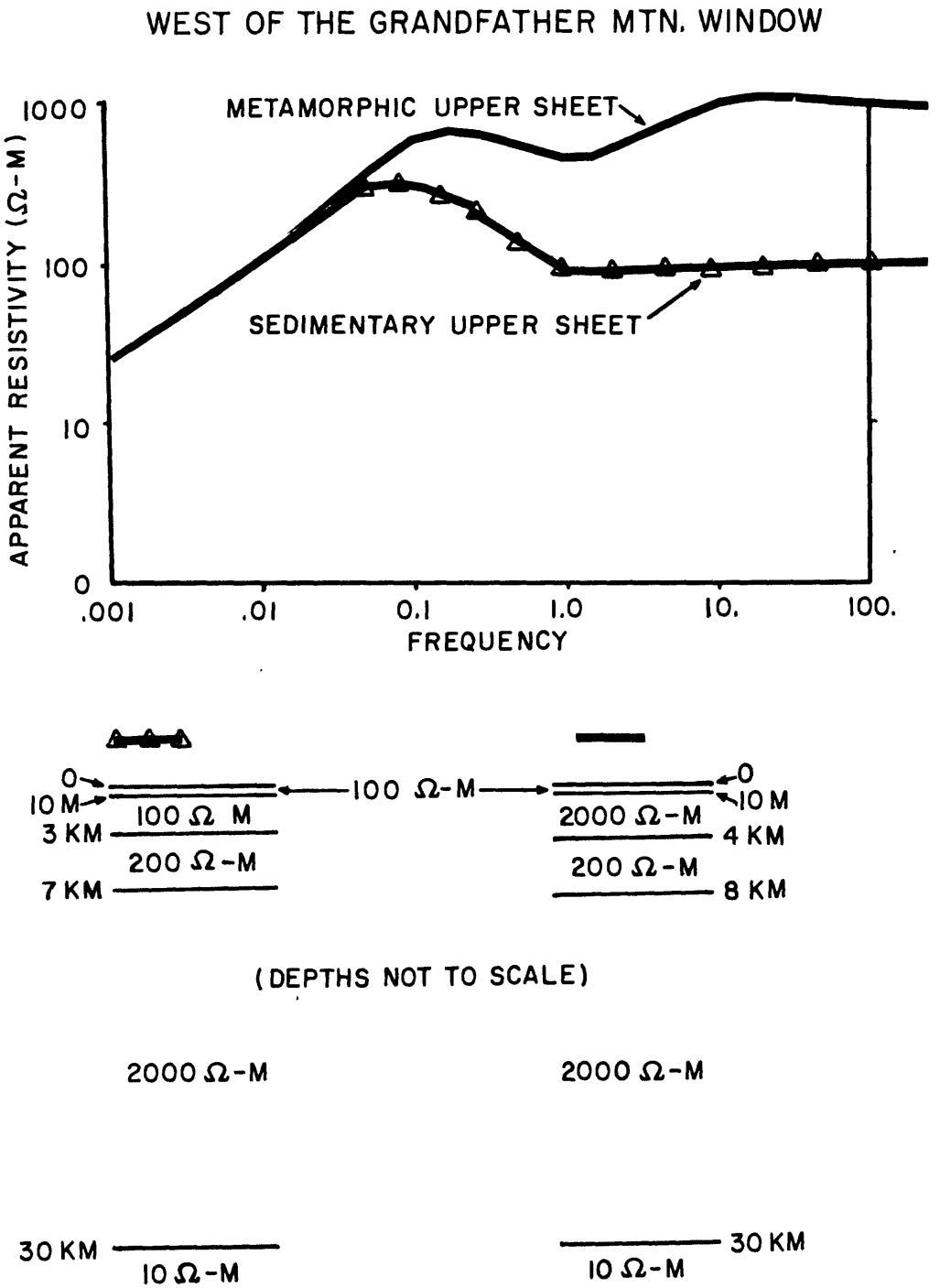

Figure 3. One-dimensional magnetotelluric models for the overthrust sheet west of the Grandfather Mtn. Window in North Carolina. Triangles indicate model of the overlying sheet made up principally of non-indurated sediments.

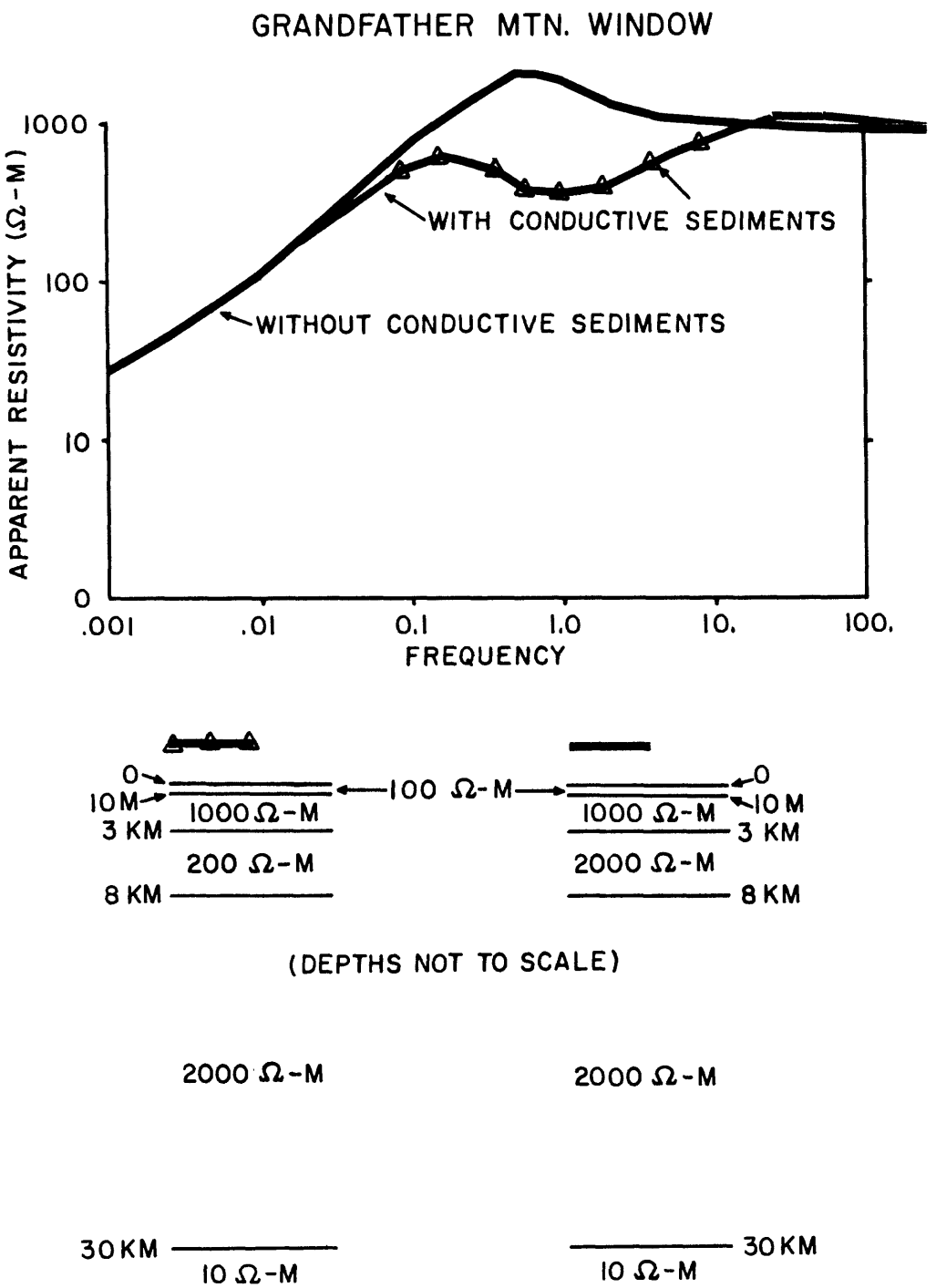

Figure 4. One-dimensional magnetotelluric models for the overthrust sheet at the Grandfather Mtn. Window in North Carolina. Triangles indicate model of metamorphic rocks overlying sedimentary rocks, and indicate that sufficient resolution exists to detect with MT.

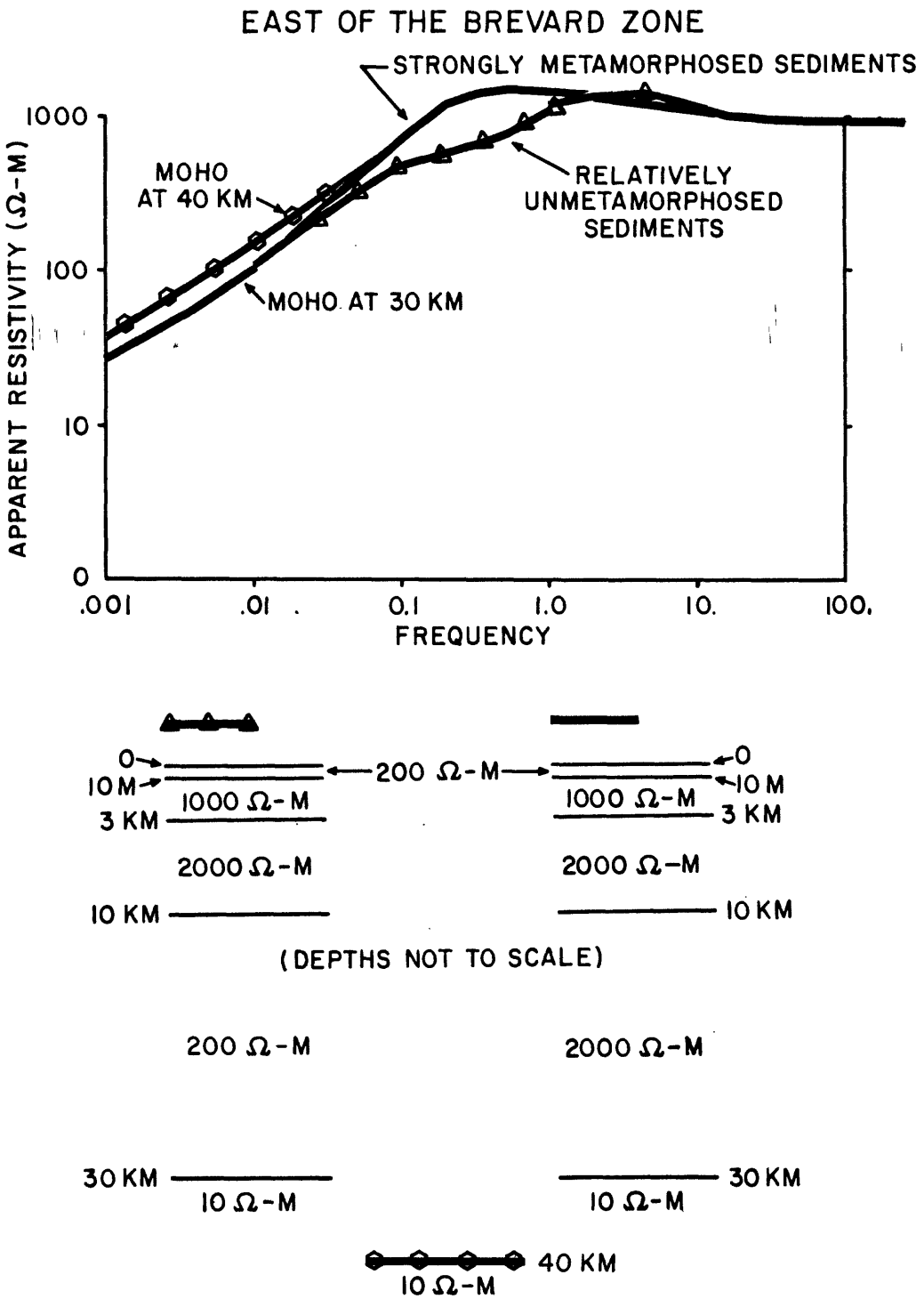

Figure 5. One-dimensional magnetotelluric models for the overthrust sheet east of the Brevard Fault Zone in North Carolina. Triangles indicate the appearance of relatively unmetamorphosed sediments underlying the thrust sheet, and resolution can be seen to be limited due to the increased thickness of overlying metamorphic rocks.

ARGONAUT ENTERPRISES

1480 HOYT ST., SUITE 26
P. O. BOX 15277
DENVER, COLORADO 80215
(303) 237-0418

CONTRACT NO. 14-08-0001-18958

BUYER:

U. S. GEOLOGICAL SURVEY
PROCUREMENT AND CONTRACTS, EASTERN REGION
12201 SUNRISE VALLEY DRIVE
RESTON, VIRGINIA 22902

CONTRACTOR:

ARGONAUT ENTERPRISES
7860 W. 16TH AVENUE, SUITE 115
P. O. BOX 15277
DENVER, COLORADO 80215

TITLE:

MAGNETOTELLURIC SURVEY IN THE SOUTHERN APPALACHIANS

DATE:

28 SEPTEMBER 1981

TABLE OF CONTENTS

INTRODUCTION

The U.S. Geological Survey is carrying out studies of the eastern overthrust belt in the southern Appalachians. To date, this work has included regional geologic mapping and seismic reflection profiles in southeastern Tennessee and western North Carolina. These and other studies have led to the recent scientific papers that raise the possibility that there are sediments buried beneath the crystalline rocks of the thrust sheet. If these sedimentary rocks do in fact exist, and are relatively unmetamorphosed, then a potential new hydrocarbon province may be opened. If the sedimentary rocks are relatively unmetamorphosed, they should be more conductive then the underlying and overlying crystalline rocks. This type of geologic model is ideally suited to the magnetotelluric method. Data collected from tensor magnetotelluric soundings should determine the presence or absence of conductive rocks to depths of 4 - 8 kilometers and may permit an approximate evaluation of the degree of metamorphism along the profile (the more resistive, the greater the degree of metamorphism).

To this end, the U.S. Geological Survey contracted Argonaut Enterprises to perform a magnetotelluric survey along its previously-obtained seismic lines, where the geologic and seismic control are the best in the region. The stations were located as closely as possible to the existing seismic profiles, within the constraints of avoiding artifacts of human culture that might degrade the quality of the data.

Because there is a much higher incidence of these artifacts, including powerlines and pipelines, in the eastern United States, the U.S.G.S. decided it was necessary that the MT stations be acquired using a remote reference to help reduce the electrical noise in the data. Following these guidelines, 10 magnetotelluric stations were acquired in five pairs with each pair remotely referenced to the other. Figure 1 is a regional index map showing the outline of the area covered by Plate 1; detailed site locations are presented in Appendix A.

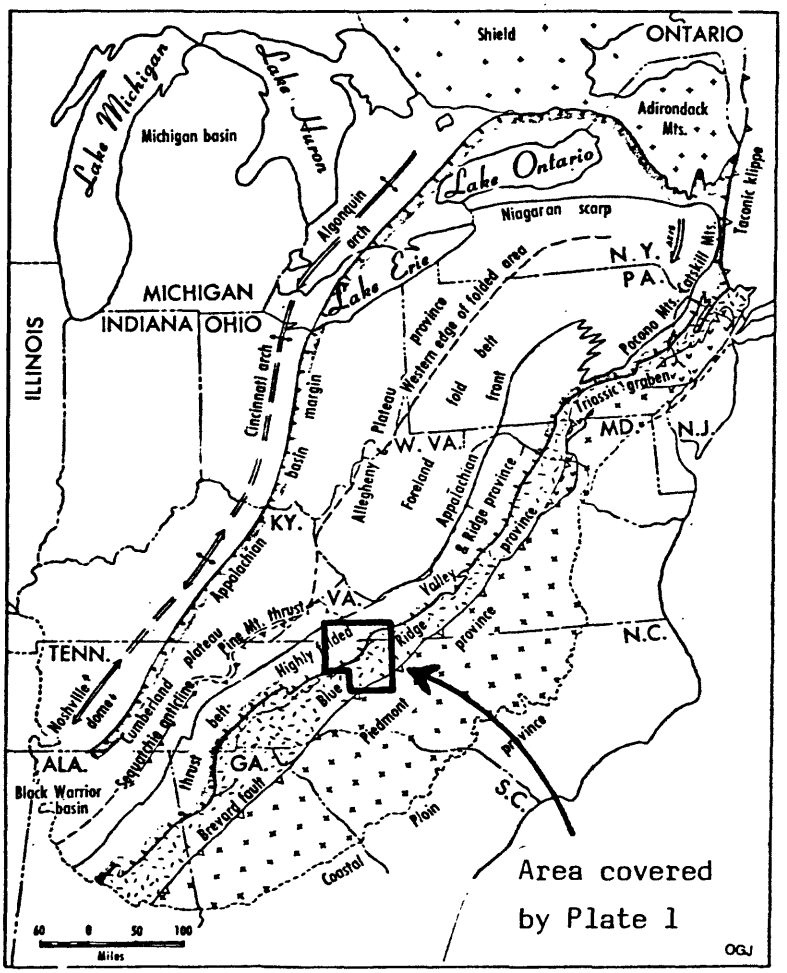

Figure 1: Index map of the Appalachian area showing the major geologic features and the area covered by Plate 1.

PREVIOUS WORK

Classic geologic mapping in the Southern Appalachian Mtns. survey area is summarized by Rankin and others (1972) at a scale of 1:250,000. This work is a good reference for work at more detailed scales. The Southern Appalachians are made up of four major topographic features trending from northeast to southwest: the Valley and Ridge province, the Blue Ridge province, the Piedmont province (including the Inner Piedmont, the Charlotte belt, and the Carolina slate belt), and the costal plain.

Cook and others (1979, 1980) reviewed the classic geology in light of COCORP (Consortuim for Continental Reflection Profiling) seismic data and concluded that "the crystalline Precambrian and Paleozoic rocks of the Blue Ridge, Inner Piedmont, Charlotte belt, and Carolina slate belt constitute an allochthonous sheet, generally 6 to 15 km thick; which overlies relatively flat-lying autochthonous lower Paleozoic sedimentary rocks, 1 to 5 km thick, of the proto-Atlantic continental margin". Thus, the crystalline rocks of the southern Appalachians appear to have been thrust at least 260 km to the west, and they overlie sedimantary rocks that cover an extensive area of the central and southern Appalachians.

The sedimentary rocks beneath the crystalline thrust sheet have unknown hydrocarbon potential. Stearns (1971) noted that future targets for hydrocarbon exploration in the southern Appalachians are the Cambrian Ordovician Knox Group and various Cambrian formations. It is this sequence of rocks, or a part thereof, that most likely

extend beneath the southern Appalachian thrust sheet. The depths and implied degree of metamorphism of the Paleozoic sedimentary rocks suggest that if hydrocarbons are present in producible quantities, they would be in the form of natural gas. Many questions remain regarding the nature of these sedimentary rocks and their degree of metamorphism, but it is clear that the discovery of these strata calls for reconsideration of the resource possibilities of the crystalline southern Appalachians.

Very little electrical geophysical data pertaining to the southern Appalachians was found in the literature. Heinrichs (1966) discusses induced-polarization and dipole-dipole resistivity measurements on a mining prospect in Ashe County, N.C., located 35 km northeast of the magnetotelluric profile (see Plate 1 for location). Resistivities to a maximum depth of 650 meters varied between 200 and 10,000 ohm-m with most of the values in the range 2000 to 7500 ohm-m.

Anderson and Keller (1966) conducted a series of Schlumberger and dipole resistivity soundings in and along the flanks of the central and northern Appalachians. Source 7 was located near Philipsburg, Pennsylvania about 15 km northwest of the boundary between the Appalachian Plateau and the Valley and Ridge Province. As expected the results indicate a thick (6000 m) sequence of moderately conductive (85 ohm-m) sedimentary rocks under a 1000 m thick surface layer of 900 ohm-m material. Basement rock appears resistive but the

sounding was not deep enough to obtain a value. Source 6 was taken near Watkins Glen, New York where the Paleozoic section is similar to that in western Pennsylvania except that the Precambrain basement is thought to be closer to the surface in the northern section of the Appalachian Plateau province (about 4000 to 4300 m). The surface layer of 80 ohm-m resistivity was found to be only 2400 m thick and appears to be underlain by rocks of 4500 ohm-m resistivity. Keller and Anderson ascribe the discrepancy in projected depths to basement to the probability that the several thousand meters of Cambrian and Ordovician limestones overlying basement are closer in resistivity to the Precambrian basement than the surface sedimentary rocks.

From source 5 in the Adirondack area between Plattsburgh and Elizabethtown, New York, they interpret a geoelectric section consisting of 3500 meters of 5000 ohm-m (probably granite) overlying rocks with "a much higher resistivity". Near North Woodstock, New Hampshire, even higher resistivities were obtained from source 4 in a three layer sequence:

layer	resistivity (ohm-m)	thickness (m)
1	1,300	50
2	20,000 or more	8,000
3	1,000 or less	

Source 3 located near Montpelier, Vermont will not be considered here because the soundings obtained from it appear to have anomalously

low resistivity values probably caused by high percentages (as much as 10 percent) of graphite and pyrite. Source 2 was located north of Kokadjo, Maine and source 1 was located south of Sourdnahunk, Maine, seperated a distance of 20 km. Omitting surface layers less than 100 m thick, the data indicate resistivities of at least 10,000 ohm-m beneath the soundings and "much more conductive rocks to the northwest".

THE THEORY OF THE MAGNETOTELLURIC METHOD

The magnetotelluric (often abbreviated as MT) method is a way of determining the electrical conductivity distribution of the subsurface from measurements of natural transient electric and magnetic fields on the surface. The MT method depends on the penetration of electromagnetic energy into the earth. Depth control comes as a natural consequence of the greater penetration of the lower frequencies.

Results interpreted from measurements at a single site are often considered analogous to an induction log, very heavily smoothed, obtained without drilling a well. Results from a line of measuring stations are interpreted to give underlying conductivity distribution and structure. That picture of the subsurface can in turn be related to porosity and salinity, since conductivity depends primarily on those

= = = = = = = = = = = = = = =

This chapter summarizing the theory of the magnetotelluric method was produced largely by lifting sections from the papers of many of the authors, especially Vozoff (1972, 1976).

two factors in common sedimentary rocks. A third factor, temperature, is an important variable in geothermal areas. In the past few years the MT method has been applied increasingly to problems in exploration and in earth sciences generally. These problems range from studies of the interior of the earth (on a regional scale), to the search for oil and gas and geothermal energy (on an intermediate scale), to the search for minerals (on a small scale).

The time variations of the earth's electric and magnetic fields at a site are recorded simultaneously over a wide range of frequencies, usually on digital tape. The variations are analyzed by computer to obtain their spectra, and various parameters (such as apparent resistivity) are computed as functions of frequency from the spectra. Interpretation consists of matching the computed plots to curves calculated for simplified models.

The Signals

The time-varying magnetic (H) signal is the always present "noise" in the earth's magnetic field. When very large, it interferes with magnetic surveys. In the

conducting earth, the changing magnetic field induces telluric (eddy) currents and voltages; the latter are proportional to the electric (E) signals. They are very similar in appearance to the H signals. On chart records, both sets of variations look irregular and noise-like for the most part. At times, in certain frequency bands, the variations may appear sinusoidal, but the sinusoids are not an important part of the signal for MT purposes. Signal amplitudes fall off rapidly with increasing frequency over most of the range of frequencies used. Signal level can increase very rapidly at the onset of magnetic storms, an increase of a factor of 10 being common, and even a factor of 100 is not unusual.

Most of the magnetic noise reaching the earth below 1 Hz is due to current flow in the ionized layers surrounding the earth. The currents are powered by solar activity and by the relative motions of the earth, sun, and moon. At frequencies above 1 Hz, worldwide electrical thunderstorm activity within the atmosphere is the major contributor. The transient fields due to thunderstorms can be exceedingly large locally, while those associated with tornadoes are greater still.

In the low-frequency range, mean directional properties from the source are fairly random so that, given sufficient

recording time, all source directions are sampled. This is very fortunate since individual observations should then be reproducible even though the electric field does not always flow perpendicular to the source field, due to local anisotropy. At higher frequencies the source fields are not so uniform in direction, depending on the location of thunderstorm centers, and one can obtain sets of nonrepeatable data depending upon the relative directions of source field and lateral resistivity contrast.

Effect of Earth Conductivity on H

When the magnetic fluctuations reach the surface of the earth, reflection and refraction occur. It is now well established that the signals can be approximated by electromagnetic plane waves. This will not be true under all conditions, but holds for the vast majority of geological situations of interest in petroleum prospecting (Madden and Nelson, 1964; Rikitake, 1966; Vozoff and Ellis, 1966).

Although the majority of the incident energy is reflected, a small portion is transmitted into the earth and travels vertically downward. To the conducting rocks, this

energy appears as a magnetic field which is changing with time, and electric fields are induced so that telluric currents can flow. These telluric currents are completely analogous to the eddy currents which flow in transformers due to the changing magnetic fields caused by the alternating current in the primary windings.

Energy in the downgoing disturbance is quickly dissipated as heat. As a result the field penetration is relatively small in terms of its wavelength in air. The penetration mechanism in this situation is actually diffusion rather than wave propagation.

Current density in the earth depends on resistivity ρ, as might be expected. Within a rock, the normal relationship between the electric field and the current density at each point is

$$j = E/\rho.$$

This differential form of Ohm's law is really a definition of resistivity and is very similar to the Ohm's law definition of resistance,

$$I = V/R.$$

In mks units E is in volts/meter, j is in amperes/square

meter, ρ is in ohm-meters, and H is in amperes/meter. However, because the fields are so small, the more commonly used practical units are mv/km for E and gammas for H. The practical units will be used in later sections.

The E measurement is actually a voltage difference measurement between two electrodes. In a uniform earth, the voltage difference V between electrodes a distance l apart would be

$$V = lE.$$

In the MT method it is usually assumed that E is constant over the length of the wire; i.e.,

$$E = V/l.$$

The depth of penetration of the fields into the earth is inversely related to rock conductivity. In a uniform earth E and H weaken exponentially with depth; the more conductive the earth, the less the penetration. The depth at which the fields have fallen off to (1/e) of their values at the surface is called the skin depth δ.

$$\begin{aligned}\delta &= \sqrt{2/\omega\mu\sigma}\ \text{m} \\ &\approx \tfrac{1}{2}\sqrt{\rho/f}\ \text{km},\end{aligned}$$

where f is frequency, $\omega = 2\pi f$, and μ is permeability.

(μ in the earth is taken equal to μ_0 except in highly magnetic materials.) Frequency enters into the equations because the magnitudes of the induced telluric currents depend on the time rate of change of the magnetic fields.

In a uniform or horizontally layered earth all currents, electric fields, and magnetic fields are practically horizontal, regardless of the direction from which these fields enter the earth. This comes about because of the high conductivity of earth relative to air. It can be thought of in terms of Snell's law in optics, with the velocity in the earth being orders of magnitude smaller than that outside. Furthermore, the currents and electric fields are at right angles to the associated magnetic fields at each point. If E is positive to the north, H is positive to the east. That is, viewed from above, E must be rotated 90 degrees clockwise to obtain the direction of positive H.

The mathematical description of the perpendicular E and H fields in a uniform isotropic conductor includes all these features in a concise form:

$$H_y = H_y^0 e^{-i\omega t + (i-1)z/\delta};$$
$$E_x = E_x^0 e^{-i\omega t + (i-1)z/\delta};$$
$$E_x^0 = (1 - i)\omega\mu\delta H_y^0/2.$$

The superscript indicates the value at the surface.

Particularly interesting is the ratio

$$\frac{E_x^0}{H_y^0} = \frac{(1-i)\omega\mu\delta}{2} \text{ ohms} \qquad (1)$$
$$= (1-i)(\omega\mu/2\sigma)^{1/2}.$$

Since E and H are recorded at frequencies which can be accurately measured and since μ varies little from μ_0 in most rocks, the ratio shows the relationship which exists between the conductivity and the measured fields. The equation can be solved for conductivity, giving

$$\sigma^{1/2} = (1-i)(\omega\mu/2)^{1/2}\frac{H_y^0}{E_x^0}. \qquad (2)$$

Equation (2) is usually rewritten in mks units as

$$\rho = \frac{i}{\omega\mu}\left(\frac{E_x}{H_y}\right)^2$$

and the superscripts are omitted.

In practical units, where E is given in mv/km and H is in gammas, the magnitude of ρ is

$$\rho = \frac{1}{5f}\left(\frac{|E_x|}{|H_y|}\right)^2. \qquad (3)$$

When ρ (or σ) is calculated from E and H values, it is called an apparent resistivity ρ_a (or apparent

conductivity σ_a). ρ and ρ_a are related, but they must be clearly distinguished. ρ_a is the resistivity that a uniform earth must have to give the measured value of the impedance Z. ρ is a property of the medium, whereas ρ_a depends on how it is measured. The ratio of E_i to H_j at each frequency is the impedance Z_{ij} for those components at that frequency. Since E and H are usually not in phase Z_{ij} is taken to be a complex number.

In a uniform earth, ρ_a has to be the same at every frequency, and E leads H in phase by 45 degrees at all frequencies. (This can be checked by substituting Equation (1) into Equation (3).) Thus, if we plot ρ_a and phase against frequency, we see that both are constants.

In discussing kinds of electrical structure, it is useful to define two-dimensional and three-dimensional structures. In the two-dimensional case [$\sigma = \sigma(x, z)$], conductivity varies along one horizontal coordinate and with depth. The other horizontal direction is called the strike. When conductivity varies with both horizontal coordinates and with depth [$\sigma = \sigma(x, y, z)$], the structure is said to be three-dimensional and has no strike. If σ depends only on z, the structure is one-dimensional. In each case, σ at each point can depend on the direction of current flow;

if σ does depend on direction, the medium is anisotropic.

If the conductivity changes with depth, ρ_a varies with frequency, since lower frequencies penetrate more deeply. Apparent resistivity can be written and computed exactly for any desired combination of horizontal layers, whether isotropic or arbitrarily anisotropic. It can be calculated approximately for any two-dimensional model structure. As might be expected, Z for horizontally isotropic and homogeneous layers does not depend on the directions used as long as E is measured perpendicular to H.

When faulting or jointing are present, σ varies laterally or with direction, and the J and E which are induced by a given H depend on their direction relative to strike. In order to sort out these effects, we record complete horizontal E and H fields (two perpendicular components of each) at every site. In addition, the vertical component of H is also recorded, for a total of five recorded signals in all. These are designated H_x, H_y, H_z, E_x, and E_y.

In general, ρ_a at each frequency varies with measurement direction. We assume that there is a strike but that its direction is unknown. Then E_x is due partly to H_y, but also partly to currents induced by H_x, which have

been deflected by the structure. The same is true of E_y, so the relations are written

$$E_x = Z_{xx}H_x + Z_{xy}H_y, \qquad (4)$$

$$E_y = Z_{yx}H_x + Z_{yy}H_y. \qquad (5)$$

For example, Z_{yx} gives the part of E_y which is due to H_x, and so forth. Since E_y and H_x are generally not in phase, the Z's are complex. E and H component amplitudes are obtained by computer-analyzing the records using methods described in the section on data analysis.

FIELD PROCEDURE AND INSTRUMENTATION

Although basically simple, field procedures require a great deal of planning and attention to detail, since they dominate the costs; and the sensitivity of the measurement makes it highly vulnerable to disturbances at the measuring site. Sites must be chosen with care, to avoid possible sources of disturbance such as cathodic protection circuitry, power and fence lines, unprotected pipelines, and vehicle and pedestrian traffic. Two pairs of electrodes aligned at right angles must be laid out at each site, as must three mutually perpendicular magnetometer axes. A set-up is shown schematically in Figure 2.

For the E-field measurements, sheet lead electrodes provide low-resistance and low-noise electrical connections with the earth. The input to each of the E-field channels is the voltage difference between an electrode pair. (Although one usually thinks of the earth as being at zero potential, voltage differences must exist if telluric currents flow, because the earth has finite conductivity, and $j = E\sigma$.) The farther apart a pair of electrodes, the larger the signal voltage measured, so it is usually desirable to put the electrodes as far apart as possible, subject to other factors, such as obstructions, property

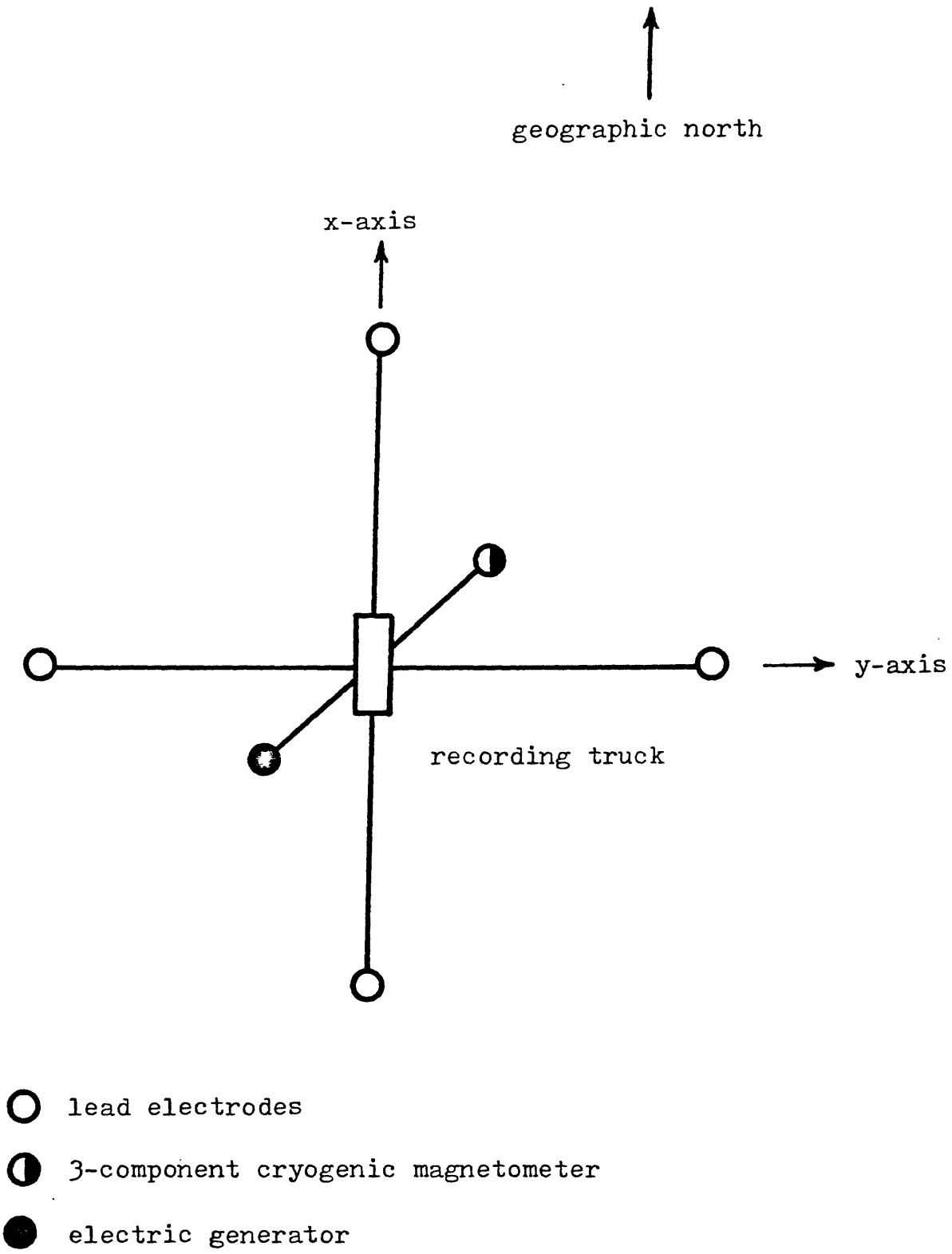

Figure 2: Magnetotelluric sensor orientation.

boundaries, the time needed to lay out connecting wires, and the minimum spacing tolerable between adjacent measurement sites. For routine operations, it is desirable to use fixed wire lengths. Finally, since the wires must not be permitted to move in the earth's main magnetic field as this induces noise, clods of dirt must sometimes be placed every few feet along the wire to restrain it, a very time-consuming task.

The two electrode pairs are intended to measure two perpendicular components of an electric field vector which exists at each site. However, it is possible for the electric field on the surface to change in both direction and intensity over very short distances, due to large lateral resistivity changes near the surface. Large electrode spacings should be used in this situation to average over as much of the variation as possible, or the resulting data will apply to conditions which are too localized to be of use. For best averaging in these circumstances, it is also important that the two electrode pairs form a cross whose four arms are as nearly equal in length as possible, rather than being arranged to form an "L" or a "T", (Swift, 1967), and that the magnetometer be near the center. Although the cross is preferable, difficult terrain may require one of the other arrays.

Topographic features can cause distortions similar to those caused by resistive heterogeneities. While these can also be modeled, it is better to avoid them if possible, especially if the relief is more than 10 percent or so of the electrode spacing.

The H-field sensors consist of a three-axis cryogenic magnetometer with a 30 liter liquid helium reservoir. Since magnetometers are even more sensitive to motions than are the wires connecting the electrodes, the magnetometer is firmly seated in a 6 inch to 12 inch deep hole and covered with a wind screen.

The recording instrumentation contains amplifiers, filters, a multiplexer, an analog-to-digital converter, and a digital cassette drive controlled by software commands from a 32K word, 16 bit mini-computer and timed by a clock synchronized with the National Bureau of Standards WWVB time code. A block diagram is shown in Figure 3, and specifications are given in Table A .

Normalized system response curves calculated for the bands used are shown in Figure 4 . System calibrations were made at the beginning of the survey and at the end of the survey and were within 3% of the calculated responses from one decade below the lower corner frequency to one octave

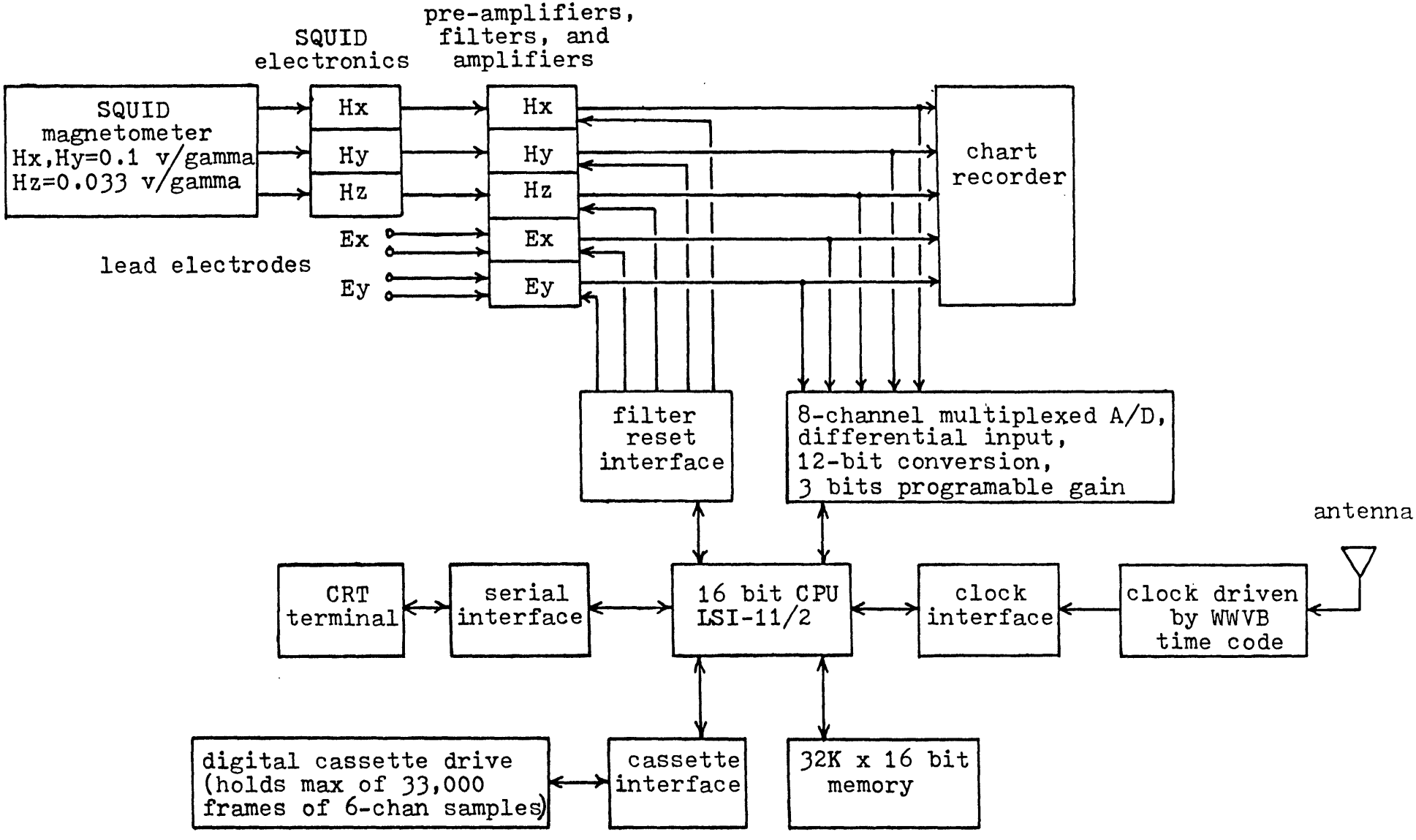

Figure 3: Argonaut Enterprises magnetotelluric data acquisition system

TABLE A : Specifications of Argonaut Enterprises MT data acquisition system as of October 9, 1979.

(1) Electrical field detectors (2 component): four electrodes in a square array using 100 to 300 m lines.
(2) Magnetic field detectors (3 component): three-axis super conducting quantum-interference device (SQUID) magnetometer with 30 liter dewar and sensitivity of better than 10 gammas.
(3) Analog signal conditioners:
    (a) instrumentation preamplifier gains of 2, 5, 10, 20, 50, and 100
    (b) post amplifier gains of 2, 5, 10, 20, 50, 100, 200, 500, 1000, and 2000
    (c) active 60 Hz notch filter with 45 db rejection and variable Q
    (d) 2 stages of passive (RC) low pass filtering: 6 db/ octave rolloff with corner frequencies of 0.16, 1.6, 16, and 160 Hz.
    (e) active low pass filter: 12 db/octave rolloff with corner frequencies of 0.02, 0.06, 0.2, 0.6, 2, 6, 20, 40, and 200 Hz.
    (f) active high pass filter: 12 db/octave rolloff with corner frequencies of 0.001, 0.002, 0.005, 0.01, 0.03, 0.1, 0.3, and 6 Hz.
    (g) The filters in each channel can be independently reset to zero by (1) manual switch on the front of each amplifier-filter board or (2) by the mini-computer under software control.
(4) 8-channel differential-input multiplexer and analog-to-digita converter with 12 bit conversion plus 3 bits of programmable gain on each sample.
(5) Timing control unit:
    (a) can be interrogated by the computer to give day of the year, hour, minute, and second.
    (b) updated millisecond interrupt clock.
    (c) accuracy to better than 1 millisecond when synchronized with WWVB.
(6) Digital tape recording with complete information for processing contained in the tape header.
(7) In-field monitoring of recording and playback processes by a 16 bit, 32K memory, mini-computer.

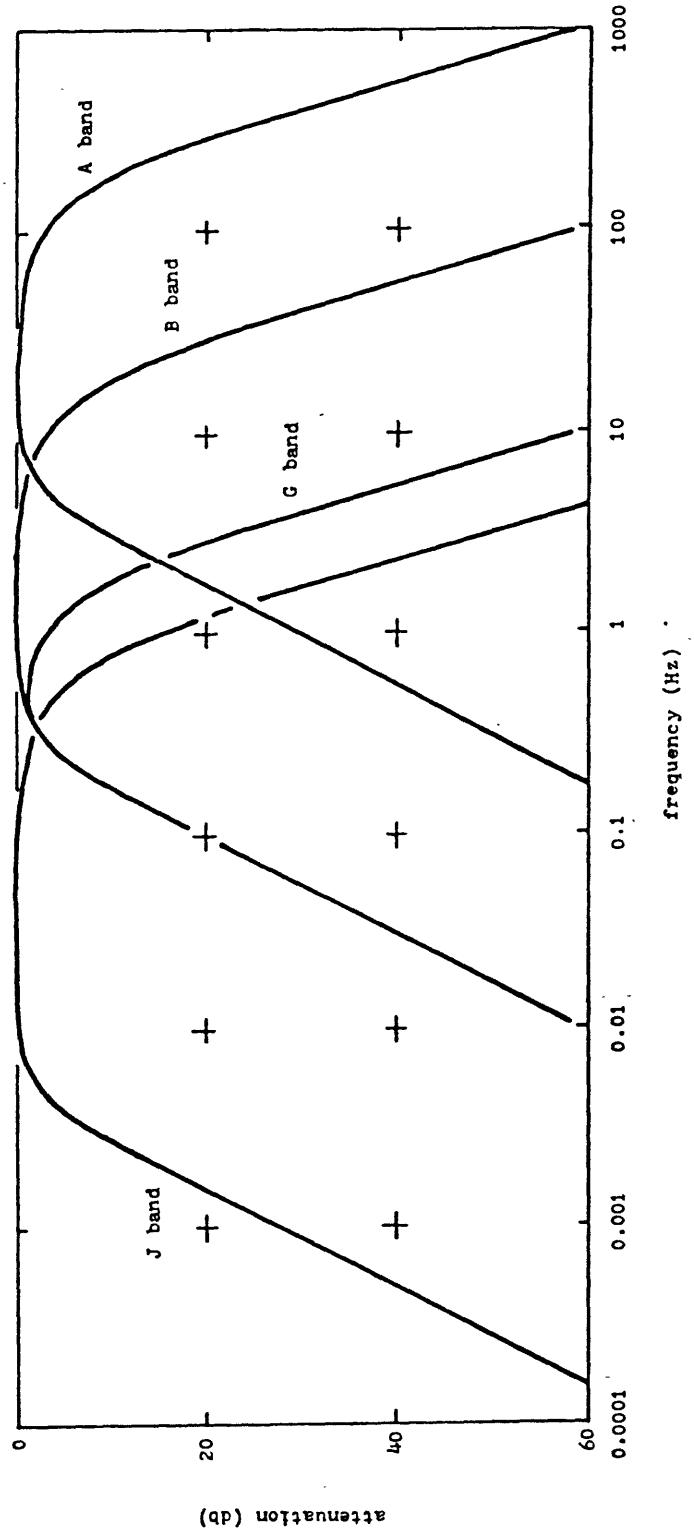

Figure 4: System response.

above the upper corner frequency. Within the pass band the match was usually better than 1%. Total filter and amplifier noise in the band from 0.001 to 1 Hz is less than eight microvolts (referred to input).

The field measurements for this survey consisted of recording simultaneously five orthogonal E and H fields over a nominal range of 0.002 to 200 Hz. Rather than record the entire frequency range at once, several narrower, overlapping bandpass segments were used. The four bands used for this survey are shown in Table B . The frequency range is divided this way for two important reasons: to make best use of the available dynamic range and for economy in digital recording. That is, dividing the frequency range permits the use of large gains in some parts of the spectrum and lower gains in others, according to the signal levels actually present at recording time. The economic aspect enters, since the total recording duration is a multiple of the longest period which is being recorded, whereas digitizing rate is at least four times the highest frequency being recorded. If the band is very wide, far more short period data will be acquired than is necessary while waiting for adequate sampling of long periods. The 1- to 2- decade segments used are a compromise. For further efficiency, recordings can be scheduled so as to avoid known or

Table B: Magnetotelluric recording bands.

band	digitizing interval	3 db down corner frequencies			average number of points recorded
		active high pass	active low pass	passive low pass (two stages)	
I	0.0005	5.7	200	160	60,000
B	0.01	0.32	20	16	60,000
G	0.04	0.32	2	1.6	60,000
J	0.3	0.005	0.64	1.6	20,000

anticipated noise. Customarily, several recordings are obtained in each frequency band at different times of the day, because noise and signal are both variable and largely unpredictable.

DATA ANALYSIS

The purpose of data analysis is to extract reliable values of impedances, apparent resistivities, and the other earth response functions (ERF) from the field records, and to present them in a form convenient for interpretation. Operationally, data analysis consists of (a) manual editing of records to reject those judged to be contaminated by noise; (b) computer manipulation of tape-recorded data to transform all records into the frequency domain, to derive the ERF which are used for interpretations, to screen each value computed, and to plot in a form convenient for interpretation the values which pass the screening; and (c) manual evaluation of the results to reject suspect data and to attempt to extract useful portions of previously rejected data when necessary.

The first phase, manual editing, involves the examination of both recording log books and chart records for evidence the artificial or wind noise is large enough to downgrade a record. Records degraded by noise are not used if their use can be avoided, although it is sometimes necessary to reconsider using their quieter parts when insufficient quiet data exist.

Normally, 20 to 35 data sets (each 2048 points long) per band are picked for processing. Each data set has its mean removed and then is tapered by a cosine bell so that harmonics as low as the second might be used. Then a FFT (Fast Fourier Transform) is performed and the resulting Fourier coefficients are used to compute power spectra. All power spectra in a band are then averaged.

It is helpful at this point to describe a few of the properties of the ERF, in order to explain some of the procedures which are used in data analysis. In two-dimensional structures when neither of the coordinate axes is along strike, all four elements of the impedance tensor Z_{ij} are nonzero and have different values. Magnetic field components in the x direction give rise to some currents along x, in addition to the y-directed currents, which would be the only ones if the earth were uniform or horizontally layered. Magnetic y components are likewise associated with both E_x and E_y, so that Z_{xx}, Z_{xy}, Z_{yx}, and Z_{yy} will all have some finite values. Now if the coordinate axes are rotated (either physically or by computation) until one of them is along strike, then currents due to H_x can no longer be deflected into the x direction and those due to H_y flow only in the x direction. In this situation, Z_{xx} and Z_{yy} must be zero. The other pair are nonzero and unequal,

since current densities will differ in the two directions, and the E components must also differ. If the coordinates are rotated a further 90 degrees, the same situation is found, except that the Z values are interchanged. Some of the other properties of the impedence elements are not so apparent. One of these is that

$$Z_{xx} = -Z_{yy} \qquad (6)$$

regardless of the angle between the coordinate axes and strike. Equation (6) was also found by computation to be valid for an arbitrary number of horizontal layers, each of which is arbitrarily anisotropic. Another important property is that

$$Z_{xy} - Z_{yx} = \text{constant}$$

at all orientations.

In three-dimensional structures, the tensor elements are still well behaved, according to Sims and Bostick (1969). By plausibility arguments, they arrived at

$$Z_{xx} + Z_{yy} = \text{constant}$$

and

$$Z_{xy} - Z_{yx} = \text{constant.}$$

The Z_{ij} are first found from the transformed data by solving Equations (4) and (5) (see The Theory of the Magnetotelluric Method). This involves using two equations in four unknowns. The apparent discrepancy is resolved by taking advantage of the facts that the Z_{ij} change very slowly with frequency and can therefore be computed at far fewer frequencies than there are transform values. That is, the Z_{ij} are calculated as averages over frequency bands with each band including many points of the transform. There are six different ways of computing each of the four tensor components (Word and others, 1970; Sims and others, 1971; Vozoff, 1971). Two of the expressions tend to be relatively unstable for the one-dimensional earth, particularly when the incident fields are unpolarized. Another pair of the expressions are biased down by random noise on H and are not biased by random noise on E, while the remaining two are biased up by random noise on H. The six expressions are computed and checked to see if they are stable and fit a two-dimensional structure. The ones which pass the tests are then averaged and used to compute the impedance tensor.

Once the Z_{ij} have been found in the original (x, y, z) coordinate system, they can be rotated to any other system (x', y', z') by an angle θ in the clockwise direction. The principal axes of Z are the values of θ at which Z'_{xy} and

Z'_{yx} take on their largest and smallest values, respectively. One way of finding these directions is to compute Z for many values of θ and interpolate to find maxima and minima. It is preferable to use an analytical technique if possible, to reduce computation. However, the only such technique which has thus far been developed does not directly maximize either $Z'_{xy}(\theta)$ or $Z'_{yx}(\theta)$. Instead it solves for the angle θ_0 at which

$$|Z'_{xy}(\theta_0)|^2 + |Z'_{yx}(\theta_0)|^2 = \text{maximum.}$$

Setting the derivative with respect to θ of this sum equal to zero gives (Swift, 1967)

$$\tan 4\theta = \frac{(Z_{xx} - Z_{yy})(Z_{xy} + Z_{yx})^* + (Z_{xx} + Z_{yy})^*(Z_{xy} - Z_{yx})}{|Z_{xx} - Z_{yy}|^2 - |Z_{xy} + Z_{yx}|^2}.$$

This same value of θ_0 also satisfies

$$|Z'_{xx}(\theta_0)|^2 + |Z'_{yy}(\theta_0)|^2 = \text{minimum},$$

so that in the case of two-dimensional structures the scheme finds the true principal axes. In the three-dimensional case, the method picks a slightly more general maximum, i.e.,

$$|Z'_{xy}(\theta) + Z'_{yx}(\theta)| = \text{maximum}$$

(Sims and Bostick, 1969). The results are seldom shown as impedance values. Instead, the Z'_{ij} are converted to apparent resistivities ρ' , with

$$\rho'_{ij} = \frac{1}{5f} |Z'_{ij}|^2.$$

Apparent resistivity has the phase of Z'_{ij} , that is, the phase difference between E_i and H_j.

Four different Z'_{ij} are extracted at each frequency: Z'_{xx}, Z'_{xy}, Z'_{yx}, and Z'_{yy}. The main purpose of analysis and plotting is to permit interpretation, which is now practically possible only for two-dimensional structures. Hence, only ρ'_{xy} and ρ'_{yx} are routinely plotted, since they are the only two which appear in two-dimensional models.

As noted above, both $(Z_{xx} + Z_{yy})$ and $(Z_{xy} - Z_{yx})$ are independent of θ , as is their ratio. The magnitude of the complex ratio of these quantities is called skewness,

$$S = \frac{|Z_{xx} + Z_{yy}|}{|Z_{xy} - Z_{yx}|}.$$

If S is large, structure at the site must appear to be three-dimensional in that frequency range.

The multiple coherence values are a result of analyzing the MT problem as a multiple input single output linear system. In particular it is a measure of the correlation between an electric field measured and one predicted by the radial magnetic fields.

There are two multiple coherence values corresponding to the different electric fields. The functions are computed from the power spectra according to the following formula

$$(MCE_x)^2 = \frac{H_y H_y^* |H_x E_x^*|^2 \; H_x H_x^* |H_y E_x^*|^2 - 2\,Re(H_x H_y^* H_y E_x^* E_x H_x^*)}{E_x E_x^* (H_x H_x^* H_y H_y^* - |H_x H_y^*|^2)} .$$

A similar expression exists for the E_y function by substituting E_y for E_x above. (Reddy and Rankin, 1974).

The other ERF are designed to use the vertical magnetic component H_z to help determine which of the two principal impedance axes is the strike direction. At the same time, the remaining ERF aid the interpreter in understanding the cause of apparent anisotropy, point out distant lateral conductivity changes, and often provide additional warning when three-dimensional structural conditions occur.

From the field data, we want to find the horizontal direction in which the magnetic field is most highly coherent with H_z. In two-dimensional structures, that direction will be constant and perpendicular to strike.

The procedure, due to T. R. Madden (1968, unpublished), is to assume that H_z is linearly related to H_x and H_y and to write at each frequency

$$H_z = AH_x + BH_y,$$

where A and B are unknown complex coefficients.

Using a least-squares derivation, we can solve for A and B. This pair of coefficients can be thought of as operating on the horizontal magnetic field and tipping part of it into the vertical. For that reason, (A and B) is called the "tipper". Its magnitude in each frequency band,

$$\begin{aligned} |T| &= \{|A|^2 + |B|^2\}^{1/2} \\ &= (A_r^2 + A_i^2 + B_r^2 + B_i^2)^{1/2}, \end{aligned}$$

shows the relative strength of H_z. For a two-dimensional structure striking in the direction ($\phi \pm 90$) degrees from x, the tipper strike ϕ can be determined by a natural extension of the tensor rotation method, proposed by Sims

and Bostick (1969). Here ϕ is chosen to maximize

$$|A'|^2 = |A \cos\phi + B \sin\phi|^2,$$

and is denoted ϕ_2.

We find the necessary condition to be

$$\tan(2\phi_2) = \frac{2(a_r b_r + a_i b_i)}{(a_r^2 + a_i^2) - (b_r^2 + b_i^2)}.$$

If we use the Fortran function ATAN, so that -90 degrees $\leq 2\phi_2 \leq 90$ degrees, then $|A'|^2$ is a maximum if $(a_r^2 + a_i^2) \geq (b_r^2 + b_i^2)$, and $|A'|^2$ is a minimum if $(a_r^2 + a_i^2) \leq (b_r^2 + b_i^2)$. If $|A'|^2$ is minimum, we need to add 180 degrees to $2\phi_2$. In either case, the final angle ϕ_2 is determined to within 180 degrees. A definite choice for ϕ_2 is made by taking ϕ_2 as the angle for which the phase of A' is in the range (-90 degrees, 90 degrees).

A single site recording is subject to biasing by noise on any of the measured fields. The recording of a remote pair of H-fields can be used to minimize uncorrelated noise. If we denote the remote channels by H_x^{R*} and H_y^{R*} and multiply through Equation (4), we have

$$\overline{E_x H_x^{R*}} = Z_{xx}\,\overline{H_x H_x^{R*}} + Z_{xy}\,\overline{H_y H_x^{R*}}$$

$$\overline{E_x H_y^{R*}} = Z_{xx}\,\overline{H_x H_y^{R*}} + Z_{xy}\,\overline{H_y H_y^{R*}}$$

If we then solve simultaneously for Z_{xx} and Z_{xy}, we find

$$Z_{xx} = \frac{\overline{E_x H_x^{R*}}\ \overline{H_y H_y^{R*}} - \overline{E_x H_y^{R*}}\ \overline{H_y H_x^{R*}}}{D}$$

$$Z_{xy} = \frac{\overline{E_x H_y^{R*}}\ \overline{H_x H_x^{R*}} - \overline{E_x H_x^{R*}}\ \overline{H_x H_y^{R*}}}{D}$$

where $D = \overline{H_x H_x^{R*}}\ \overline{H_y H_y^{R*}} - \overline{H_x H_y^{R*}}\ \overline{H_y H_x^{R*}}$, and the bars denote averages. Similar treatment of Equation (5) yields estimates of Z_{yx} and Z_{yy}:

$$Z_{yx} = \frac{\overline{E_y H_x^{R*}}\ \overline{H_y H_y^{R*}} - \overline{E_y H_y^{R*}}\ \overline{H_y H_x^{R*}}}{D}$$

$$Z_{yy} = \frac{\overline{E_y H_y^{R*}}\ \overline{H_x H_x^{R*}} - \overline{E_y H_x^{R*}}\ \overline{H_x H_y^{R*}}}{D}$$

These solutions for the impedance elements contain no autopowers and include only crosspowers between the base and the remote station. The impedance estimate will then be unbiased by noise, provided the noise is uncorrelated. (Goubau and others, 1978)

INTERPRETATION

The quality of the data collected during this survey is, at the best, fair and, often, very poor. Noise sources of importance were water well pumps, 60 Hz power distribution lines, and virtually continuous rain and lightning storms during the entire survey period. Remote reference recording, parallel E-field checks, and system calibrations gave assurance that Argonaut's equipment was functioning correctly. As a final check, stations 2, 4, 5, and 6 were completely retaken including new E-field wires and electrodes. Minor improvement was observed for the repeated stations 2 and 4, but none for 5 and 6. Coherencies also indicate the poor quality of this data, and so extreme caution should be observed in using the results of the following interpretive comments.

Probably the single most important step in MT interpretation is the systematic examination of the apparent resistivity verses frequency data for the survey area (Appendix B). This step, roughly equivalent to the familiar seismic "brute stack", yields (a) the approximate vertical sequence of resistive and conductive units, (b) approximate location of faults and structural trends, and (c), most important, the structural complexity as evidenced in the data, which will indicate which modeling route to take for

the continuation of the interpretation. The above procedures involve examining all of the MT data with an eye to the interrelation between sites, as impressions gained from an individual site by itself or even a single profile may be misleading. As shown in Appendix E (Arnold Orange, 1981, unpublished), it is most important to identify evidence of strong two and three-dimensional effects. While one is usually forewarned by preliminary geologic and regional geophysical (gravity, magnetics) studies, frequently the MT data will exhibit unanticipated effects. The qualitative examination step identifies these effects, and leads to the determination of the appropriate modeling procedures.

The interpretation of MT data as currently practiced by most geophysicists active in the field relies heavily on one-dimensional inversions of the parallel to strike (TE) component of apparent resistivity. Two-dimensional models are used as an aid to interpretation but final resistivity and geologic sections are most frequently seen as contoured or "picked" sections with the one-dimensional (TE) inversions as the base. This technique is applicable in many instances, and excellent MT interpretations have been produced as a result. There are, however, important geologic structures where the TE based, one-dimensional

inversion interpretation will be seriously in error (see Appendix E). To avoid this the interpreter must learn to recognize those situations where the procedure is inappropriate, and to have available alternate procedures to follow in order to arrive at a successful interpretation.

Table C shows electrical strike determined for each station. It is readily apparent that except for station 3, the strike is northeast or east which agrees reasonably well with the major structural trends in the area. Station 3 is inside a Precambrian porphyry body and less than three kilometers from the noise of the plunging Fries Fault.

The station density of this survey is too sparse by at least a factor of three for a cross section of any confidence, but the attempt was made as it was a requirement of the contract. Therefore, a northwest-southeast section was drawn between stations 1 and 10 (Plate 2), with an offset between stations 7 and 8. Using the Bostick (1977) continuous inversion in Appendix D as a first start, analytic discrete layer inversions using a program by Anderson (1978) were made for the ten stations on the profile (see Table C). Because this highly speculative cross section clearly shows the strong two-dimensional character of the structure, it should only be used as a starting point for a two-dimensional analysis.

Table C: Strike direction, TE mode choice, and analytic one-dimensional inversions for TE mode.

station	strike	TE mode	layer number	resistivity (ohm-m)	depth to bottom of layer (km)
1	60	xy	1	5,000	3.9
			2	10,200	40
			3	900	70
			4	200	
2	60	yx	1	500	0.43
			2	1,000	11
			3	20	49
			4	1,000	
3	135	xy	1	1,400	0.87
			2	19,000	35
			3	1,700	
4	70	xy	1	2,100	0.32
			2	16,000	57
			3	1,000	230 (?)
			4	100,000 (?)	
5	80	xy	1	2,300	0.44
			2	320	0.80
			3	9,000	
6	30	xy	1	2,000	0.21
			2	85,000	30
			3	10,000	57
			4	550	
7	60	xy	1	12,000	17
			2	500	39 (?)
			3	30,000 (?)	
8	90	xy	1	1,000	17
			2	200	39
			3	20	
9	50	yx	1	250	0.37
			2	2,700	35
			3	440	
10	80	xy	1	20	0.19
			2	125	7
			3	30	

REFERENCES

Specific to this survey

Anderson, L.A., and Keller, G.V., 1966, Experimental deep resistivity probes in the central and eastern United States: Geophysics, v. 31, no. 6, p. 1105-1122.

Cook, F.D., and others, 1979, Thin-skinned tectonics in the crystalline southern Appalachians, COCORP seismic-reflection profiling of the Blue Ridge and Piedmont: Geology, v. 7, p. 563-567.

Cook, F.D., Brown, L.D., and Oliver, J.E., 1980, The southern Appalachians and the growth of continents: Scientific American, v. 243, no. 4, p. 156-169.

Heinrichs, W.E., 1966, Geophysical investigations, Ore Knob Mine, Ashe County, North Carolina: Mining Geophysics, v. 1, p. 179-184.

Kaufman, S., 1979, COCORP southern Appalachian data: Geophysics, v. 44, no. 9, p. 1598-1599.

Rankin, D.W., Espenshade, G.H., and Neuman, R.B., 1972, Geologic map fo the Winston-Salem Quadrangle, North Carolina, Virginia, and Tennessee: U.S.G.S. Map I-709-A.

REFERENCES

General

Bostick, F.X., 1977, A simple almost exact method of MT analysis in Ward, S.H., ed., Workshop on electrical methods in geothermal exploration: Univ of Utah, Salt Lake City, UT, pp. 175-183.

Goubau, W.M., Gamble, T.D., and Clarke, J., 1978, Magnetotelluric data analysis: removal of bias: Geophysics, v.43, pp. 1157-1169.

Jupp, D.L.B., and Vozoff, K., 1976, Discussion of "The magnetotelluric method in the exploration of sedimentary basins" by K. Vozoff (Geophysics, 1972): Geophysics, v.41, pp. 325-328.

Madden, T., and Nelson, P., 1964, A defense of Cagniard's magnetotelluric method: Geophysics Lab, MIT Project NR-371-401.

Reddy, I.K., and Rankin, D., 1974, Coherence functions for magnetotelluric analysis: Geophysics, v.39, pp. 312-320.

Ritatake, T., 1966, Electromagnetism and the earth's interior: Amsterdam, Elsevier Pub. Co.

Sims, W.E., and Bostick, F.X., Jr., 1969, Methods of magnetotelluric analysis: EGRL Tech. Rep. no. 58, Univ of Texas at Austin.

Sims, W.E., and Bostick, F.X., Jr., and Smith, H.W., 1971 The estimation of magnetotelluric impedence tensor elements from measured data: Geophysics, v. 36, no. 5, pp.938-942.

Swift, C.M., Jr., 1967, A magnetotelluric investigation of electrical conductivity anomaly in the southwestern United States: Ph.D. thesis, MIT.

Vozoff, K., 1972, The magnetotelluric method in the exploration of sedimentary basins: Geophysics, v. 37, pp.98-141.

Vozoff, K., and Ellis, R.M., 1966, Magnetotelluric measurements in southern Alberta: Geophysics, v. 31, p. 1153.

Word, D.R., Smith H.W., and Bostick F.X., Jr., 1970, An investigation of the magnetotelluric tensor impedence method: EERL Tech. Rep. no. 82, Univ of Texas at Austin.

APPENDIX A

STATION LOCATIONS

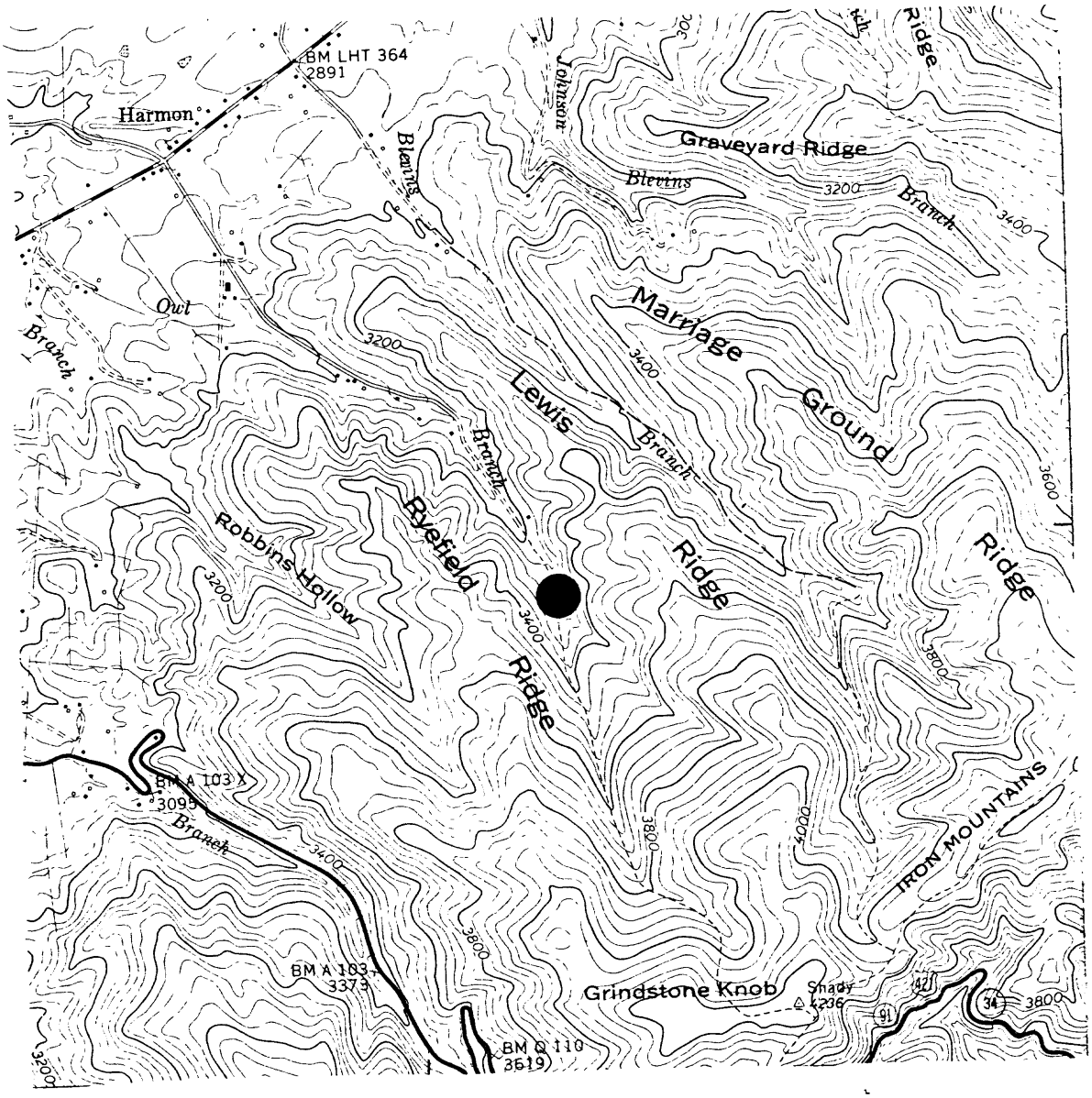

Station 1
Shady Valley Quad.
Tennessee
7.5 minute
Lat 36°30.879', Long 81°53.686'

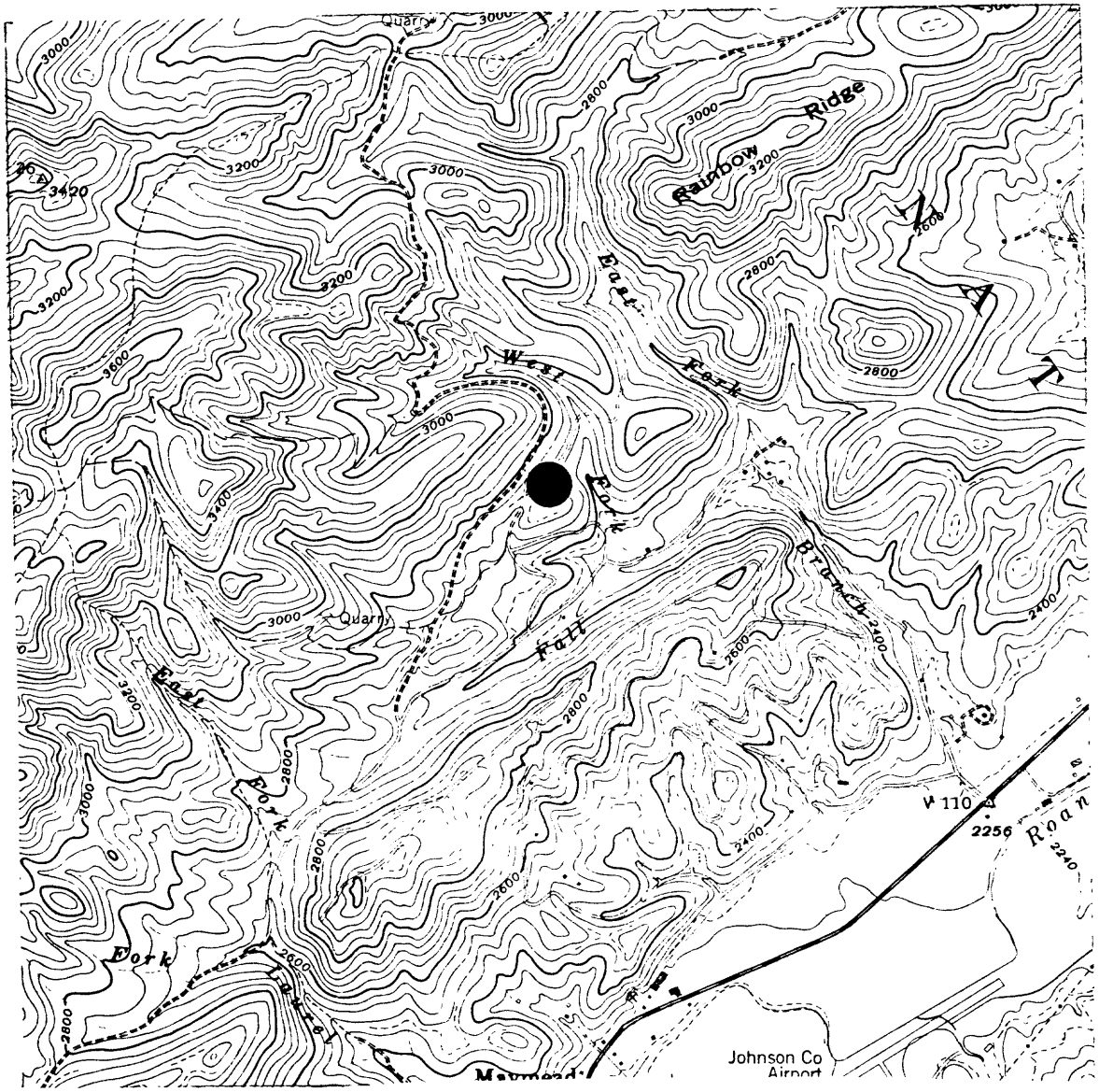

Station 2
Mountain City Quad.
Tennessee
7.5 minute series
Lat 36°26.109', Long 81°50.270'

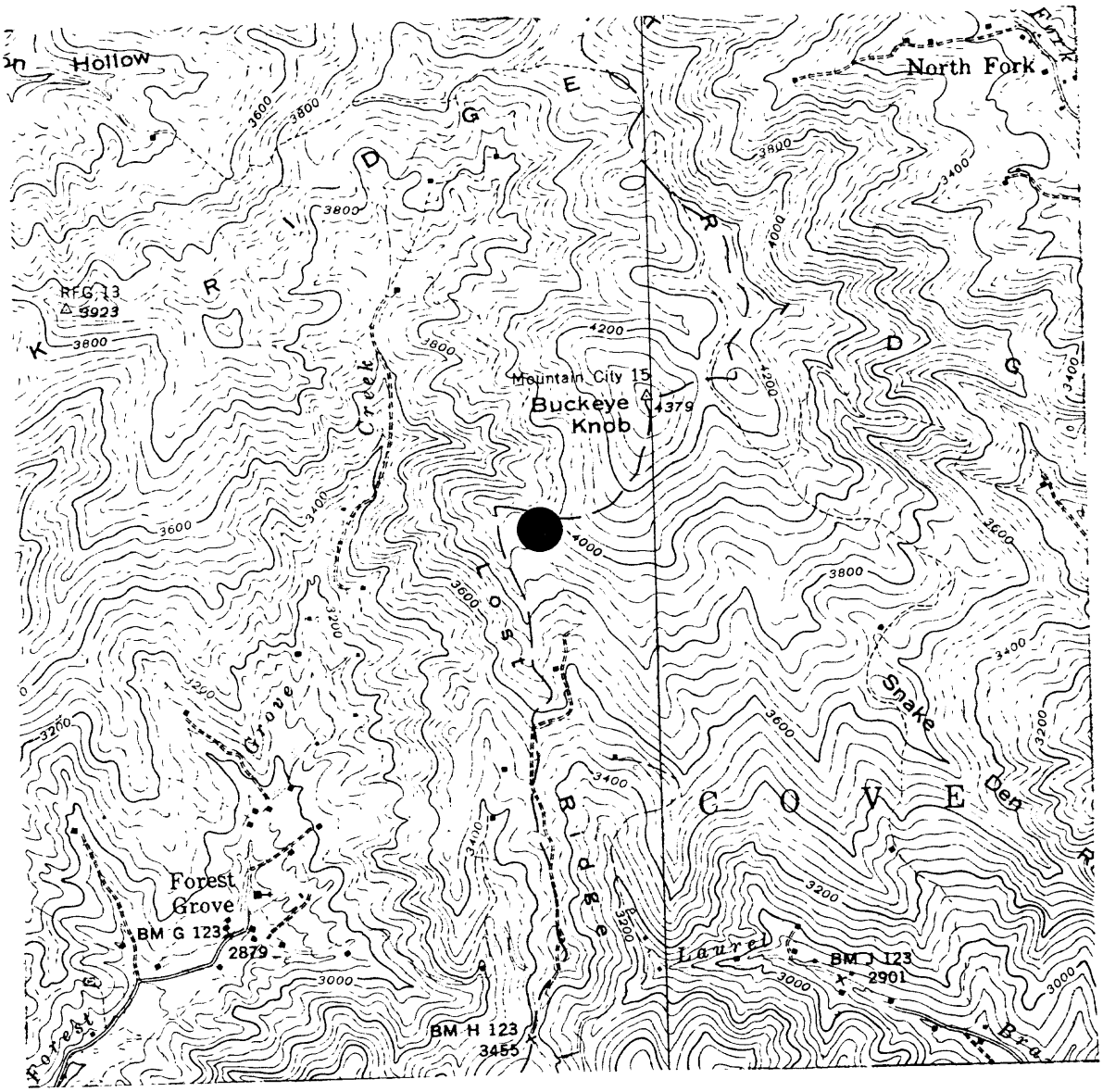

Station 3
Sherwood Quad.
North Carolina
7.5 minute series
Lat 36°18.752', Long 81°47.781'

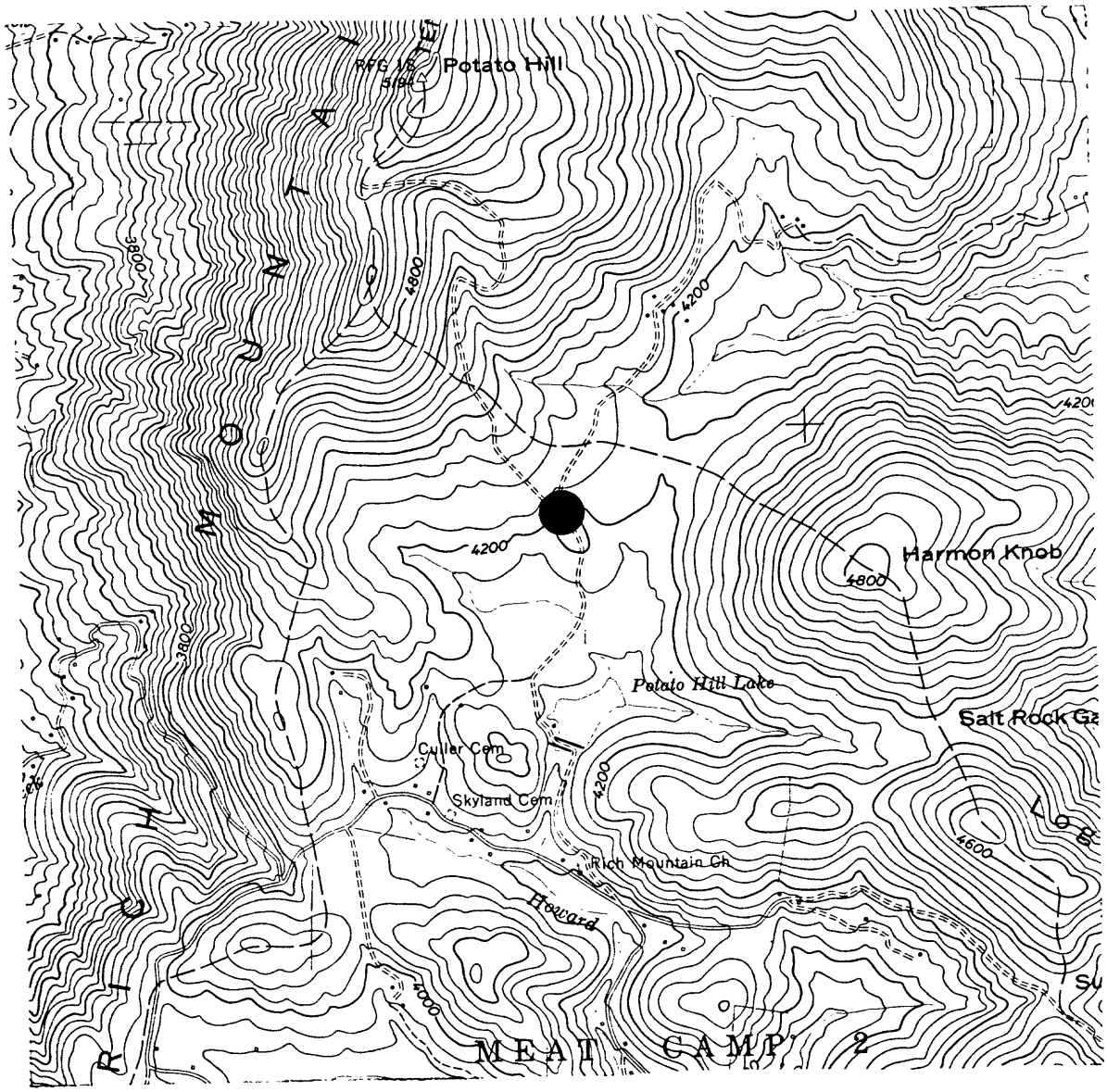

Station 4
Zionville Quad.
North Carolina
7.5 minute series
Lat 36°17.357', Long 81°43.045'

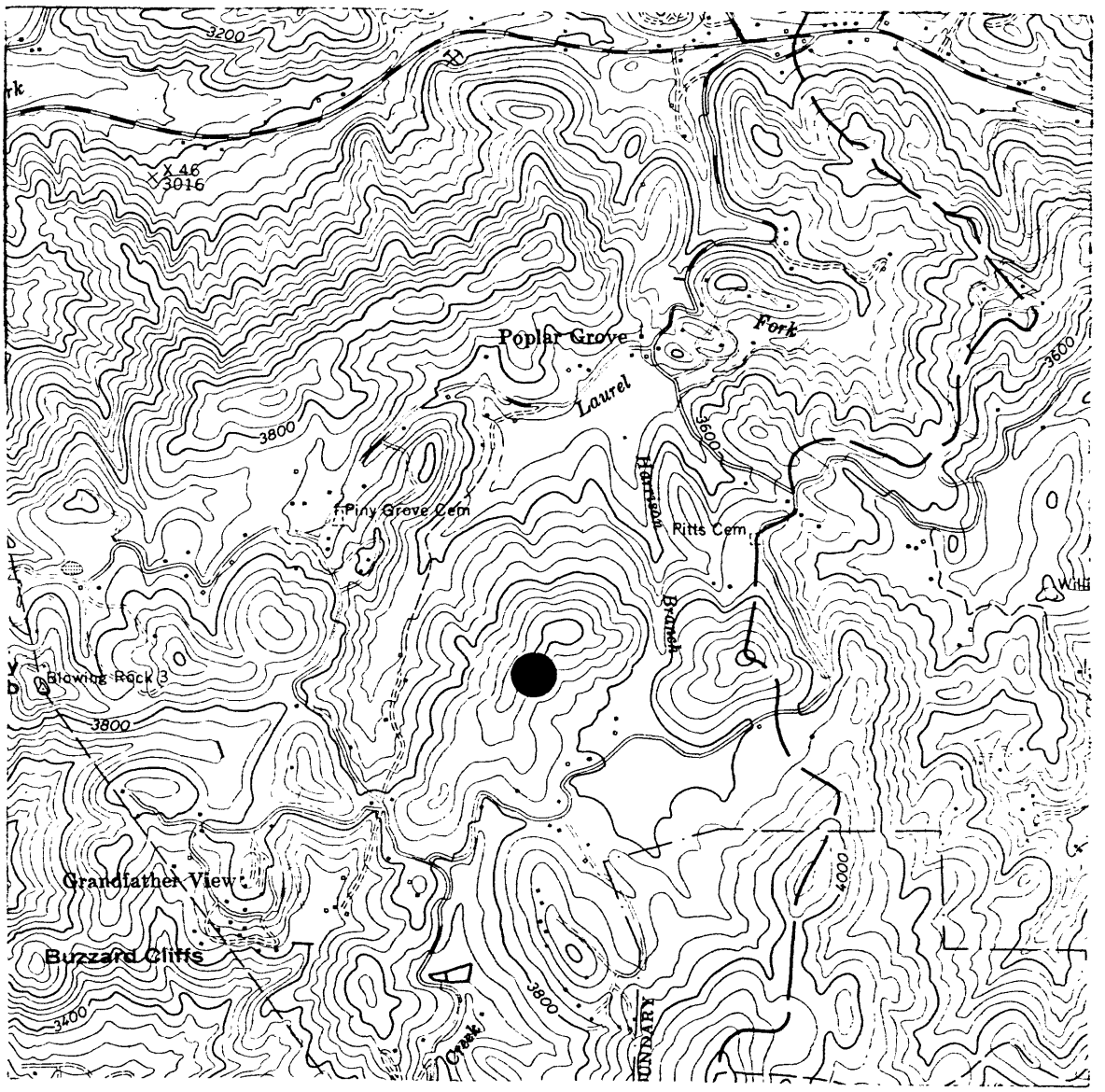

Station 5
Boone Quad.
North Carolina
7.5 minute series
Lat 36°11.252', Long 81°42.824'

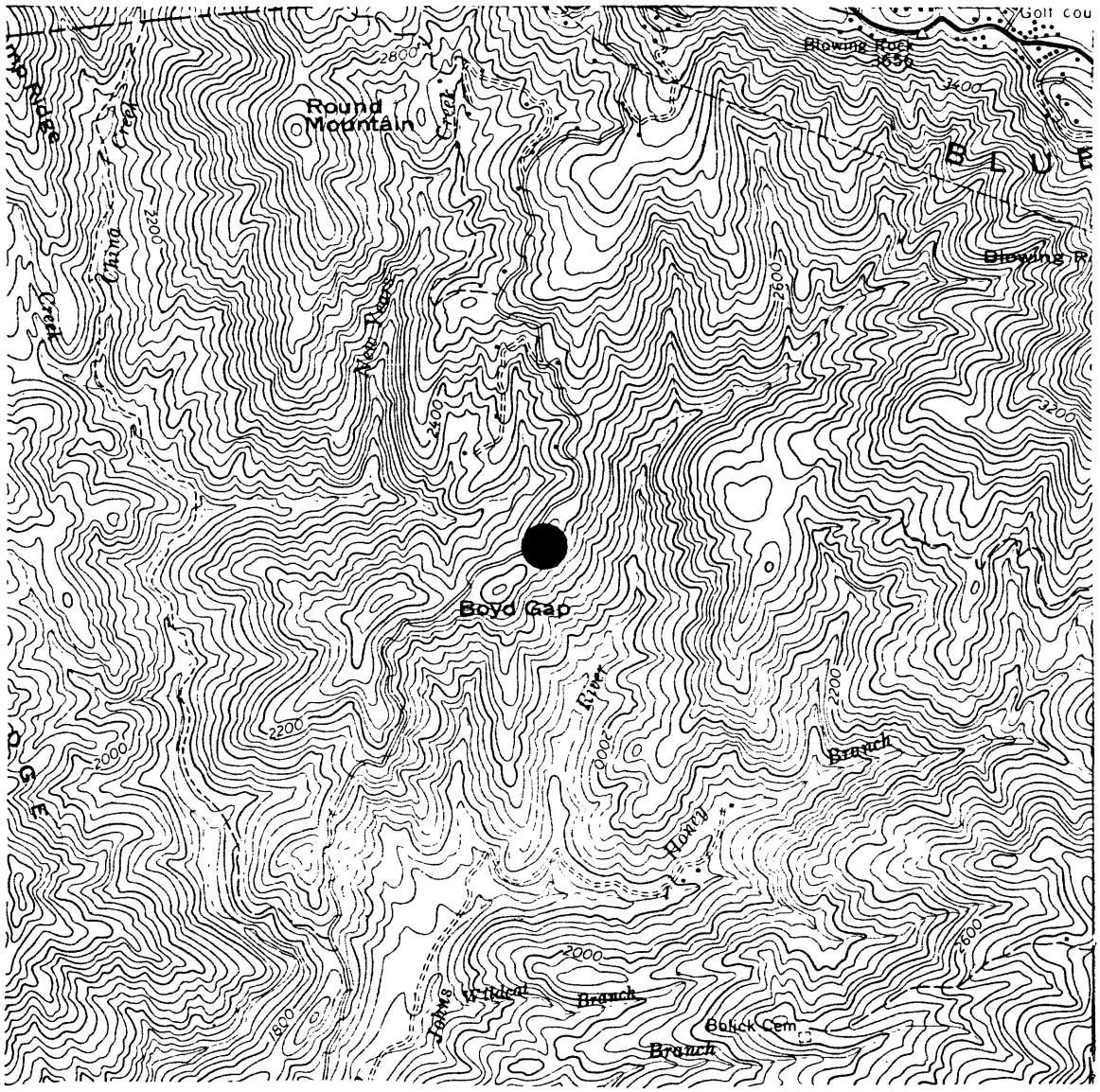

Station 6
Globe Quad.
North Carolina
7.5 minute series
Lat 36°6.295', Long 81°40.997'

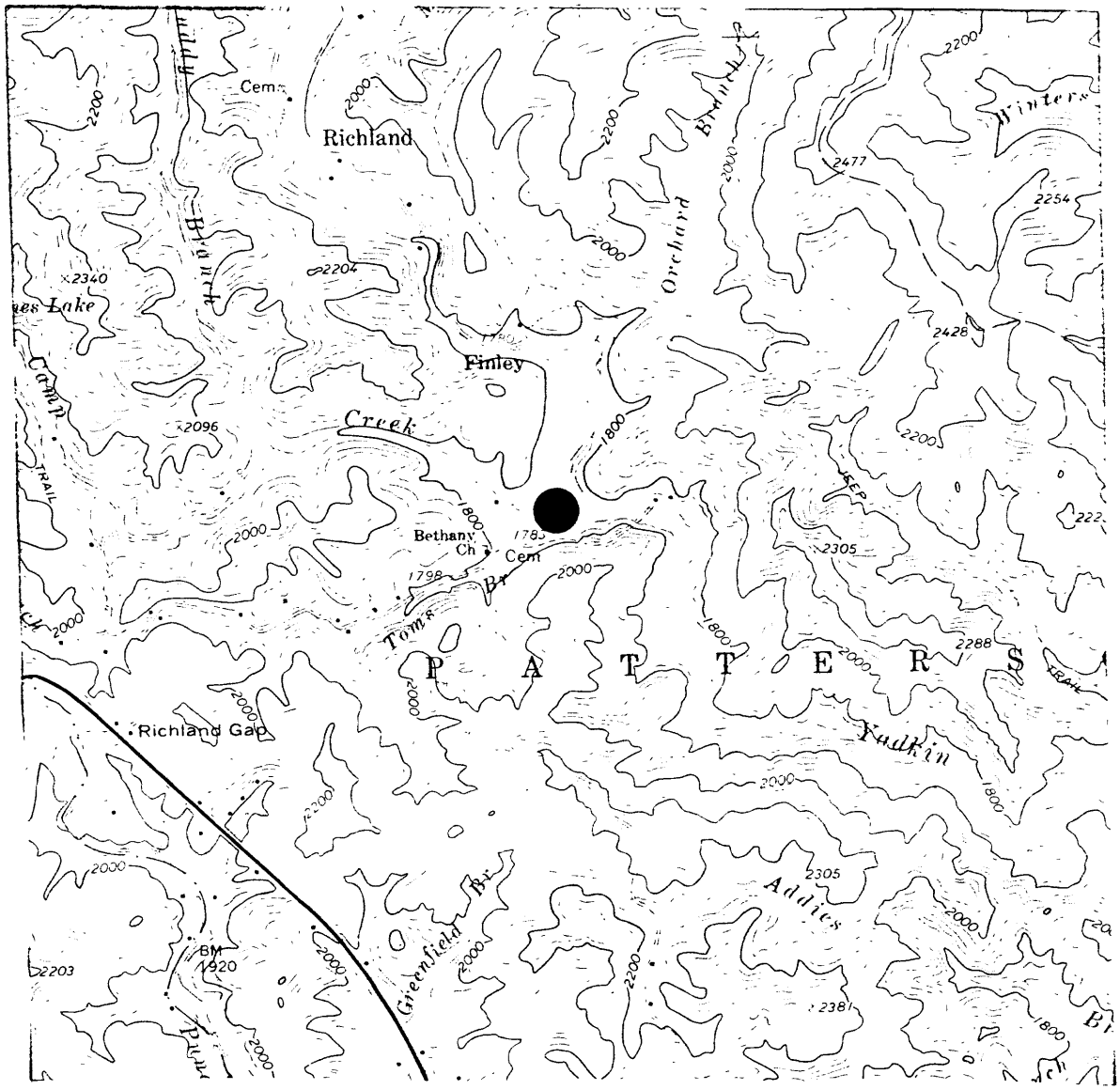

Station 7
Buffalo Cove Quad.
North Carolina
7.5 minute series
Lat 36°4.137', Long 81°35.410'

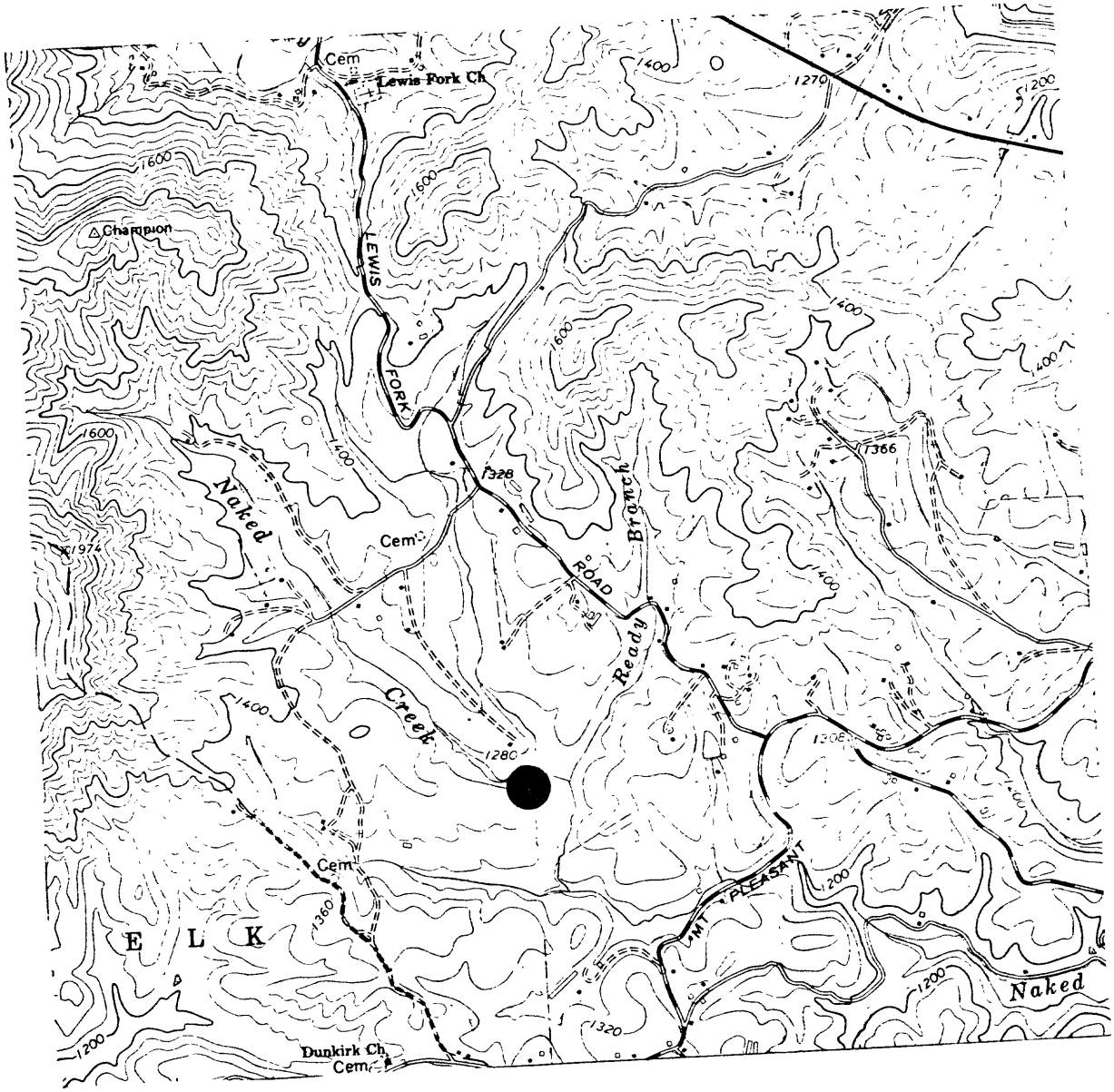

Station 8
Purlear Quad.
North Carolina
7.5 minute series
Lat 36°8.008', Long 81°21.396'

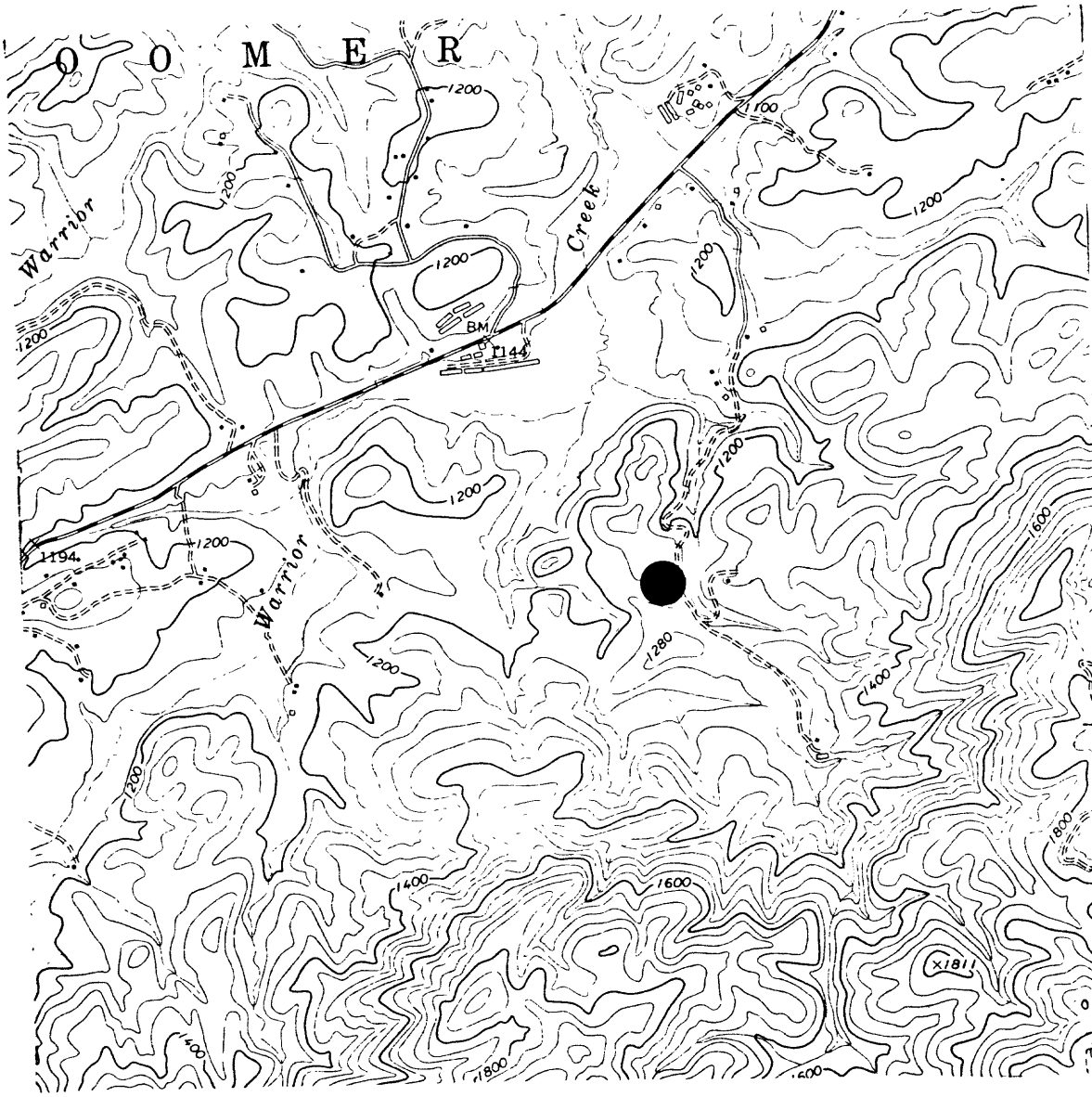

Station 9
Boomer Quad.
North Carolina
7.5 minute series
Lat 36°2.782', Long 81°15.969'

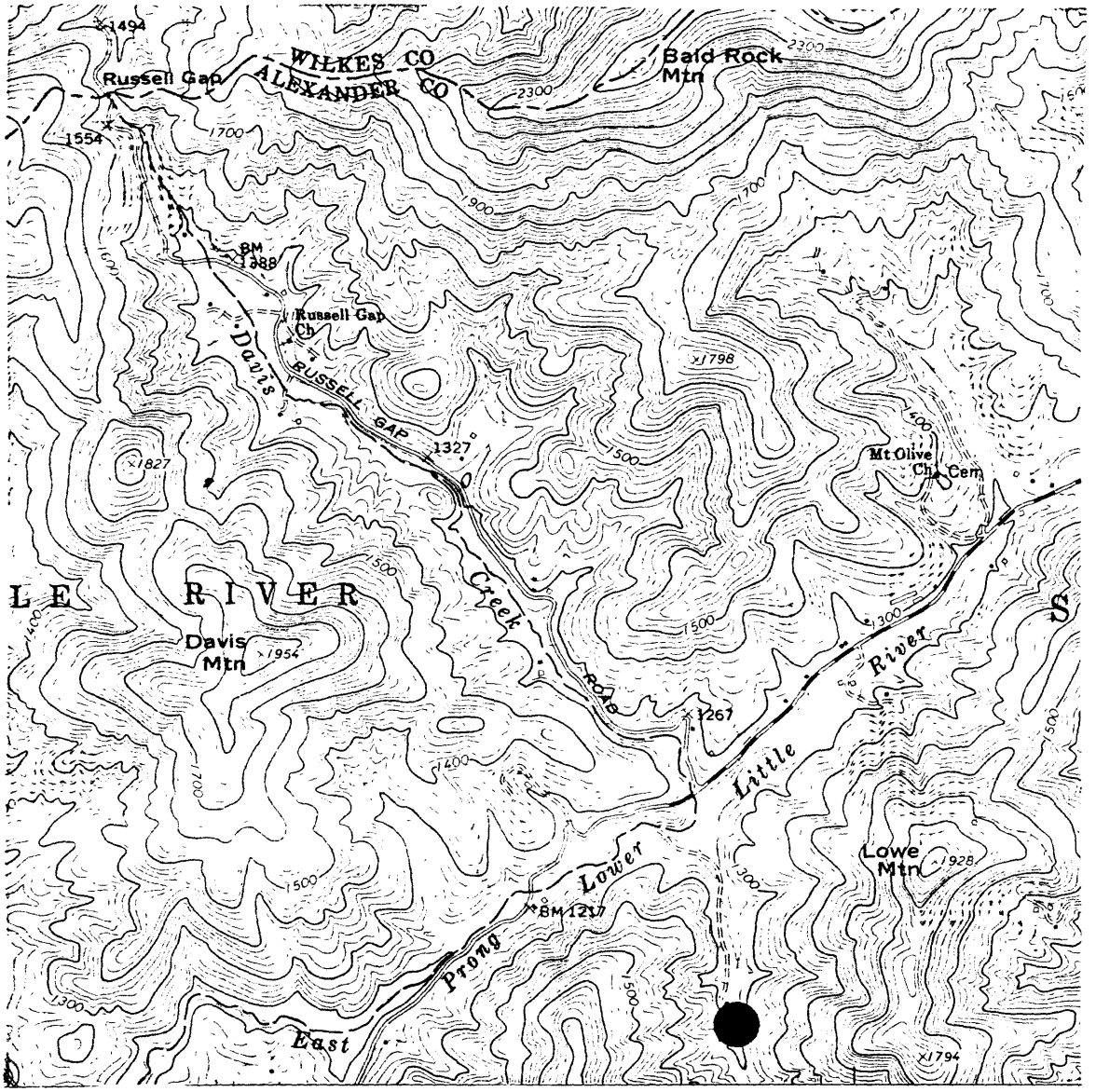

Station 10
Moravian Falls Quad.
North Carolina
7.5 minute series
Lat 36°0.120', Long 81°12.767'

APPENDIX B1

COMPUTER PLOTS OF DATA

Tensor Apparent Resistivity

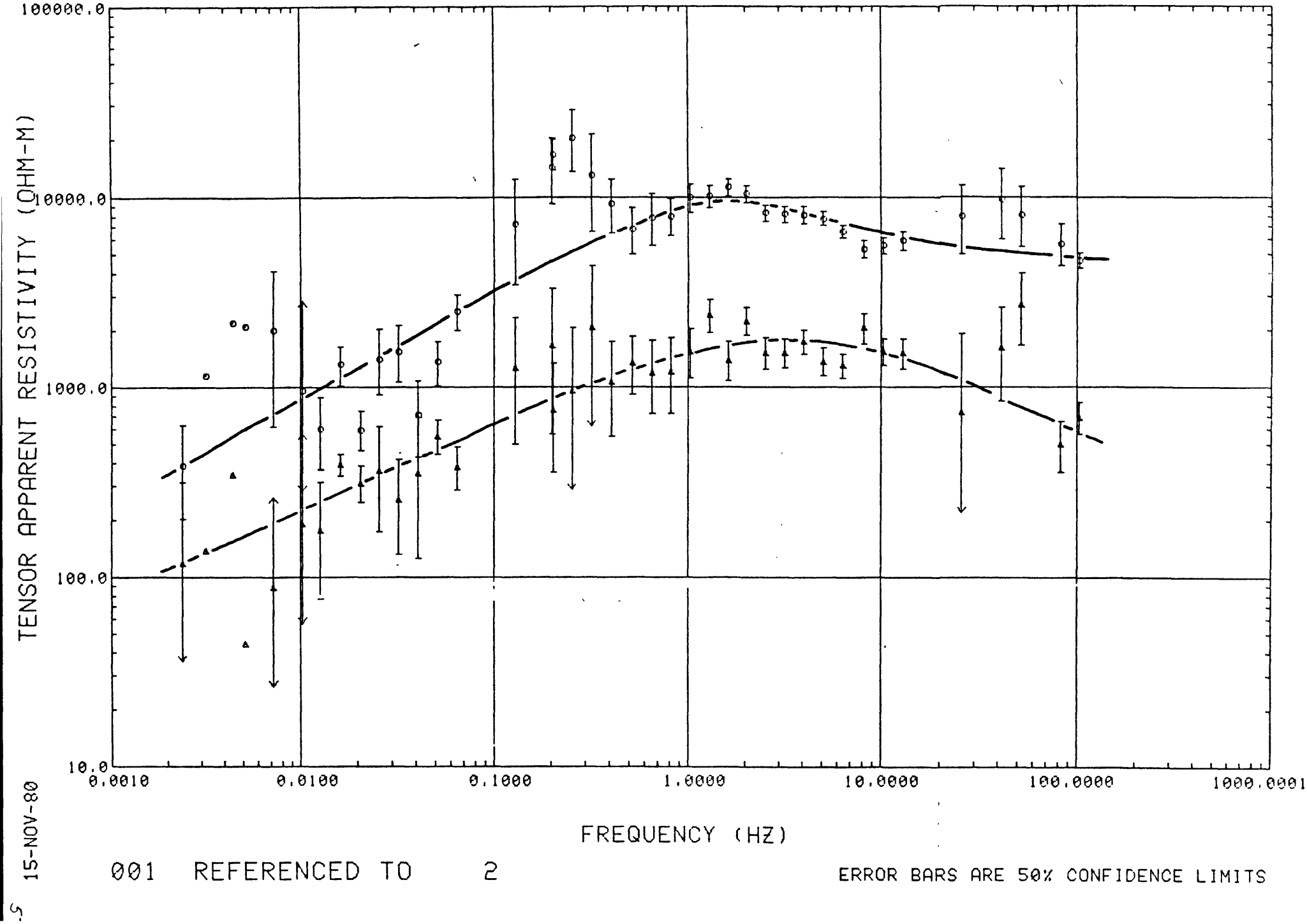
100000.0
10000.0
1000.0
100.0
10.0
TENSOR APPARENT RESISTIVITY (OHM-M)
0.0010
0.0100
0.1000
1.0000
10.0000
100.0000
1000.0001
FREQUENCY (HZ)
15-NOV-80
001 REFERENCED TO 2
ERROR BARS ARE 50% CONFIDENCE LIMITS

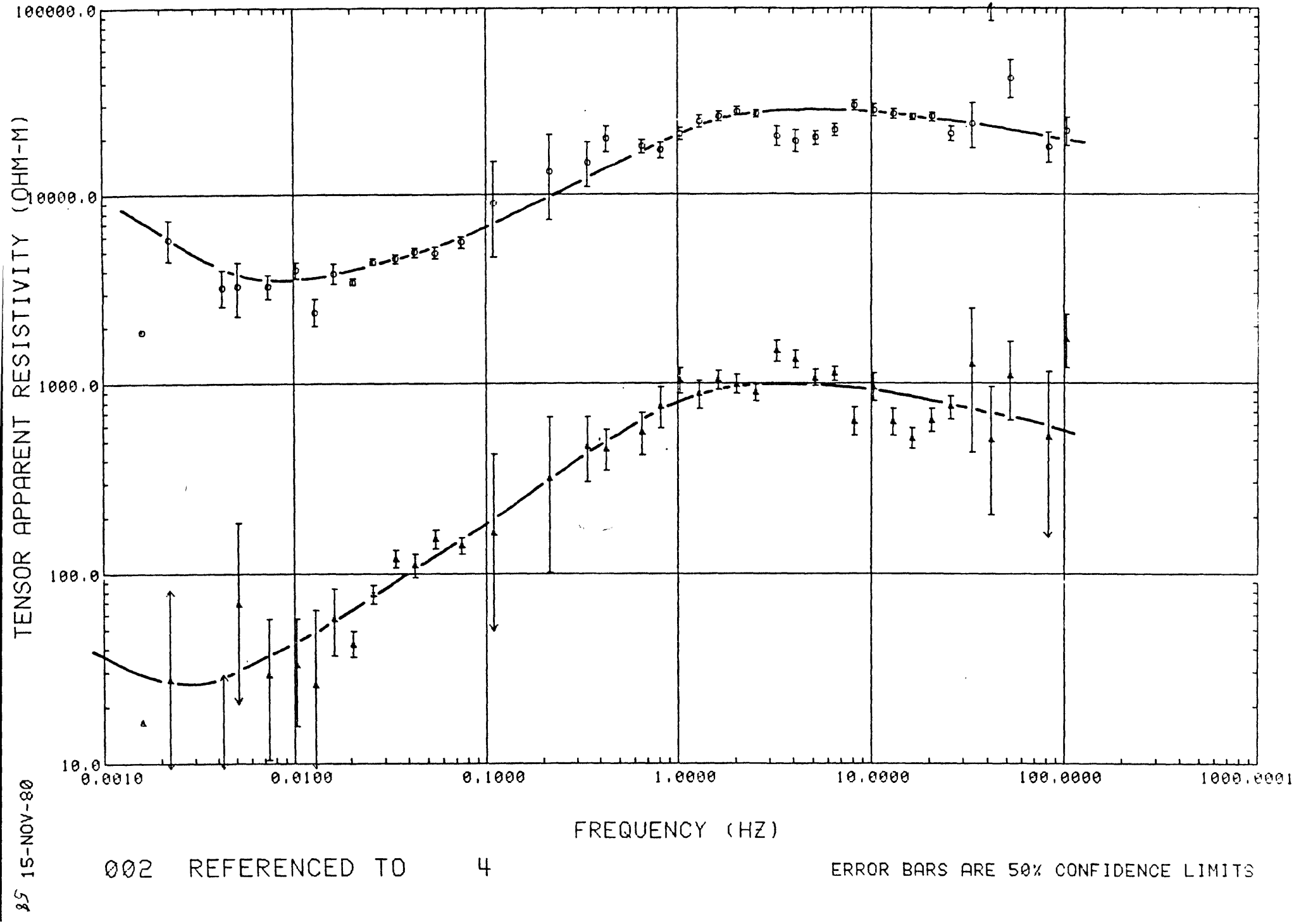
100000.0
10000.0
1000.0
100.0
10.0
TENSOR APPARENT RESISTIVITY (OHM-M)
0.0010
0.0100
0.1000
1.0000
10.0000
100.0000
1000.0001
FREQUENCY (HZ)
002 REFERENCED TO 4
ERROR BARS ARE 50% CONFIDENCE LIMITS
15-NOV-80

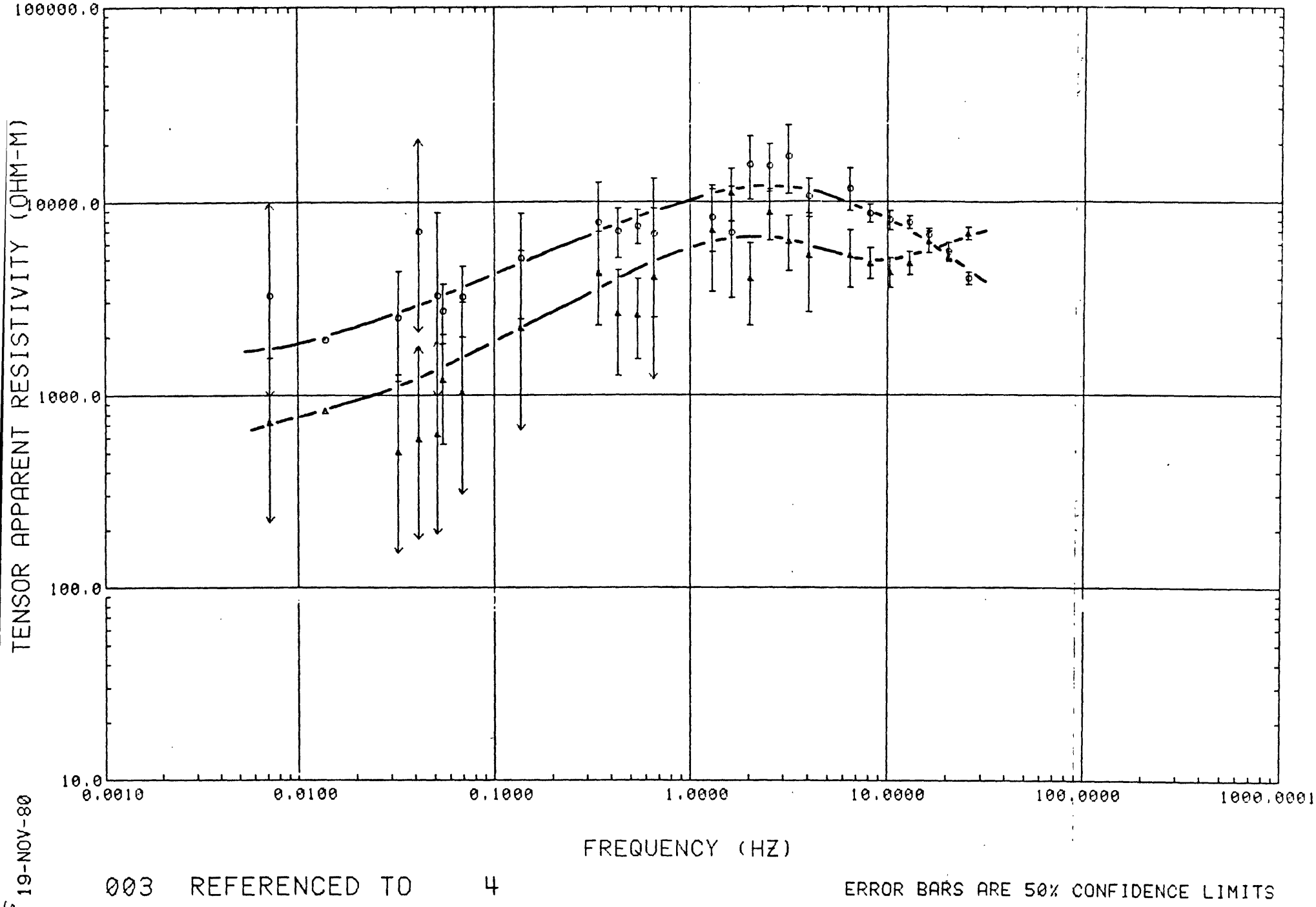
100000.0
10000.0
1000.0
100.0
10.0
TENSOR APPARENT RESISTIVITY (OHM-M)
0.0010
0.0100
0.1000
1.0000
10.0000
100.0000
1000.0001
FREQUENCY (HZ)
19-NOV-80
003 REFERENCED TO 4
ERROR BARS ARE 50% CONFIDENCE LIMITS

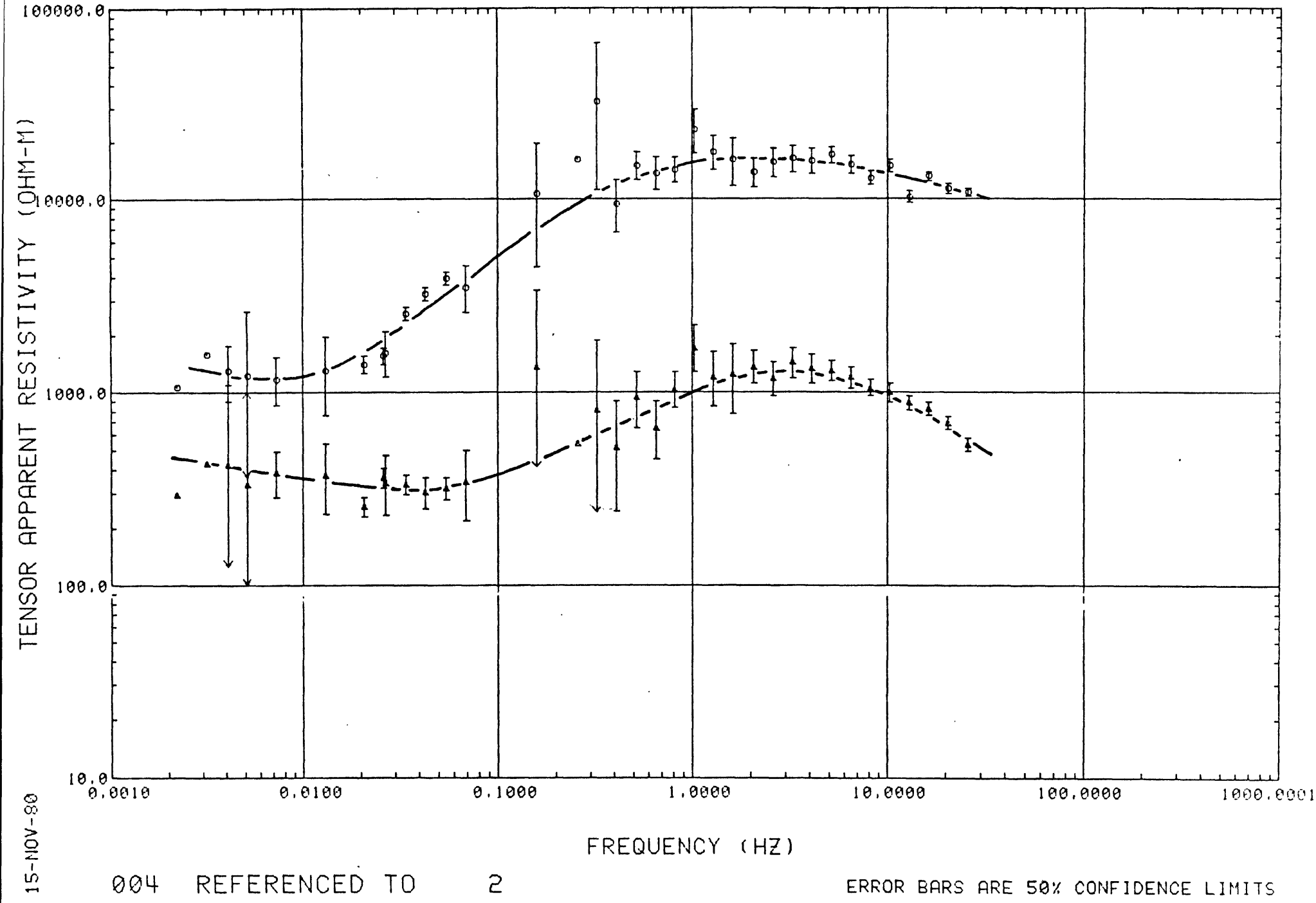

15-NOV-90

004 REFERENCED TO 2

ERROR BARS ARE 50% CONFIDENCE LIMITS

09

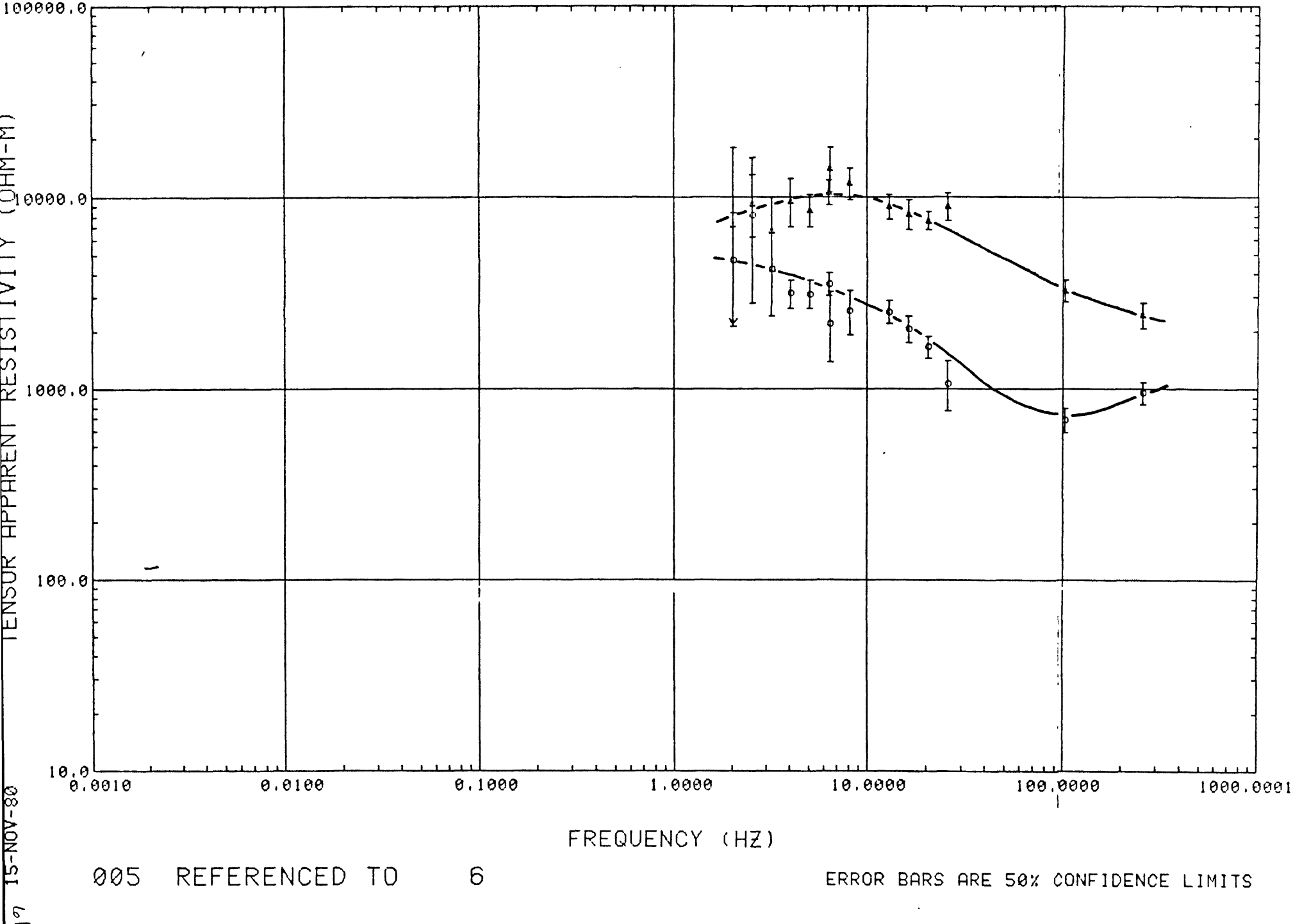

005 REFERENCED TO 6

ERROR BARS ARE 50% CONFIDENCE LIMITS

15-NOV-80

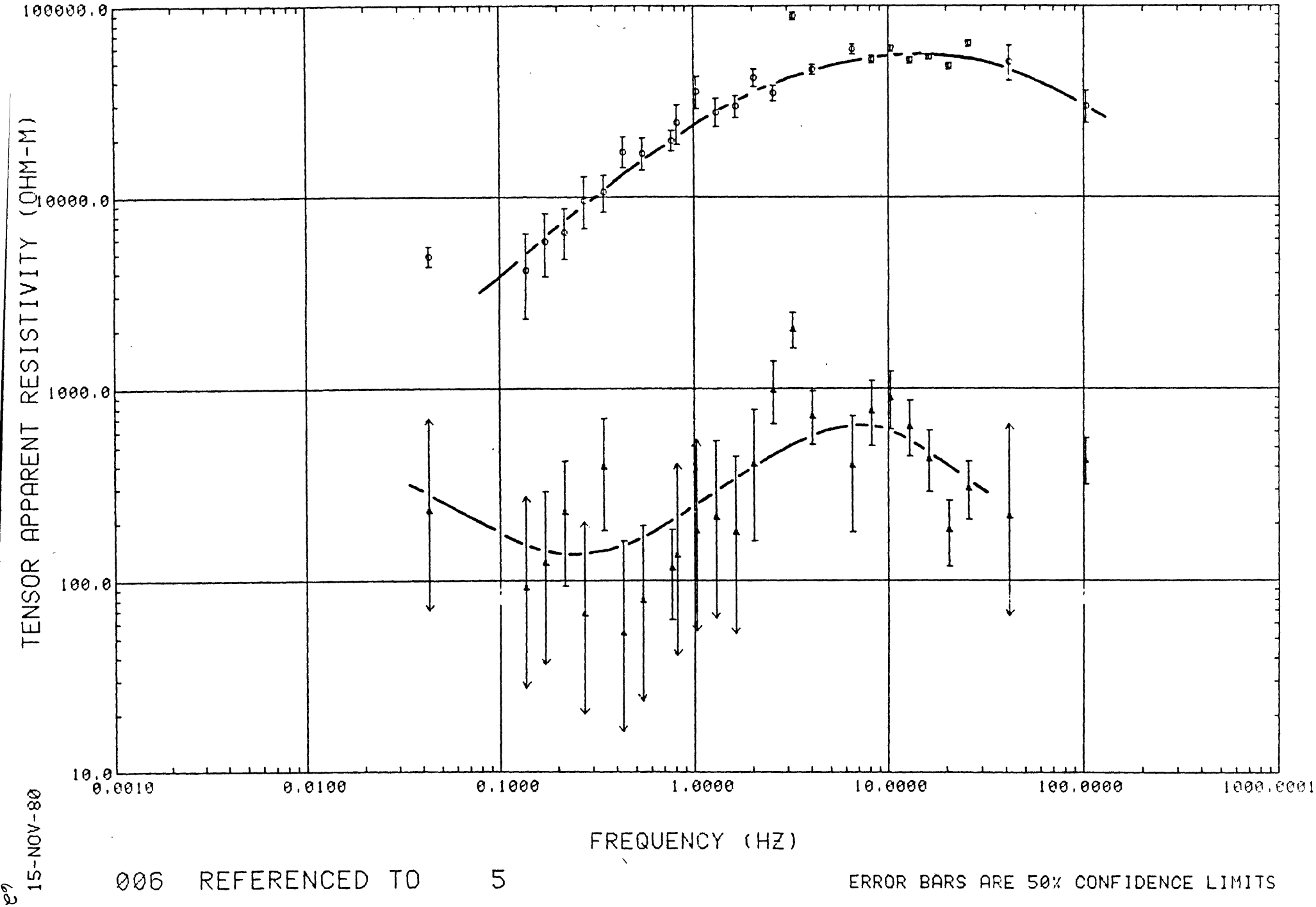
100000.0
10000.0
1000.0
100.0
10.0
TENSOR APPARENT RESISTIVITY (OHM-M)
0.0010
0.0100
0.1000
1.0000
10.0000
100.0000
1000.0001
FREQUENCY (HZ)
15-NOV-80
006 REFERENCED TO 5
ERROR BARS ARE 50% CONFIDENCE LIMITS

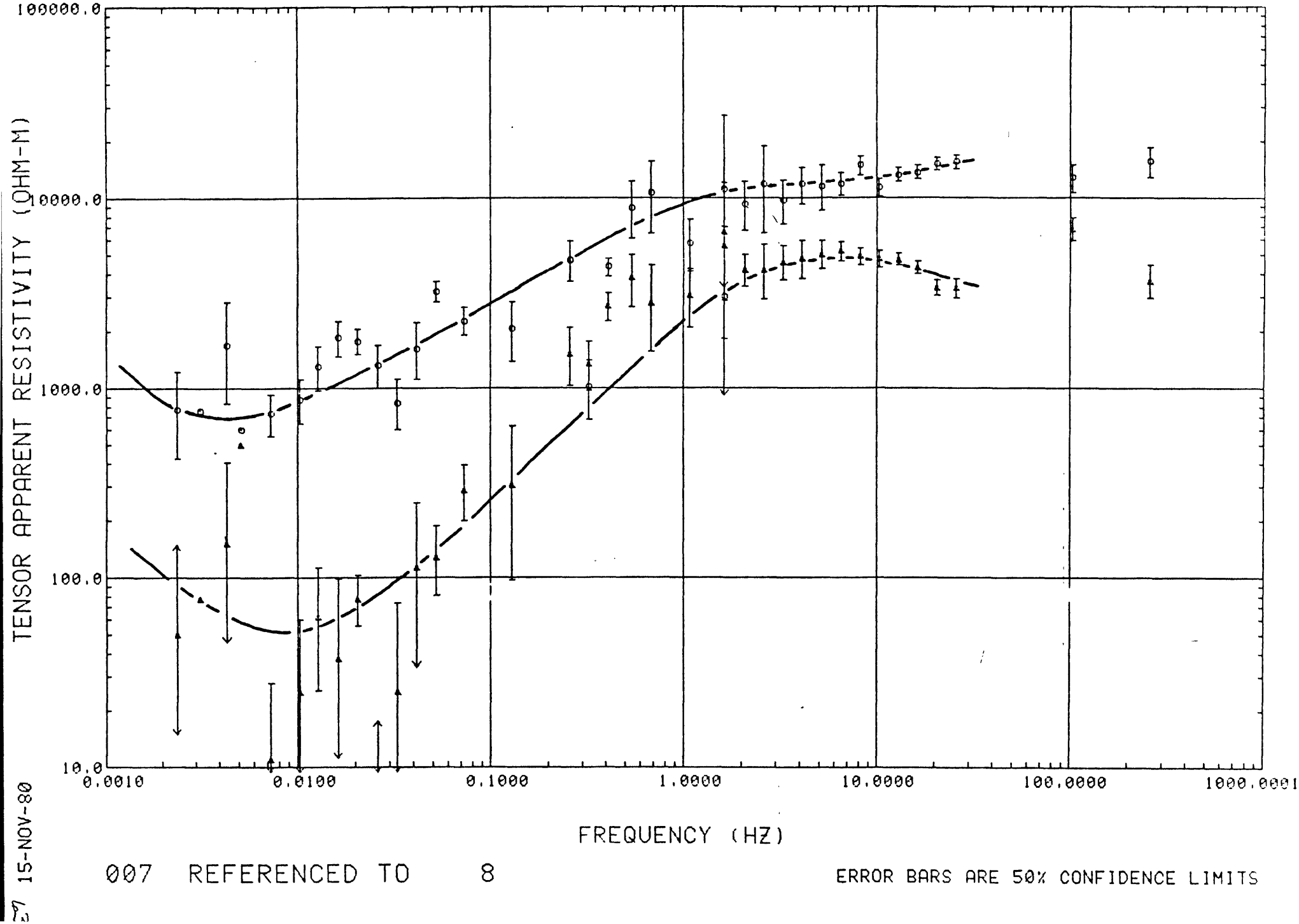
100000.0
10000.0
1000.0
100.0
10.0
TENSOR APPARENT RESISTIVITY (OHM-M)
0.0010
0.0100
0.1000
1.0000
10.0000
100.0000
1000.0001
FREQUENCY (HZ)
007 REFERENCED TO 8
ERROR BARS ARE 50% CONFIDENCE LIMITS
15-NOV-80

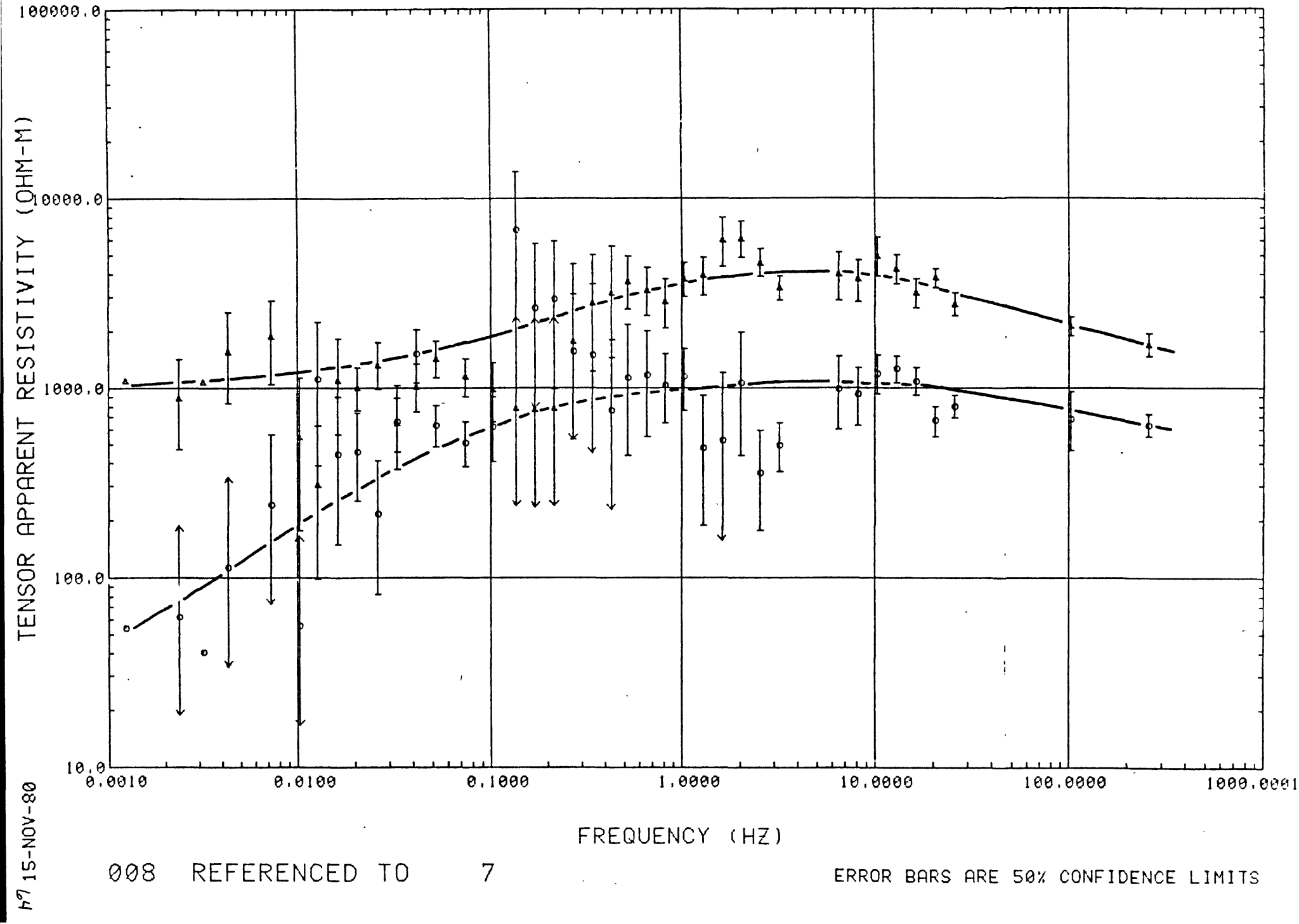

h7 15-NOV-80

008 REFERENCED TO 7

ERROR BARS ARE 50% CONFIDENCE LIMITS

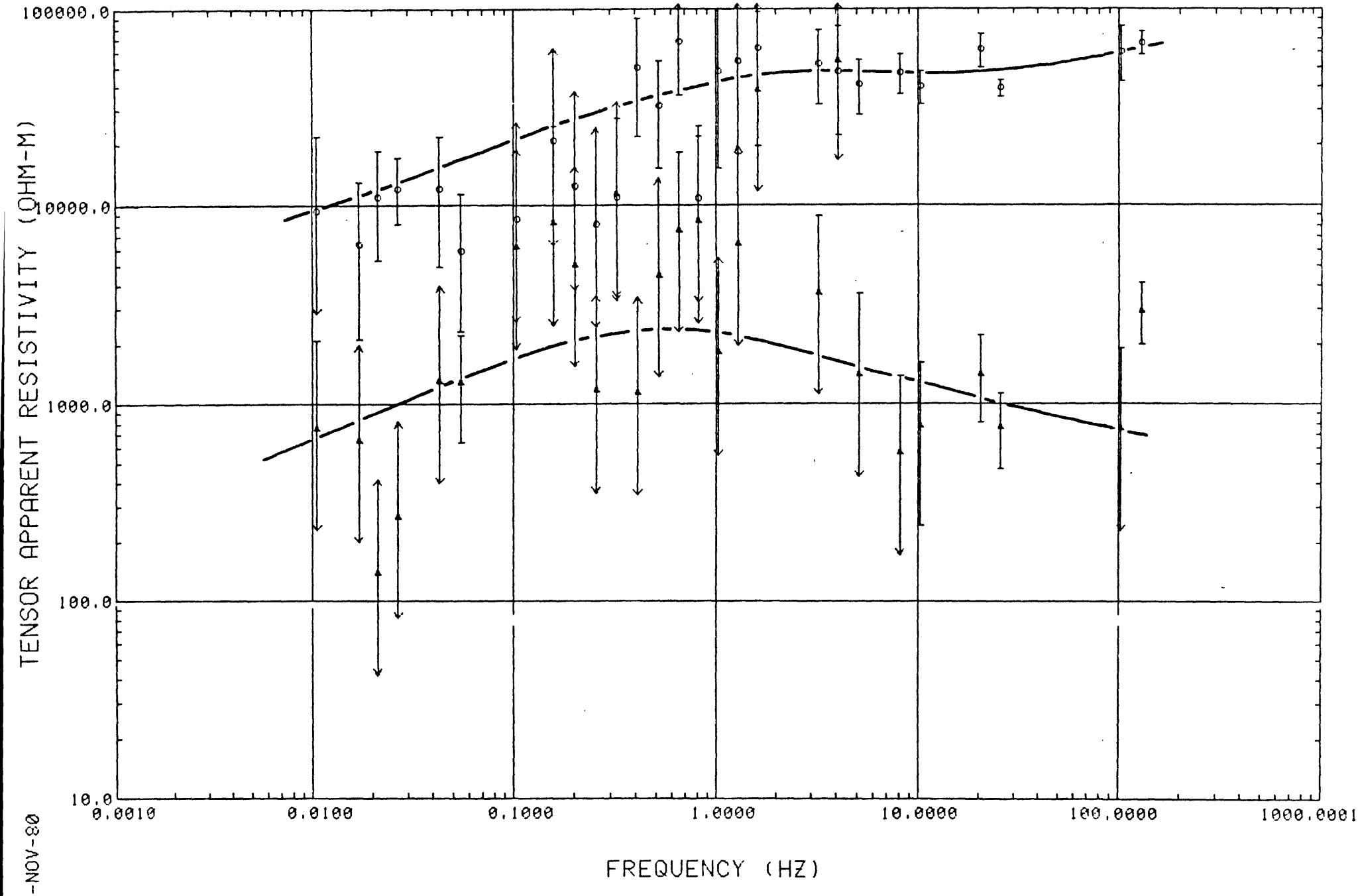

15-NOV-80

009 REFERENCED TO 10

ERROR BARS ARE 50% CONFIDENCE LIMITS

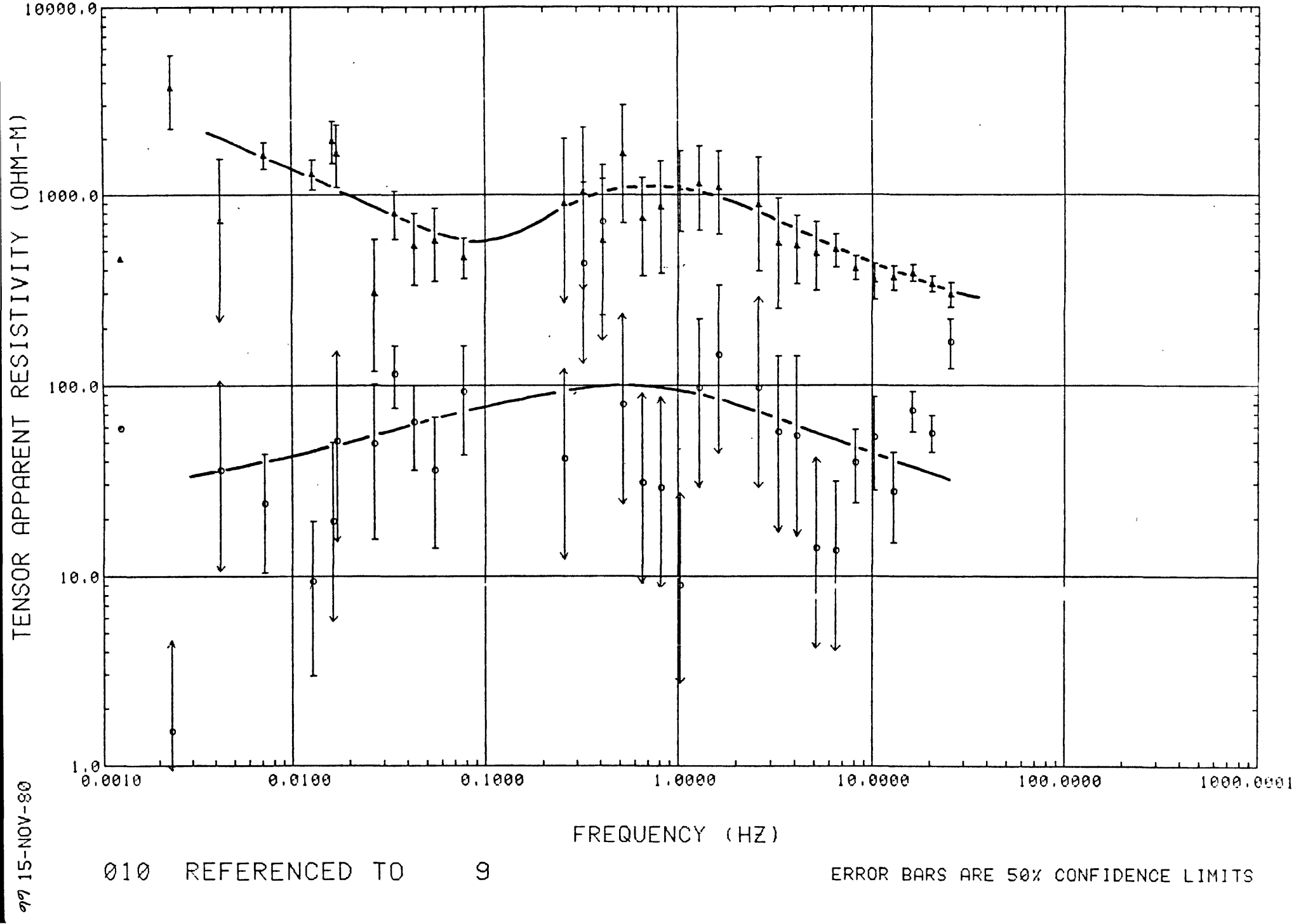

010 REFERENCED TO 9

ERROR BARS ARE 50% CONFIDENCE LIMITS

99 15-NOV-80

APPENDIX B2

COMPUTER PLOTS OF DATA

Tensor Phase, Multiple Coherencies, Rotation,

Tipper "Strike", Tipper, Skewness

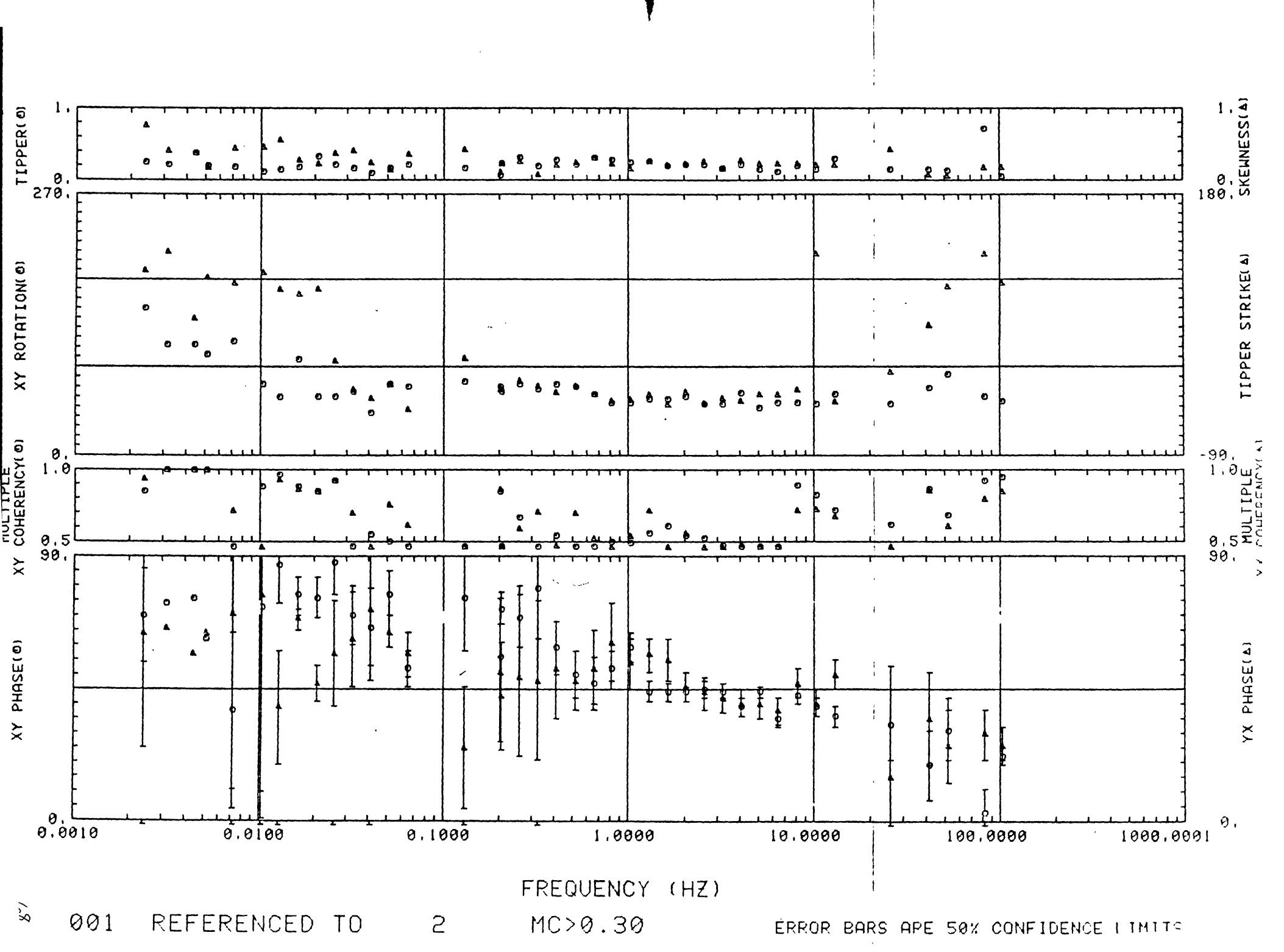

001 REFERENCED TO 2 MC>0.30 ERROR BARS ARE 50% CONFIDENCE LIMITS

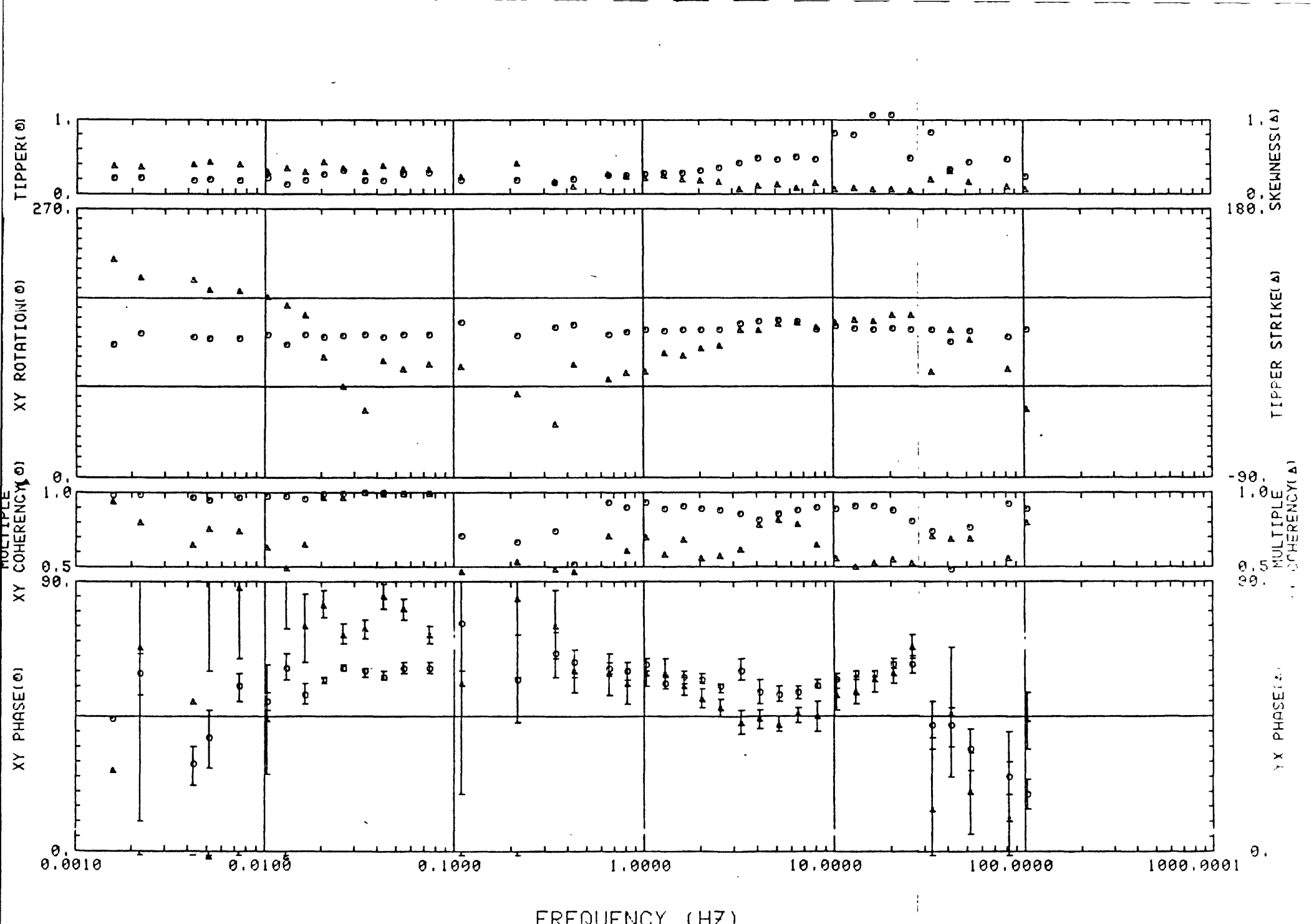

002 REFERENCED TO 4 MC>0.20 ERROR BARS ARE 50% CONFIDENCE LIMITS

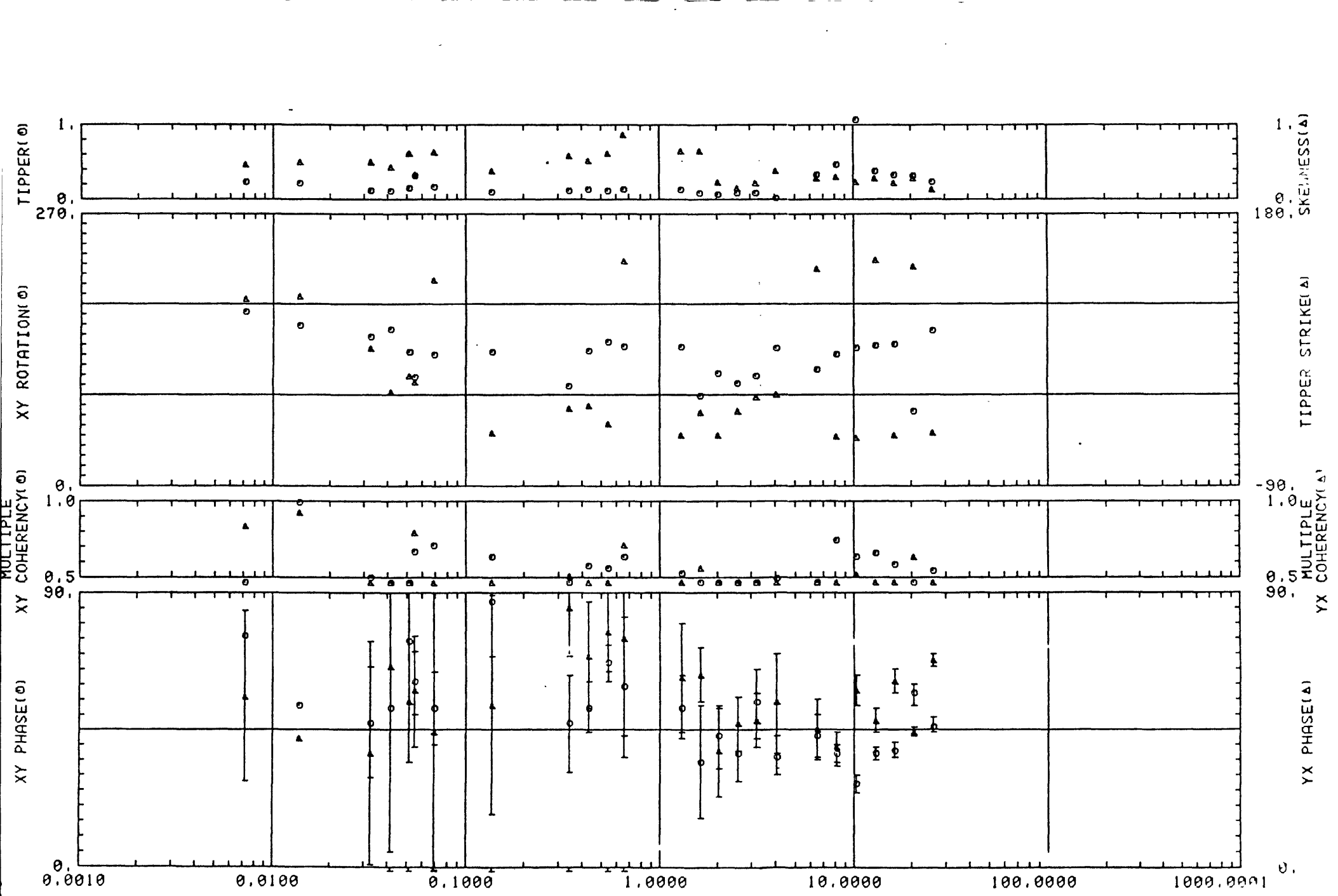

003 REFERENCED TO 4 MC>0.10 ERROR BARS ARE 50% CONFIDENCE LIMITS

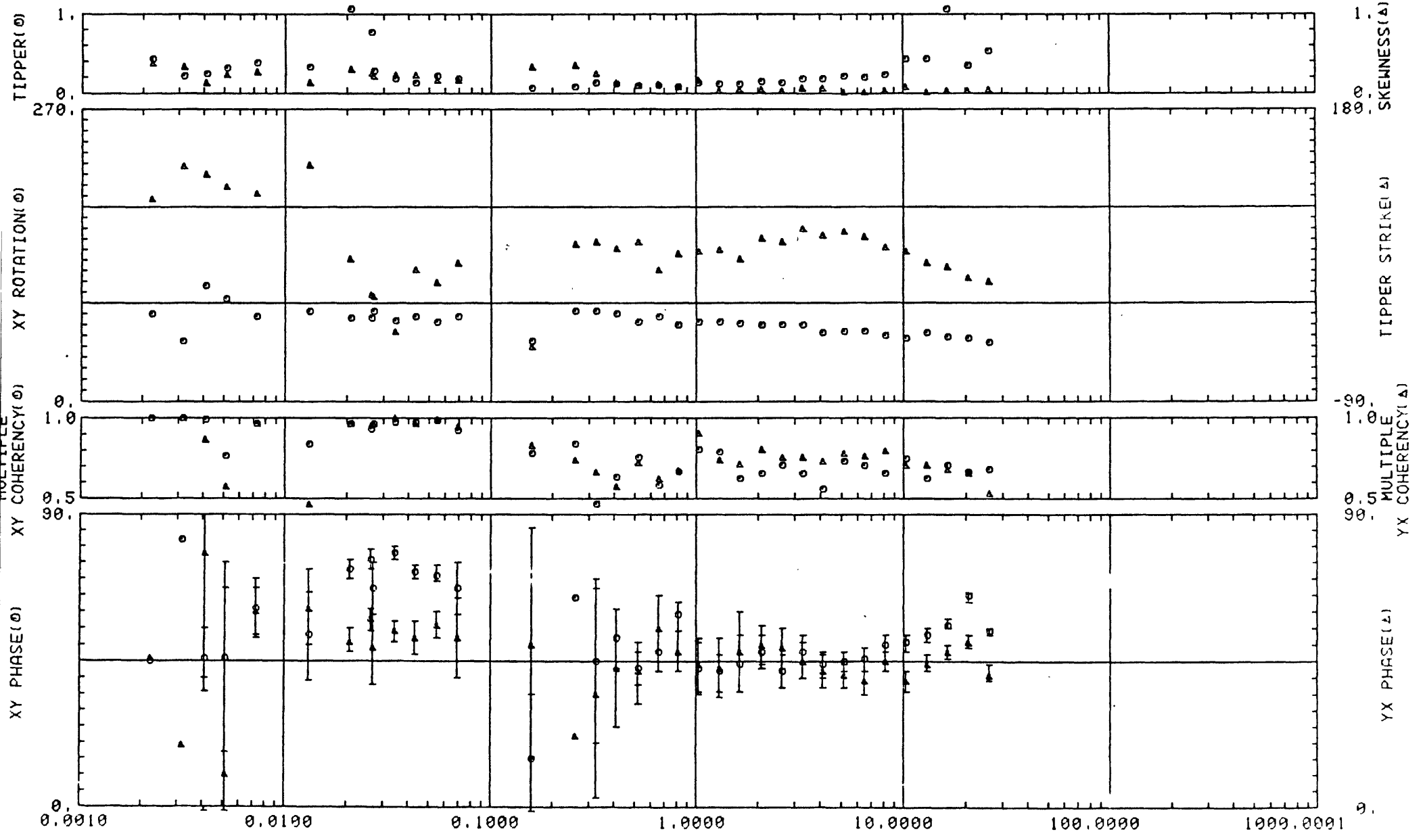

004 REFERENCED TO 2 MC>0.20 ERROR BARS ARE 50% CONFIDENCE LIMITS

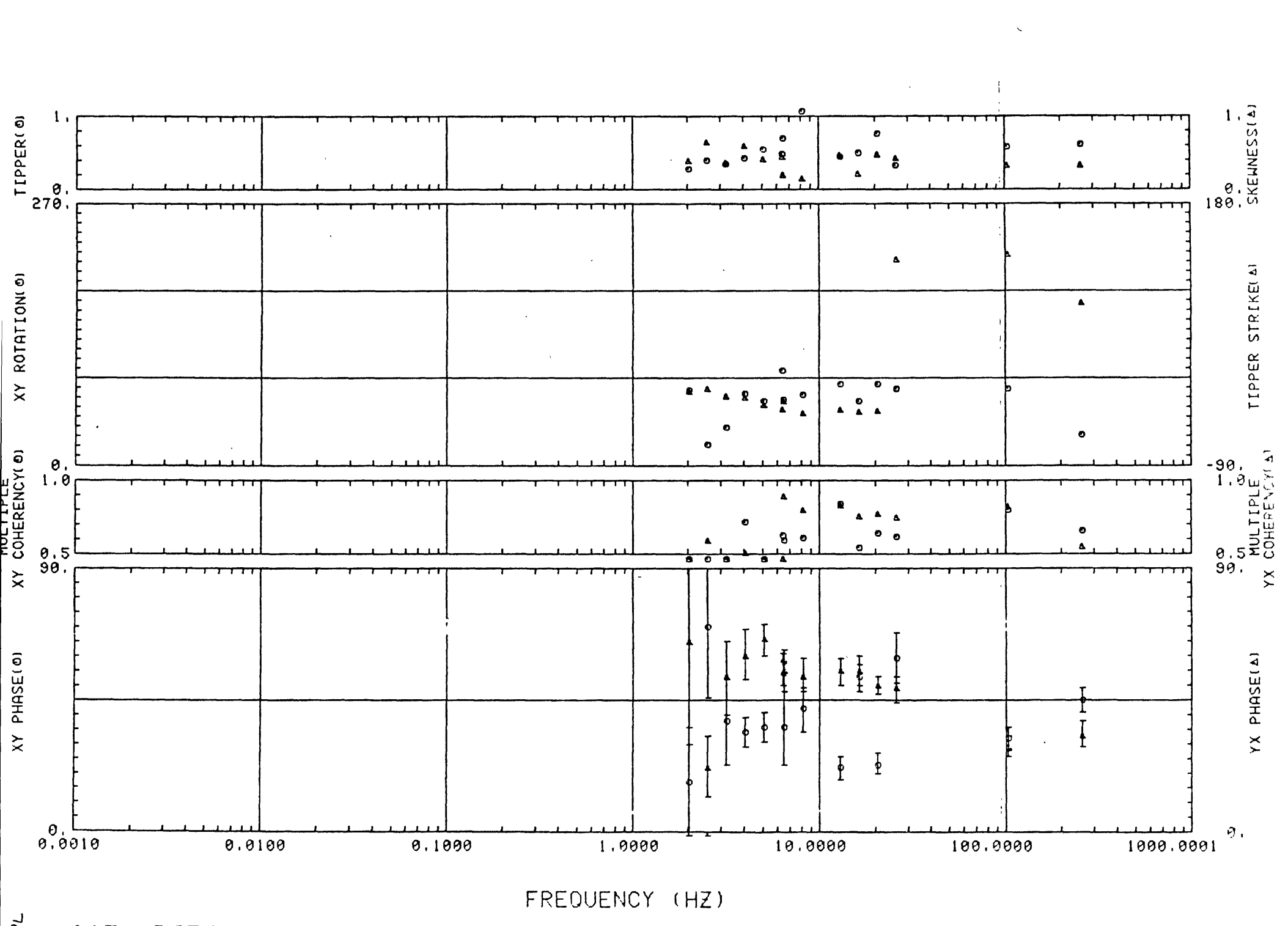

005 REFERENCED TO 6 MC>0.10 ERROR BARS ARE 50% CONFIDENCE LIMITS

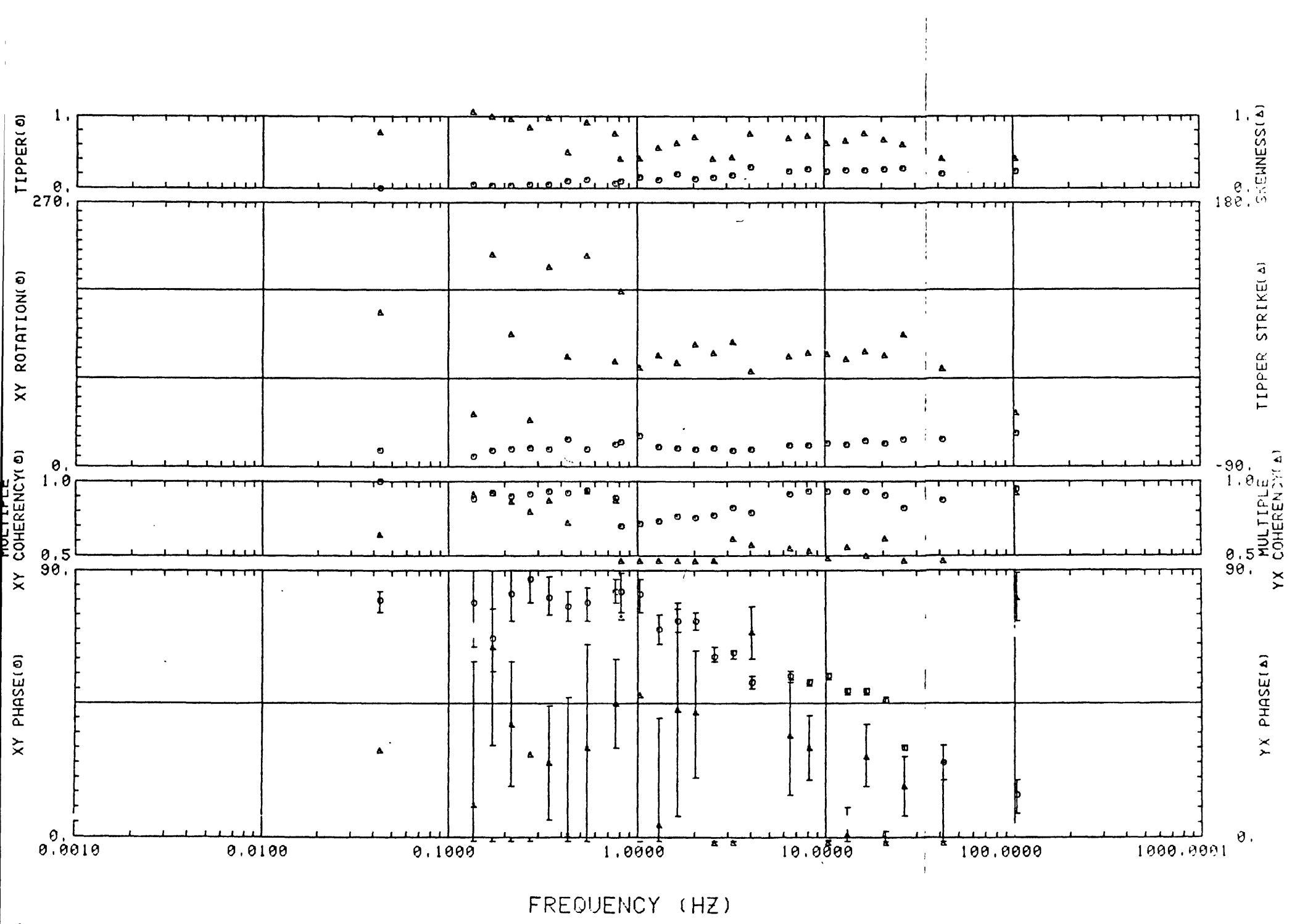

006 REFERENCED TO 5 MC>0.10 ERROR BARS ARE 50% CONFIDENCE LIMITS

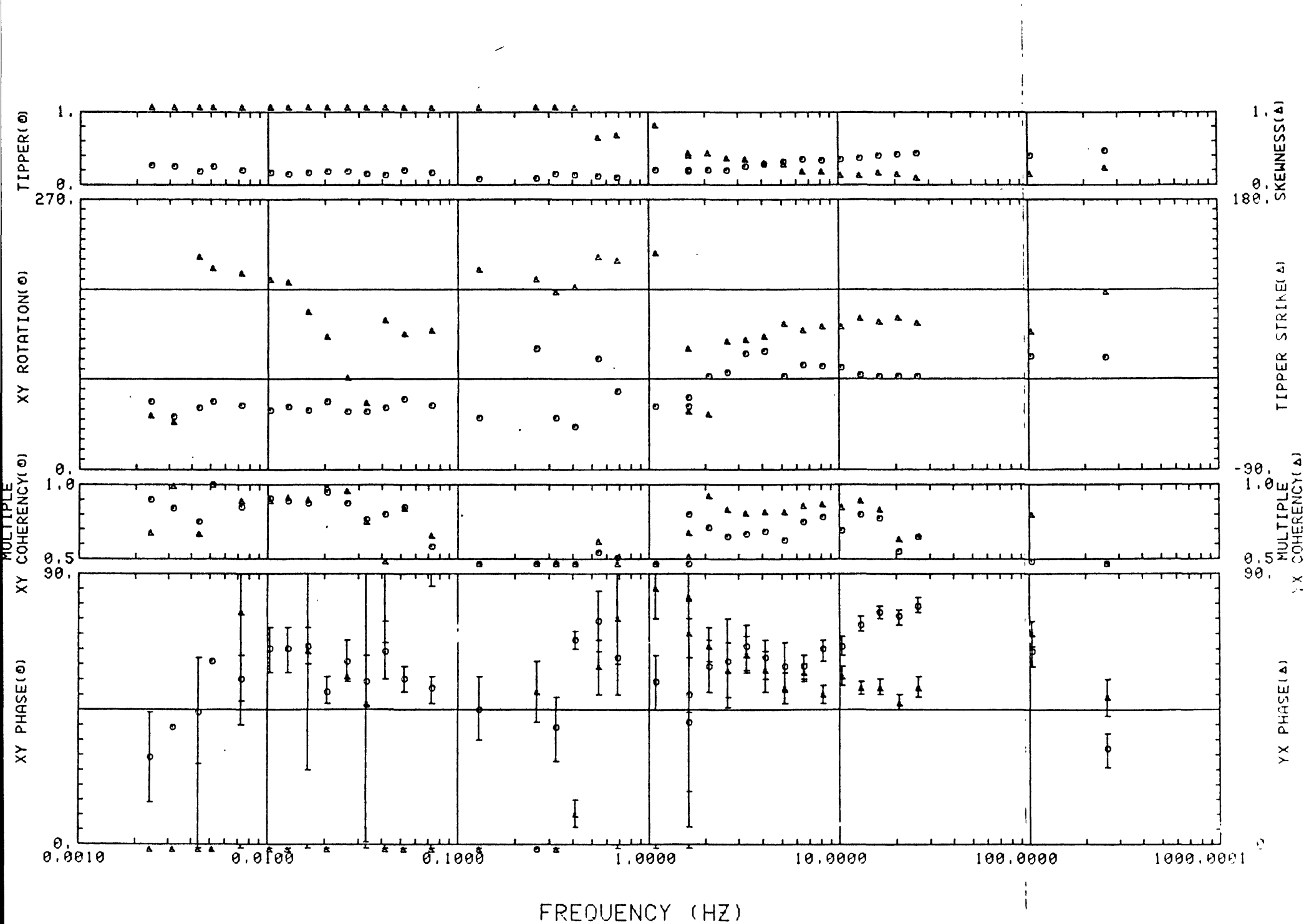

HL 007 REFERENCED TO 8 MC>0.20 ERROR BARS ARE 50% CONFIDENCE LIMITS

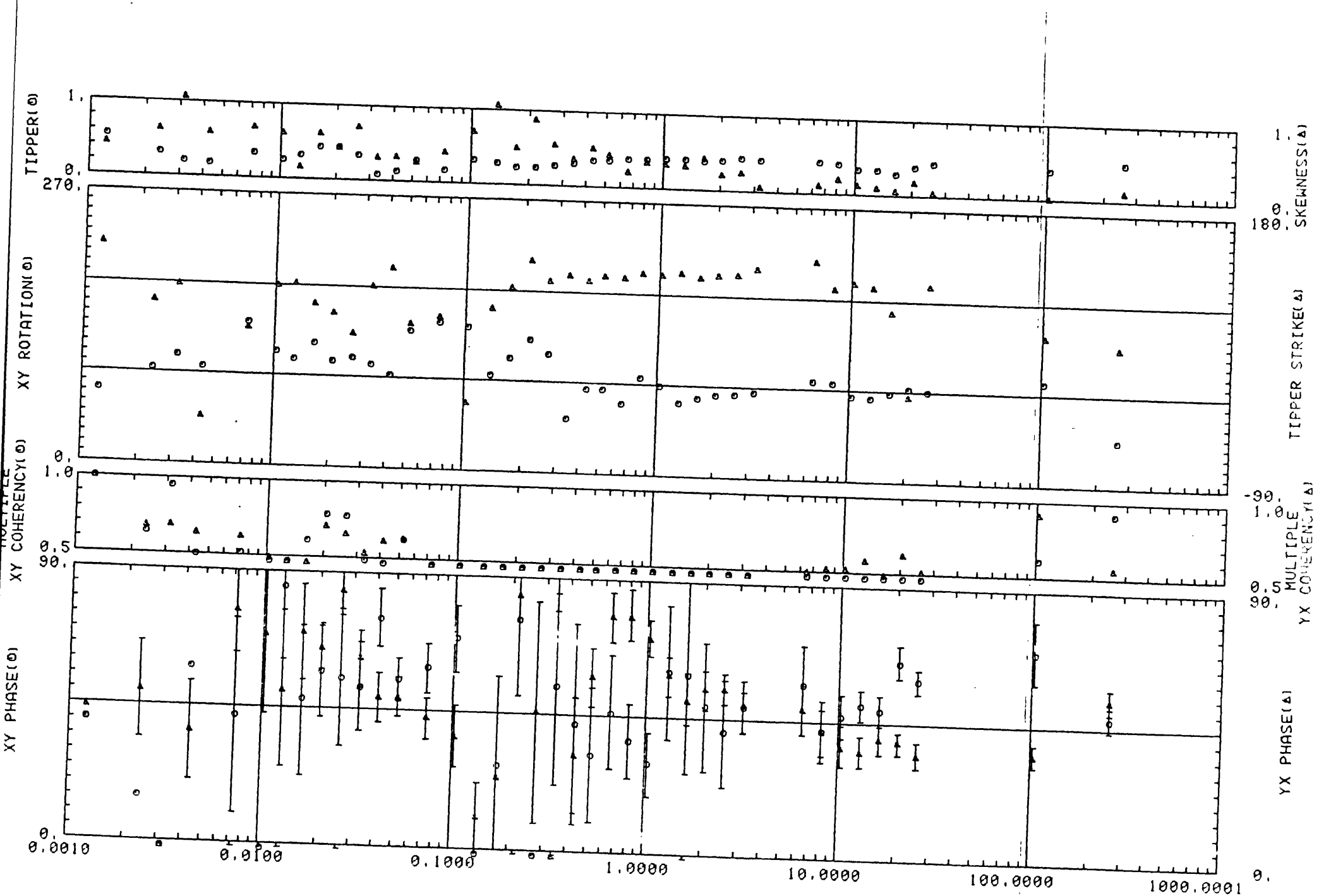

008 REFERENCED TO 7

MC>0.10

ERROR BARS ARE 50% CONFIDENCE LIMITS

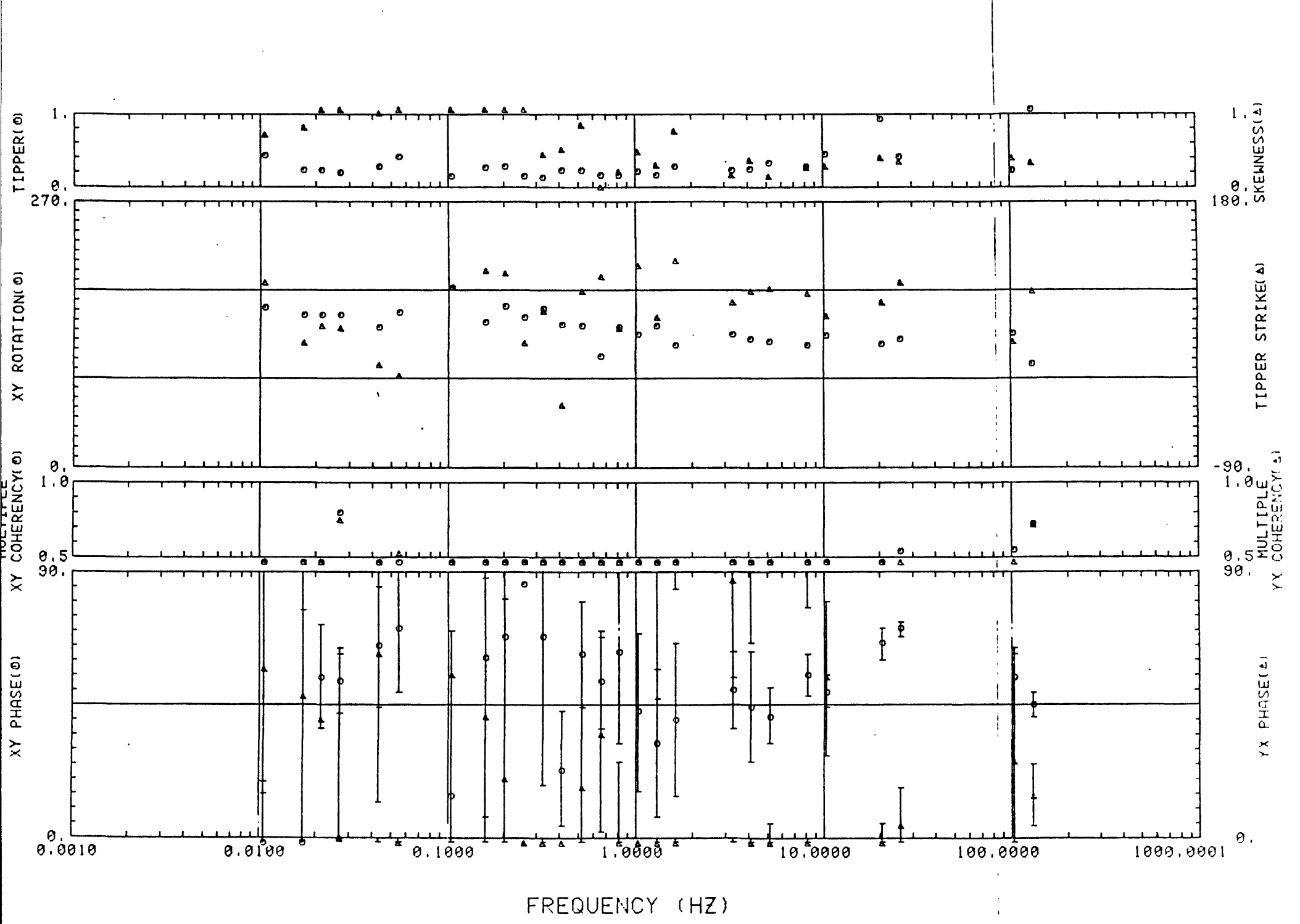

009 REFERENCED TO 10 MC>0.10 ERROR BARS ARE 50% CONFIDENCE LIMITS

APPENDIX C

COMPUTER LISTINGS OF DATA

The calculated results are printed out for the power spectra averaged data sets. These include:

FREQ = frequency (hertz)

RHOXY = xy rotated apparent resistivity (ohm-m)

RHOYX = yx rotated apparent resistivity (ohm-m)

PHASEXY = xy rotated phase angle (degrees)

PHASEYX = yx rotated phase angle (degrees)

ROT ANG = rotation angle (degrees)

SKEWNESS = skewness

TIPPER = tipper magnitude

TIP STRIK = tipper strike as defined by Vozoff (Geophysics, 1976, p. 327)

TIP PHASE = tipper phase

COHXY = xy multiple coherency

COHYX = yx multiple coherency

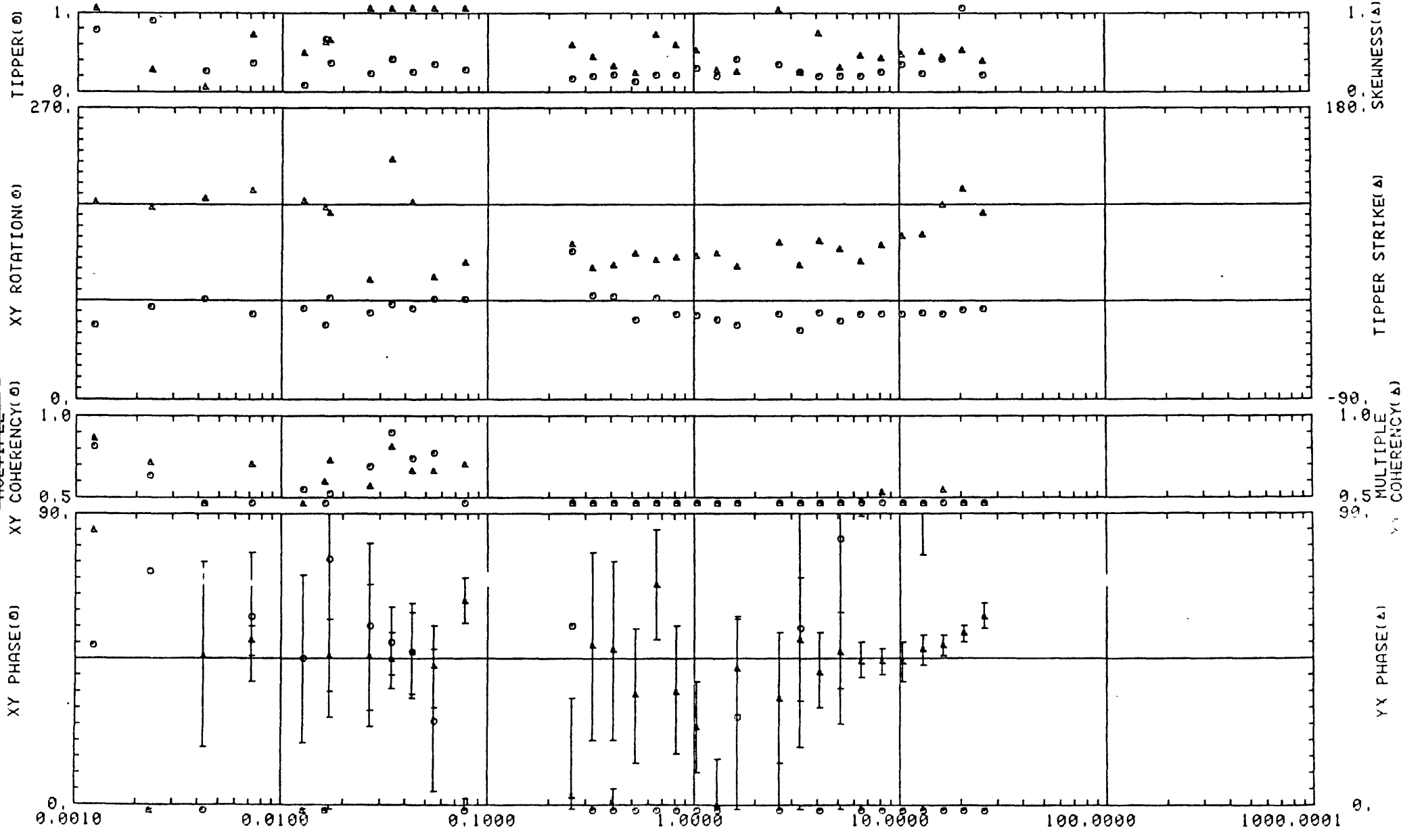

77 010 REFERENCED TO 9 MC>0.10 ERROR BARS ARE 50% CONFIDENCE LIMITS

MAGNETOTELLURIC STATION 001 UNREFERENCED

FREQ	RHOXY	RHOYX	PHASEXY	PHASEYX	ROT ANG	SKEWNESS	TIPPER	TIP STRIK	TIP PHASE	COHXY	COHYX
25.878922	7902.46	731.45	33.	15.	53.	0.43	0.14	-5.	-65.	0.62	0.44
41.503918	9640.30	1611.61	19.	35.	69.	0.08	0.15	42.	34.	0.86	0.86
52.246094	8108.37	2709.35	31.	26.	83.	0.07	0.13	83.	14.	0.68	0.61
0.000000	4387.03	16227.08	47.	-70.	93.	0.66	1.84	81.	-42.	0.74	0.93
82.031235	5688.70	498.38	3.	30.	60.	0.19	0.72	118.	-57.	0.92	0.80
103.027351	4643.94	693.38	22.	26.	55.	0.18	0.06	86.	82.	0.95	0.85

MAGNETOTELLURIC STATION 001 REMOTE REFERENCED TO STATION 2

FREQ	RHOXY	RHOYX	PHASEXY	PHASEYX	ROT ANG	SKEWNESS	TIPPER	TIP STRIK	TIP PHASE	COHXY	COHYX
0.002378	388.35	119.04	70.	64.	150.	0.76	0.25	100.	-15.	0.85	0.95
0.003174	1141.01	137.84	74.	66.	112.	0.41	0.21	120.	-27.	1.00	1.00
0.004395	2189.93	347.68	76.	57.	113.	0.39	0.39	50.	25.	1.00	1.00
0.005127	2095.32	44.19	62.	64.	103.	0.19	0.20	93.	-18.	1.00	1.00
0.007178	1984.36	88.11	38.	71.	116.	0.46	0.18	86.	-15.	0.39	0.72
0.010254	948.94	189.86	73.	77.	72.	0.47	0.11	97.	-28.	0.88	0.42
0.012817	601.03	176.63	87.	39.	60.	0.57	0.15	80.	-13.	0.97	0.94
0.016235	1312.41	390.33	77.	69.	98.	0.28	0.18	75.	-23.	0.88	0.87
0.020605	597.66	312.70	76.	47.	60.	0.23	0.33	80.	20.	0.85	0.85
0.025818	1406.37	364.39	88.	57.	60.	0.39	0.21	6.	29.	0.92	0.93
0.032623	1541.53	253.73	70.	62.	65.	0.41	0.16	-22.	12.	0.40	0.70
0.040649	715.12	353.50	66.	72.	44.	0.26	0.11	-31.	27.	0.55	0.37
0.051634	1360.17	550.43	77.	64.	73.	0.15	0.17	-18.	37.	0.50	0.76
0.065001	2494.62	382.88	52.	57.	70.	0.36	0.21	-42.	3.	0.45	0.62
0.129394	7269.70	1250.60	76.	25.	75.	0.43	0.17	9.	40.	0.39	0.38
0.201416	14271.25	1656.43	56.	51.	70.	0.12	0.07	-23.	38.	0.85	0.86
0.204590	16681.32	764.41	72.	43.	65.	0.23	0.23	-23.	58.	0.32	0.37
0.256348	20230.48	958.89	69.	49.	72.	0.27	0.32	-14.	51.	0.67	0.59
0.323486	12888.08	2064.85	79.	48.	67.	0.09	0.20	-19.	28.	0.37	0.71
0.408935	9256.93	1060.57	59.	52.	73.	0.21	0.28	-25.	15.	0.54	0.48
0.518799	6790.25	1337.76	50.	48.	70.	0.25	0.22	-19.	10.	0.36	0.70
0.653076	7843.38	1184.79	47.	52.	62.	0.32	0.32	-28.	1.	0.43	0.53
0.817871	7959.38	1208.04	52.	61.	54.	0.23	0.28	-34.	-14.	0.50	0.40
1.025391	9944.13	1540.28	59.	54.	54.	0.16	0.25	-32.	-15.	0.49	0.55
1.287842	10118.16	2380.88	44.	57.	57.	0.27	0.27	-28.	-33.	0.56	0.72
1.617431	11227.69	1385.75	44.	55.	58.	0.22	0.21	-38.	-34.	0.61	0.43
2.032470	10433.07	2233.30	44.	46.	60.	0.23	0.22	-25.	-33.	0.54	0.56
2.557373	8306.88	1520.31	45.	44.	52.	0.26	0.22	-36.	-52.	0.53	0.40
3.216552	8141.05	1517.01	44.	42.	53.	0.17	0.16	-31.	-68.	0.48	0.42
4.046630	8068.01	1728.22	39.	40.	64.	0.28	0.22	-34.	-72.	0.29	0.49
5.096435	7758.47	1367.02	44.	40.	49.	0.23	0.14	-27.	-22.	0.40	0.24
6.414794	6631.30	1288.63	35.	38.	54.	0.23	0.12	-28.	-11.	0.39	0.34
8.129883	5338.33	2042.27	43.	47.	54.	0.23	0.20	-23.	38.	0.89	0.72
10.229492	5544.13	1530.37	39.	40.	52.	0.22	0.16	118.	-1.	0.82	0.73
12.866213	5922.60	1510.73	36.	50.	63.	0.22	0.30	-35.	-50.	0.71	0.67

MAGNETOTELLURIC STATION 002 UNREFERENCED

FREQ	RHOXY	RHOYX	PHASEXY	PHASEYX	ROT ANG	SKEWNESS	TIPPER	TIP STRIK	TIP PHASE	COHXY	COHYX
32.714840	23821.29	1252.38	42.	14.	148.	0.20	0.83	15.	-15.	0.74	0.71
41.503918	110684.20	509.66	42.	46.	135.	0.32	0.33	58.	-49.	0.48	0.69
52.246094	42474.61	1093.97	34.	20.	146.	0.16	0.44	47.	31.	0.76	0.69
82.031235	17876.47	522.17	25.	11.	140.	0.10	0.47	17.	-37.	0.93	0.55
103.027351	21918.15	1719.35	19.	44.	148.	0.06	0.24	-23.	-41.	0.89	0.80

MAGNETOTELLURIC STATION 002 REMOTE REFERENCED TO STATION 4

FREQ	RHOXY	RHOYX	PHASEXY	PHASEYX	ROT ANG	SKEWNESS	TIPPER	TIP STRIK	TIP PHASE	COHXY	COHYX
0.001587	1870.33	16.50	44.	27.	133.	0.39	0.22	130.	-4.	0.98	0.94
0.002224	5848.61	27.42	59.	68.	144.	0.37	0.21	111.	1.	0.98	0.80
0.004269	3282.76	9.77	29.	50.	140.	0.39	0.18	109.	-27.	0.97	0.65
0.005127	3289.54	69.06	38.	-78.	139.	0.43	0.19	99.	9.	0.95	0.76
0.007357	3296.48	29.31	55.	88.	139.	0.40	0.19	98.	-2.	0.97	0.74
0.010303	4027.48	33.31	50.	44.	142.	0.31	0.22	91.	15.	0.97	0.63
0.012877	2407.52	25.90	61.	-70.	133.	0.35	0.13	83.	-44.	0.97	0.49
0.016276	3880.66	57.51	52.	75.	143.	0.30	0.18	72.	-14.	0.96	0.65
0.020548	3487.07	42.64	57.	82.	140.	0.43	0.27	30.	-61.	0.99	0.97
0.025948	4460.24	77.85	61.	72.	141.	0.36	0.31	0.	69.	0.99	0.97
0.034180	4627.23	120.53	60.	74.	143.	0.30	0.19	-24.	0.	1.00	1.00
0.043131	4999.39	111.25	58.	85.	140.	0.39	0.19	26.	-75.	1.00	1.00
0.054525	4964.10	152.80	61.	81.	142.	0.33	0.26	17.	53.	1.00	0.99
0.074689	5624.28	142.28	61.	72.	143.	0.33	0.28	23.	52.	0.99	0.99
0.109049	9044.74	165.76	76.	56.	155.	0.23	0.18	20.	19.	0.71	0.44
0.215658	13219.61	322.81	57.	84.	141.	0.42	0.19	-7.	-11.	0.66	0.53
0.340983	14676.79	472.46	66.	75.	150.	0.17	0.14	-37.	3.	0.74	0.49
0.428874	19997.47	459.14	63.	60.	152.	0.11	0.20	22.	5.	0.51	0.25
0.653076	18108.91	555.85	61.	59.	143.	0.27	0.24	7.	14.	0.94	0.71
0.817871	17292.63	760.11	60.	56.	145.	0.23	0.26	14.	23.	0.90	0.60
1.025391	21146.05	1041.71	62.	59.	147.	0.21	0.27	15.	23.	0.93	0.70
1.287842	24831.60	881.12	56.	59.	146.	0.25	0.29	34.	21.	0.89	0.59
1.617431	26407.17	1046.09	58.	55.	148.	0.20	0.28	31.	21.	0.91	0.68
2.032470	28059.05	992.25	57.	51.	147.	0.18	0.32	39.	23.	0.89	0.56
2.557373	26983.22	898.09	55.	48.	147.	0.17	0.35	41.	20.	0.88	0.58
3.271484	20640.10	1487.95	60.	43.	154.	0.07	0.41	57.	45.	0.86	0.62
4.101563	19343.66	1339.37	53.	44.	156.	0.11	0.49	58.	48.	0.81	0.78
5.151367	20147.19	1068.39	52.	42.	158.	0.14	0.46	64.	37.	0.85	0.82
6.469726	22319.03	1130.95	53.	46.	156.	0.08	0.51	65.	35.	0.88	0.79
8.129883	30267.57	633.69	55.	45.	147.	0.15	0.47	60.	10.	0.90	0.65
10.229492	28416.91	961.81	57.	52.	151.	0.07	0.82	65.	38.	0.89	0.56
12.866213	27066.85	631.70	59.	53.	149.	0.08	0.80	67.	38.	0.91	0.50
16.186522	26154.79	516.17	59.	57.	148.	0.07	2.48	66.	80.	0.91	0.53
20.385744	26119.46	642.35	62.	59.	149.	0.06	5.26	73.	69.	0.88	0.55
25.659182	21339.89	755.12	62.	68.	148.	0.05	0.48	72.	-22.	0.81	0.52

MAGNETOTELLURIC STATION 003 REMOTE REFERENCED TO STATION 4

FREQ	RHOXY	RHOYX	PHASEXY	PHASEYX	ROT ANG	SKEWNESS	TIPPER TIP STRIK	TIP PHASE	COHXY	COHYX
0.007205	3271.23	728.19	76.	56.	173.	0.47	0.23	95.	-25.	0.23	0.83
0.013835	1948.79	836.70	53.	42.	159.	0.50	0.22	97.	-26.	0.99	0.93
0.032592	2515.60	505.90	47.	37.	147.	0.51	0.11	46.	-25.	0.50	0.11
0.041341	7027.36	594.25	52.	66.	155.	0.44	0.11	2.	20.	0.19	0.15
0.051514	3267.58	635.81	74.	54.	132.	0.62	0.15	19.	35.	0.16	0.14
0.054525	2720.28	1193.35	61.	58.	107.	0.33	0.32	12.	47.	0.67	0.79
0.069173	3194.07	1025.10	52.	44.	130.	0.64	0.17	114.	19.	0.71	0.45
0.136719	5101.73	2211.37	87.	53.	133.	0.38	0.10	-37.	-27.	0.64	0.31
0.340983	7800.25	4318.02	47.	85.	99.	0.59	0.12	-14.	34.	0.39	0.51
0.428874	7016.39	2618.01	52.	69.	134.	0.52	0.13	-11.	27.	0.58	0.43
0.539551	7453.54	2606.39	67.	77.	142.	0.61	0.12	-29.	28.	0.56	0.33
0.653076	6815.58	4022.41	59.	75.	137.	0.86	0.13	133.	39.	0.64	0.71
1.287842	8311.72	7158.10	52.	62.	138.	0.64	0.13	-40.	33.	0.53	0.34
1.617431	6878.56	11192.75	34.	63.	89.	0.64	0.08	-17.	20.	0.28	0.56
2.032470	15615.11	3986.73	43.	38.	111.	0.23	0.06	-40.	22.	0.32	0.34
2.557373	15287.71	8810.87	37.	47.	101.	0.15	0.08	-16.	23.	0.33	0.46
3.216552	17136.31	6238.47	54.	48.	109.	0.22	0.08	-3.	35.	0.29	0.36
4.046630	10623.61	5264.89	36.	54.	136.	0.39	0.02	0.	50.	0.49	0.33
6.469726	11685.62	5225.61	43.	45.	115.	0.29	0.34	125.	48.	0.44	0.39
8.129883	8711.99	4822.26	37.	39.	130.	0.31	0.46	-41.	44.	0.74	0.44
10.229494	8009.97	4286.14	27.	58.	136.	0.24	17.74	-42.	75.	0.64	0.51
12.866208	7841.17	4813.38	37.	48.	139.	0.29	0.39	134.	29.	0.66	0.44
16.186522	6671.70	6203.28	38.	61.	140.	0.22	0.34	-40.	24.	0.58	0.44
20.385740	5533.40	5170.51	57.	44.	74.	0.28	0.32	128.	11.	0.41	0.64
25.659182	3968.64	6821.06	46.	68.	154.	0.13	0.23	-37.	-32.	0.54	0.47

MAGNETOTELLURIC STATION 004 , REMOTE REFERENCED TO STATION 2

FREQ	RHOXY	RHOYX	PHASEXY	PHASEYX	ROT ANG	SKEWNESS	TIPPER TIP STRIK	TIP PHASE	COHXY	COHYX
0.002197	1071.06	299.17	45.	46.	80.	0.39	0.43	97.	2.	1.00	1.00
0.003174	1581.64	427.14	82.	19.	55.	0.34	0.22	128.	-35.	1.00	1.00
0.004089	1303.74	422.74	46.	78.	106.	0.14	0.26	120.	-44.	1.00	0.87
0.005127	1217.83	334.98	46.	10.	94.	0.24	0.31	109.	-56.	0.77	0.57
0.007274	1170.15	383.37	61.	60.	77.	0.27	0.38	102.	-78.	0.97	0.97
0.013000	1289.88	373.46	53.	61.	83.	0.14	0.34	129.	-14.	0.84	0.39
0.020691	1399.80	257.26	73.	51.	76.	0.29	5.88	41.	7.	0.96	0.96
0.025976	1560.97	361.31	76.	58.	76.	0.25	0.77	8.	-77.	0.94	0.96
0.026855	1611.56	340.42	67.	49.	82.	0.22	0.28	6.	29.	0.96	0.97
0.034180	2599.41	335.57	78.	54.	74.	0.24	0.18	-26.	-16.	0.98	1.00
0.043131	3267.19	306.76	72.	52.	78.	0.23	0.13	31.	-72.	0.97	0.97
0.054525	3936.10	321.76	71.	56.	73.	0.17	0.22	19.	61.	0.98	0.99
0.069173	3531.65	345.81	67.	52.	78.	0.16	0.19	38.	17.	0.92	0.95
0.158691	10697.30	1360.34	15.	50.	55.	0.34	0.07	-40.	-64.	0.79	0.84
0.256348	15994.06	543.93	64.	22.	83.	0.35	0.09	55.	-5.	0.85	0.74
0.323486	32798.83	802.04	45.	35.	82.	0.25	0.14	57.	-27.	0.32	0.67
0.408935	9399.68	518.06	52.	43.	80.	0.13	0.11	51.	-45.	0.64	0.58
0.518799	14998.58	937.98	43.	42.	73.	0.09	0.11	57.	-37.	0.76	0.72
0.653076	13678.76	653.83	48.	55.	77.	0.11	0.10	31.	-48.	0.58	0.63
0.817871	14302.83	1038.76	59.	48.	70.	0.09	0.09	46.	-70.	0.67	0.67
1.025391	23090.08	1723.43	43.	44.	72.	0.16	0.13	49.	9.	0.81	0.91
1.293945	17771.19	1205.63	42.	43.	72.	0.03	0.11	50.	-1.	0.79	0.74
1.635742	16032.94	1233.08	44.	48.	71.	0.05	0.12	41.	62.	0.63	0.72
2.075195	13866.91	1369.69	48.	50.	70.	0.05	0.15	61.	45.	0.66	0.81
2.612305	15558.40	1188.85	42.	49.	70.	0.03	0.14	57.	35.	0.71	0.76
3.271484	16274.83	1435.14	48.	45.	70.	0.06	0.18	70.	17.	0.66	0.76
4.101563	15916.15	1335.12	44.	42.	63.	0.07	0.19	64.	15.	0.56	0.73
5.151367	17027.38	1297.76	45.	41.	64.	0.02	0.22	68.	1.	0.73	0.78
6.469726	15232.21	1203.44	46.	39.	64.	0.01	0.21	62.	0.	0.71	0.77
8.129883	12871.39	1054.60	50.	45.	60.	0.04	0.23	52.	-2.	0.66	0.80
10.229494	14944.06	997.31	51.	39.	58.	0.08	0.44	49.	-31.	0.75	0.71
12.866213	10216.75	878.49	53.	44.	62.	0.02	0.44	38.	-42.	0.63	0.71
16.186518	13137.12	819.33	56.	48.	59.	0.04	48.98	34.	-7.	0.71	0.68
20.385744	11288.88	694.36	65.	51.	57.	0.04	0.35	24.	58.	0.66	0.66
25.659182	10840.60	532.99	54.	41.	54.	0.05	0.53	20.	-51.	0.68	0.53

MAGNETOTELLURIC STATION 005 UNREFERENCED

FREQ	RHOXY	RHOYX	PHASEXY	PHASEYX	ROT ANG	SKEWNESS	TIPPER TIP STRIK	TIP PHASE	COHXY	COHYX
103.027351	690.78	3269.97	32.	29.	79.	0.33	0.58	128.	1.	0.80	0.82
257.324463	956.74	2420.13	45.	33.	31.	0.33	0.62	78.	26.	0.66	0.95

MAGNETOTELLURIC STATION 005 REMOTE REFERENCED TO STATION 6

FREQ	RHOXY	RHOYX	PHASEXY	PHASEYX	ROT ANG	SKEWNESS	TIPPER TIP	STRIK	TIP PHASE	COHXY	COHYX
2.032470	4726.82	7249.73	17.	65.	77.	0.40	0.28	-14.	34.	0.39	0.24
2.557373	8015.46	9296.62	70.	22.	21.	0.65	0.41	-11.	-11.	0.14	0.59
3.216552	4216.20	6707.92	38.	53.	39.	0.36	0.34	-19.	13.	0.15	0.31
4.046630	3138.36	9557.07	34.	60.	74.	0.60	0.44	-20.	-1.	0.71	0.51
5.096435	3128.21	8564.54	36.	66.	66.	0.41	0.55	-28.	-10.	0.34	0.45
6.414794	3542.32	10608.75	58.	54.	98.	0.46	0.48	-33.	-7.	0.62	0.33
6.469726	2200.70	14046.96	36.	55.	67.	0.21	0.70	-24.	28.	0.60	0.89
8.129883	2539.56	11776.04	42.	53.	72.	0.15	18.76	-36.	-76.	0.61	0.80
12.866213	2515.02	8969.63	22.	55.	84.	0.47	0.45	-32.	-8.	0.84	0.83
16.186522	2054.86	8177.67	53.	55.	66.	0.22	0.51	-35.	-36.	0.54	0.76
20.385744	1647.10	7630.23	23.	50.	84.	0.48	0.77	-34.	45.	0.65	0.77
25.659182	1061.34	8966.22	59.	49.	79.	0.43	0.34	122.	19.	0.62	0.75

MAGNETOTELLURIC STATION 006 UNREFERENCED

FREQ	RHOXY	RHOYX	PHASEXY	PHASEYX	ROT ANG	SKEWNESS	TIPPER TIP	STRIK	TIP PHASE	COHXY	COHYX
41.503910	50800.07	220.27	25.	-27.	28.	0.42	0.21	10.	16.	0.88	0.44
103.027351	29844.25	431.03	14.	81.	34.	0.41	0.23	-35.	18.	0.95	0.92

MAGNETOTELLURIC STATION 007 UNREFERENCED

FREQ	RHOXY	RHOYX	PHASEXY	PHASEYX	ROT ANG	SKEWNESS	TIPPER	TIP STRIK	TIP PHASE	COHXY	COHYX
103.027351	12703.88	6800.33	64.	70.	113.	0.15	0.41	48.	-39.	0.48	0.80
257.324463	15554.05	3650.85	32.	49.	111.	0.23	0.46	88.	-76.	0.24	0.41

MAGNETOTELLURIC STATION 007 REMOTE REFERENCED TO STATION 8

FREQ	RHOXY	RHOYX	PHASEXY	PHASEYX	ROT ANG	SKEWNESS	TIPPER	TIP STRIK	TIP PHASE	COHXY	COHYX
0.002378	769.68	49.76	29.	-74.	67.	1.13	0.27	-36.	-14.	0.90	0.68
0.003174	754.31	76.51	39.	-41.	52.	1.86	0.25	-42.	-5.	0.85	0.99
0.004353	1686.67	151.80	44.	-11.	61.	1.08	0.19	123.	-14.	0.75	0.67
0.005127	603.87	499.33	61.	-84.	68.	1.76	0.24	111.	-33.	1.00	1.00
0.007232	735.06	11.03	55.	77.	64.	1.15	0.19	106.	-18.	0.85	0.89
0.010254	867.33	25.28	65.	-45.	59.	1.23	0.17	100.	-17.	0.91	0.90
0.012765	1292.43	61.86	65.	-63.	62.	1.13	0.16	97.	-34.	0.89	0.92
0.016174	1847.78	37.21	66.	64.	59.	1.24	0.16	68.	-66.	0.87	0.90
0.020569	1770.31	77.30	51.	-76.	68.	1.08	0.18	42.	80.	0.95	0.98
0.025940	1318.34	5.87	61.	56.	57.	1.69	0.19	1.	19.	0.87	0.96
0.032715	835.82	24.99	54.	47.	57.	1.72	0.15	-24.	-14.	0.76	0.75
0.041364	1620.46	112.80	64.	-83.	61.	1.33	0.14	59.	-34.	0.80	0.48
0.052062	3217.58	128.44	55.	-76.	70.	1.06	0.20	45.	87.	0.85	0.84
0.072402	2267.62	286.72	52.	-84.	64.	1.17	0.17	49.	-14.	0.58	0.66
0.129185	2044.20	307.35	45.	-63.	51.	1.96	0.08	110.	36.	0.45	0.34
0.256958	4734.37	1512.36	-31.	51.	120.	1.25	0.08	100.	29.	0.33	0.27
0.323730	1009.30	1343.67	39.	-50.	51.	1.51	0.15	88.	61.	0.32	0.19
0.407715	4338.00	2693.60	68.	10.	42.	1.76	0.13	92.	58.	0.34	0.26
0.539551	8881.28	3773.10	74.	59.	110.	0.64	0.11	123.	31.	0.54	0.61
0.679525	10565.46	2794.20	62.	75.	77.	0.69	0.11	119.	6.	0.51	0.28
1.075846	5732.00	3076.03	54.	85.	62.	0.82	0.19	126.	-29.	0.42	0.30
1.617431	11151.52	6643.70	41.	82.	71.	0.43	0.19	-32.	7.	0.28	0.51
1.635742	3023.29	5551.53	50.	70.	63.	0.39	0.21	30.	41.	0.80	0.67
2.075195	9293.79	4197.58	59.	66.	92.	0.43	0.20	-35.	-26.	0.71	0.93
2.612304	11904.44	4188.83	61.	58.	96.	0.37	0.20	37.	-35.	0.65	0.83
3.271484	9689.59	4580.15	66.	63.	115.	0.35	0.25	39.	35.	0.67	0.81
4.101563	11756.73	4758.30	62.	58.	118.	0.30	0.29	43.	36.	0.68	0.81
5.151367	11503.62	5022.75	59.	52.	92.	0.28	0.31	55.	22.	0.63	0.82
6.469726	11830.23	5214.91	59.	57.	104.	0.19	0.35	49.	17.	0.75	0.86
8.129883	14822.74	4905.49	65.	50.	102.	0.18	0.33	52.	4.	0.78	0.87
10.229492	11313.64	4764.51	66.	56.	101.	0.13	0.35	52.	1.	0.69	0.85
12.866213	13243.54	4746.47	73.	52.	94.	0.13	0.37	61.	-5.	0.80	0.89
16.186522	13686.26	4282.65	77.	52.	93.	0.16	0.39	58.	-22.	0.78	0.83
20.385744	15172.71	3350.20	76.	47.	93.	0.14	0.41	61.	-30.	0.55	0.63
25.659191	15489.82	3355.13	79.	52.	93.	0.10	0.44	56.	-45.	0.65	0.65

MAGNETOTELLURIC STATION 008 UNREFERENCED

FREQ	RHOXY	RHOYX	PHASEXY	PHASEYX	ROT ANG	SKEWNESS	TIPPER	TIP STRIK	TIP PHASE	COHXY	COHYX
103.027351	683.72	2126.95	69.	36.	101.	0.01	0.39	58.	17.	0.61	0.92
257.324463	630.29	1690.58	48.	54.	45.	0.11	0.48	47.	46.	0.92	0.55

MAGNETOTELLURIC STATION 009 UNREFERENCED

FREQ	RHOXY	RHOYX	PHASEXY	PHASEYX	ROT ANG	SKEWNESS	TIPPER TIP STRIK	TIP PHASE	COHXY	COHYX
103.027351	60431.95	761.47	54.	26.	136.	0.41	0.23	37.	-52.	0.55	0.40
129.394501	67314.01	2959.22	45.	14.	105.	0.33	1.25	89.	4.	0.73	0.72

MAGNETOTELLURIC STATION 008 REMOTE REFERENCED TO STATION 7

FREQ	RHOXY	RHOYX	PHASEXY	PHASEYX	ROT ANG	SKEWNESS	TIPPER	TIP STRIK	TIP PHASE	COHXY	COHYX
0.001221	53.80	1090.56	40.	44.	73.	0.43	0.53	129.	-35.	1.00	1.00
0.002369	62.51	883.65	15.	50.	94.	0.63	0.31	73.	-25.	0.65	0.69
0.003174	40.71	1077.10	-74.	-2.	107.	1.15	0.20	89.	-27.	0.95	0.69
0.004312	112.71	1565.64	58.	37.	96.	0.60	0.19	-42.	32.	0.50	0.64
0.007228	240.92	1862.17	42.	77.	142.	0.68	0.33	48.	-4.	0.51	0.63
0.010254	55.41	550.12	-89.	69.	114.	0.62	0.25	90.	70.	0.15	0.49
0.012765	1114.01	306.45	85.	51.	106.	0.17	0.32	93.	-82.	0.31	0.32
0.016183	444.27	1103.41	48.	70.	122.	0.61	0.44	72.	71.	0.61	0.41
0.020577	460.37	1002.02	57.	65.	105.	0.43	0.44	64.	24.	0.79	0.71
0.025948	215.41	1326.29	55.	84.	109.	0.71	0.34	44.	26.	0.78	0.66
0.032715	656.40	652.17	52.	62.	103.	0.32	0.09	91.	-4.	0.48	0.54
0.041341	1502.43	1016.74	75.	49.	92.	0.34	0.14	110.	-47.	0.40	0.62
0.052036	632.38	1429.50	55.	49.	138.	0.27	0.28	55.	-18.	0.62	0.64
0.073672	508.21	1144.68	59.	43.	146.	0.42	0.17	62.	54.	0.30	0.35
0.102818	622.95	981.33	69.	37.	143.	0.70	0.31	-23.	29.	0.09	0.10
0.136719	6858.05	784.37	-2.	11.	95.	1.12	0.28	73.	26.	0.25	0.12
0.171712	2611.91	771.95	28.	24.	112.	0.50	0.23	94.	33.	0.25	0.10
0.215658	2947.90	782.76	76.	84.	131.	0.89	0.23	121.	35.	0.18	0.23
0.270996	1554.62	1772.31	-52.	46.	117.	0.55	0.27	101.	15.	0.16	0.20
0.340983	1501.26	2802.94	54.	-80.	54.	0.37	0.30	107.	37.	0.30	0.25
0.428874	752.83	3157.84	42.	32.	84.	0.52	0.35	103.	25.	0.33	0.35
0.518799	1129.05	3657.63	32.	58.	84.	0.43	0.35	107.	24.	0.20	0.41
0.653076	1157.29	3279.16	46.	78.	70.	0.22	0.38	106.	18.	0.14	0.31
0.817871	1032.67	2838.93	37.	78.	96.	0.35	0.38	111.	21.	0.20	0.38
1.025391	1146.96	3740.91	30.	71.	89.	0.34	0.40	110.	11.	0.21	0.43
1.287842	479.20	3910.01	60.	59.	72.	0.31	0.41	113.	10.	0.08	0.34
1.617431	521.74	6018.45	59.	51.	78.	0.44	0.39	109.	0.	0.05	0.27
2.032470	1063.07	6135.19	49.	55.	81.	0.22	0.40	111.	-6.	0.03	0.28
2.557373	352.80	4581.64	41.	55.	82.	0.24	0.43	113.	-5.	0.07	0.36
3.216552	492.94	3351.34	49.	50.	85.	0.07	0.42	119.	-12.	0.12	0.31
6.469726	984.99	3955.71	57.	49.	97.	0.11	0.42	127.	-21.	0.18	0.50
8.129883	928.09	3720.53	42.	42.	96.	0.20	0.40	101.	-37.	0.27	0.53
10.229492	1186.32	4971.04	47.	37.	84.	0.13	0.34	107.	-30.	0.36	0.52
12.866213	1256.14	4231.74	51.	36.	82.	0.10	0.34	104.	-53.	0.47	0.59
16.186522	1083.34	3170.06	49.	40.	87.	0.07	0.28	79.	-42.	0.41	0.49
20.385744	667.39	3791.22	65.	39.	93.	0.19	0.38	-5.	-11.	0.32	0.62
25.659191	797.15	2764.87	59.	35.	90.	0.06	0.43	106.	-34.	0.35	0.52

MAGNETOTELLURIC STATION 009 REMOTE REFERENCED TO STATION 10

	FREQ	RHOXY	RHOYX	PHASEXY	PHASEYX	ROT ANG	SKEWNESS	TIPPER TIP STRIK	TIP PHASE	COHXY	COHYX
1	0.010579	9416.89	758.34	-12.	57.	162.	0.72	0.43	97.	84.	0.17	0.21
3	0.017090	6400.16	661.49	-77.	48.	155.	0.82	0.23	36.	33.	0.38	0.31
4	0.021139	10911.42	139.66	54.	40.	155.	1.17	0.24	54.	-24.	0.37	0.42
5	0.026855	12087.16	271.07	53.	0.	155.	1.17	0.20	51.	60.	0.80	0.75
7	0.043131	11961.89	1318.08	65.	62.	143.	1.01	0.28	14.	-71.	0.27	0.10
8	0.054525	5947.27	1307.75	71.	-21.	158.	1.56	0.42	3.	78.	0.30	0.52
10	0.103780	8621.20	6283.85	14.	55.	183.	3.76	0.15	92.	71.	0.18	0.01
12	0.158691	20889.35	8289.88	61.	41.	147.	1.39	0.26	110.	48.	0.10	0.17
13	0.201416	12453.54	5103.20	68.	20.	164.	3.19	0.28	108.	41.	0.12	0.21
14	0.256348	8067.39	1181.75	86.	-31.	152.	1.68	0.15	36.	-31.	0.06	0.18
15	0.323486	10999.53	11540.90	68.	-53.	161.	0.45	0.13	69.	37.	0.10	0.09
16	0.408935	49736.61	1147.08	23.	-62.	145.	0.51	0.24	-27.	-25.	0.25	0.06
17	0.518799	31686.94	4502.77	62.	17.	144.	0.85	0.23	89.	32.	0.15	0.03
18	0.653076	69556.94	7622.99	53.	35.	113.	0.00	0.17	104.	11.	0.17	0.06
19	0.817871	10790.11	8462.87	63.	-11.	142.	0.22	0.16	51.	12.	0.06	0.02
20	1.025391	48212.31	1835.96	43.	-45.	135.	0.48	0.21	115.	35.	0.21	0.04
21	1.293945	53813.95	6502.15	32.	-74.	144.	0.31	0.16	62.	27.	0.21	0.10
22	1.635742	62714.64	38572.71	40.	-60.	124.	0.77	0.29	120.	1.	0.16	0.05
25	3.271484	52440.22	3712.53	50.	87.	135.	0.17	0.23	78.	5.	0.19	0.03
26	4.101563	47560.36	55196.77	44.	-76.	130.	0.36	0.25	89.	6.	0.24	0.07
27	5.151367	40811.64	1431.34	41.	-30.	128.	0.15	0.34	91.	38.	0.34	0.01
29	8.129883	46821.18	573.47	55.	-68.	124.	0.26	0.29	86.	23.	0.37	0.05
30	10.229494	39603.86	777.76	49.	54.	134.	0.28	0.46	64.	49.	0.42	0.06
33	20.385744	61830.38	1423.88	66.	-8.	125.	0.41	0.93	78.	-76.	0.20	0.07
34	25.659182	39056.07	766.90	71.	4.	130.	0.36	0.42	97.	-22.	0.54	0.07

MAGNETOTELLURIC STATION 010 REMOTE REFERENCED TO STATION 9

FREQ	RHOXY	RHOYX	PHASEXY	PHASEYX	ROT ANG	SKEWNESS	TIPPER	TIP STRIK	TIP PHASE	COHXY	COHYX
0.001221	59.75	454.61	49.	85.	68.	1.36	0.79	93.	-12.	0.82	0.87
0.002316	1.51	3731.00	72.	-68.	84.	0.28	0.90	88.	38.	0.63	0.72
0.004271	35.52	721.64	-79.	46.	91.	0.06	0.27	96.	39.	0.42	0.27
0.007205	24.07	1628.34	58.	51.	77.	0.73	0.37	104.	46.	0.46	0.71
0.012817	9.38	1289.06	45.	-77.	82.	0.49	0.08	94.	86.	0.55	0.31
0.016357	19.23	1937.27	-48.	-45.	67.	0.63	0.67	88.	29.	0.28	0.60
0.017090	50.63	1671.49	76.	46.	92.	0.66	0.36	83.	-68.	0.52	0.74
0.026855	49.21	303.87	55.	46.	79.	1.84	0.23	20.	19.	0.70	0.57
0.034180	114.29	796.02	50.	45.	86.	2.04	0.41	132.	26.	0.90	0.82
0.043131	63.85	534.88	47.	47.	82.	1.64	0.25	93.	-6.	0.74	0.67
0.054525	35.96	568.61	26.	43.	91.	1.54	0.35	23.	62.	0.77	0.66
0.077610	92.91	463.54	-15.	63.	91.	1.15	0.28	36.	74.	0.43	0.71
0.256348	40.98	894.93	55.	3.	136.	0.60	0.16	54.	40.	0.01	0.03
0.323486	430.16	1041.07	-40.	49.	95.	0.46	0.20	31.	58.	0.05	0.11
0.408935	708.92	568.10	-19.	48.	94.	0.34	0.22	34.	55.	0.08	0.09
0.518799	79.09	1691.23	-6.	34.	73.	0.24	0.13	45.	40.	0.01	0.13
0.653076	30.59	742.46	-19.	68.	93.	0.73	0.21	39.	47.	0.02	0.14
0.817871	28.81	852.39	-14.	35.	78.	0.60	0.22	41.	33.	0.01	0.13
1.025391	9.04	1102.75	-62.	24.	76.	0.53	0.29	42.	24.	0.03	0.15
1.287842	96.76	1154.66	-54.	0.	72.	0.29	0.20	45.	10.	0.03	0.11
1.617431	144.54	1092.72	27.	42.	67.	0.27	0.42	33.	32.	0.10	0.04
2.612305	96.39	886.55	-16.	33.	77.	1.06	0.35	55.	-34.	0.08	0.21
3.271484	56.59	547.02	54.	51.	63.	0.25	0.25	34.	-12.	0.12	0.13
4.101563	53.94	530.59	-41.	41.	79.	0.74	0.20	56.	-12.	0.03	0.18
5.151367	13.92	488.44	82.	47.	71.	0.32	0.20	49.	-10.	0.05	0.23
6.469726	13.49	506.99	-59.	44.	77.	0.46	0.20	38.	-68.	0.11	0.48
8.129885	39.39	406.79	-69.	44.	77.	0.43	0.25	53.	2.	0.15	0.53
10.229494	53.66	352.71	-73.	44.	77.	0.48	0.36	61.	-23.	0.09	0.33
12.866208	27.69	362.18	-86.	48.	79.	0.52	0.24	62.	-35.	0.13	0.45
16.186522	73.41	382.81	-67.	49.	77.	0.45	0.41	90.	-61.	0.13	0.55
20.385740	55.89	338.76	-60.	53.	81.	0.54	1.45	105.	58.	0.14	0.47
25.659191	168.39	295.58	-77.	58.	83.	0.40	0.22	83.	-63.	0.11	0.32

APPENDIX D

ONE-DIMENSIONAL "BOSTICK" INVERSIONS

The following plots are "continuous" inversions following the approximation by Bostick (1977). Inversions are given for both modes of resistivity and phase, because the selection of TE and TM is not always obvious and both modes may be useful in structurally complex areas. Because the "Bostick" inversion is an approximation for ONE DIMENSION, caution is recommended in its utilization. Some characteristics are:

(1) the tendency to overshoot maxima

(2) the tendency to undershoot minima

(3) the tendency to omit the surface layer

Specific examples are discussed in the text.

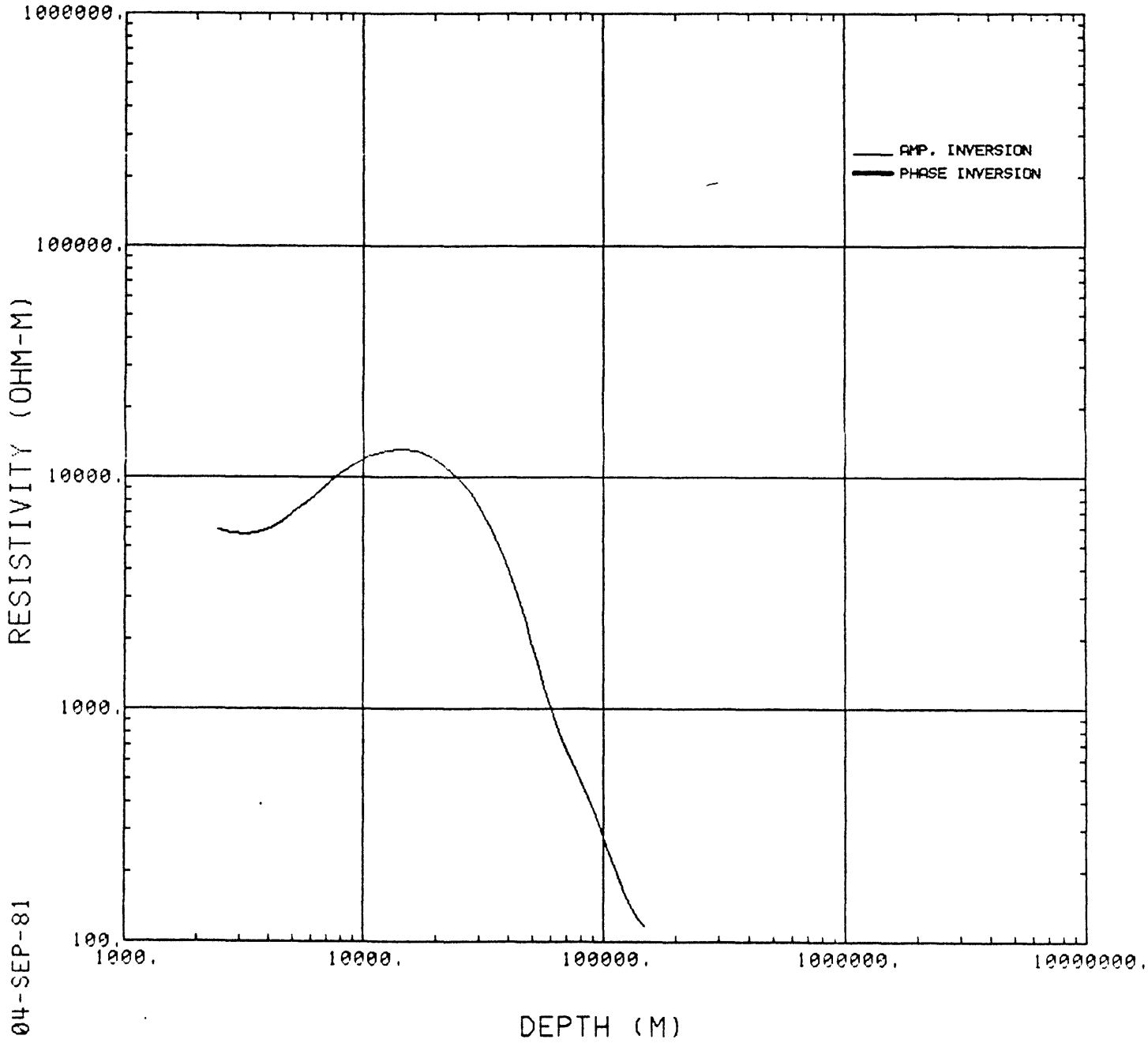
1000000.
100000.
10000.
1000.
100.
RESISTIVITY (OHM-M)
AMP. INVERSION
PHASE INVERSION
1000.
10000.
100000.
1000000.
10000000.
DEPTH (M)
04-SEP-81
U001X1

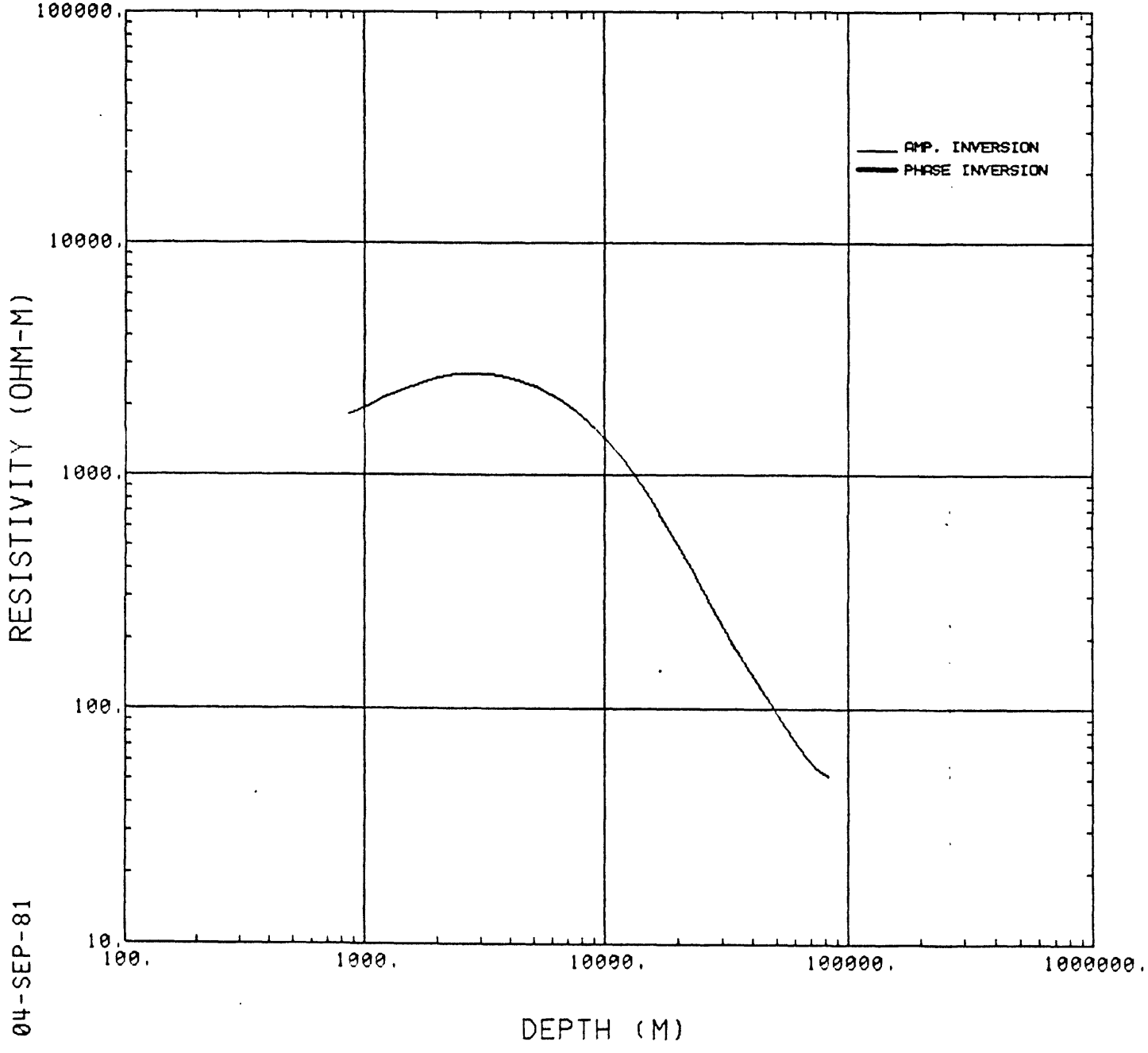
100000.
10000.
1000.
100.
10.
RESISTIVITY (OHM-M)
AMP. INVERSION
PHASE INVERSION
100.
1000.
10000.
100000.
1000000.
DEPTH (M)
04-SEP-81
U001Y1

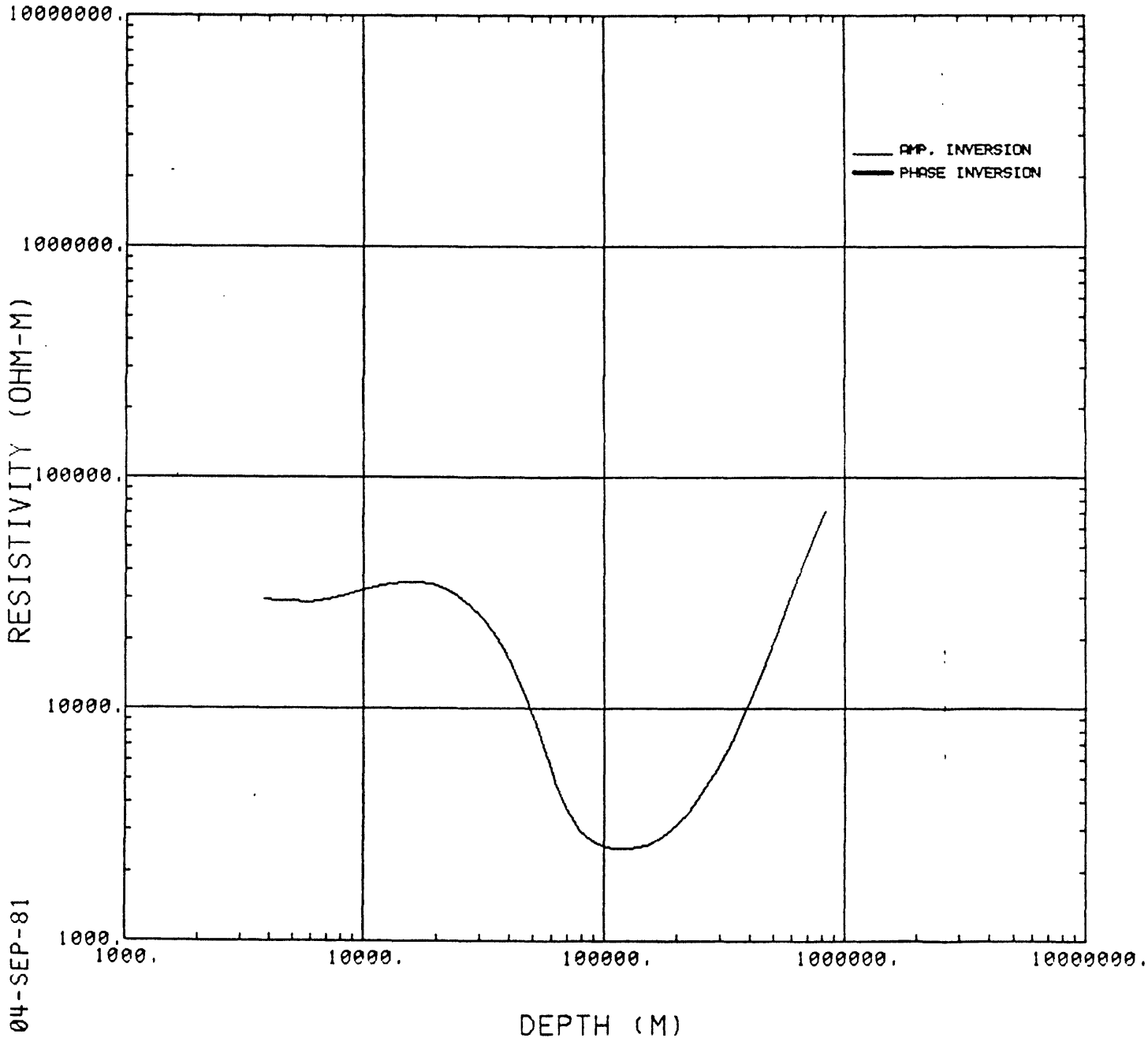
10000000.
1000000.
100000.
10000.
1000.
RESISTIVITY (OHM-M)
AMP. INVERSION
PHASE INVERSION
1000.
10000.
100000.
1000000.
10000000.
DEPTH (M)
04-SEP-81
U002X1

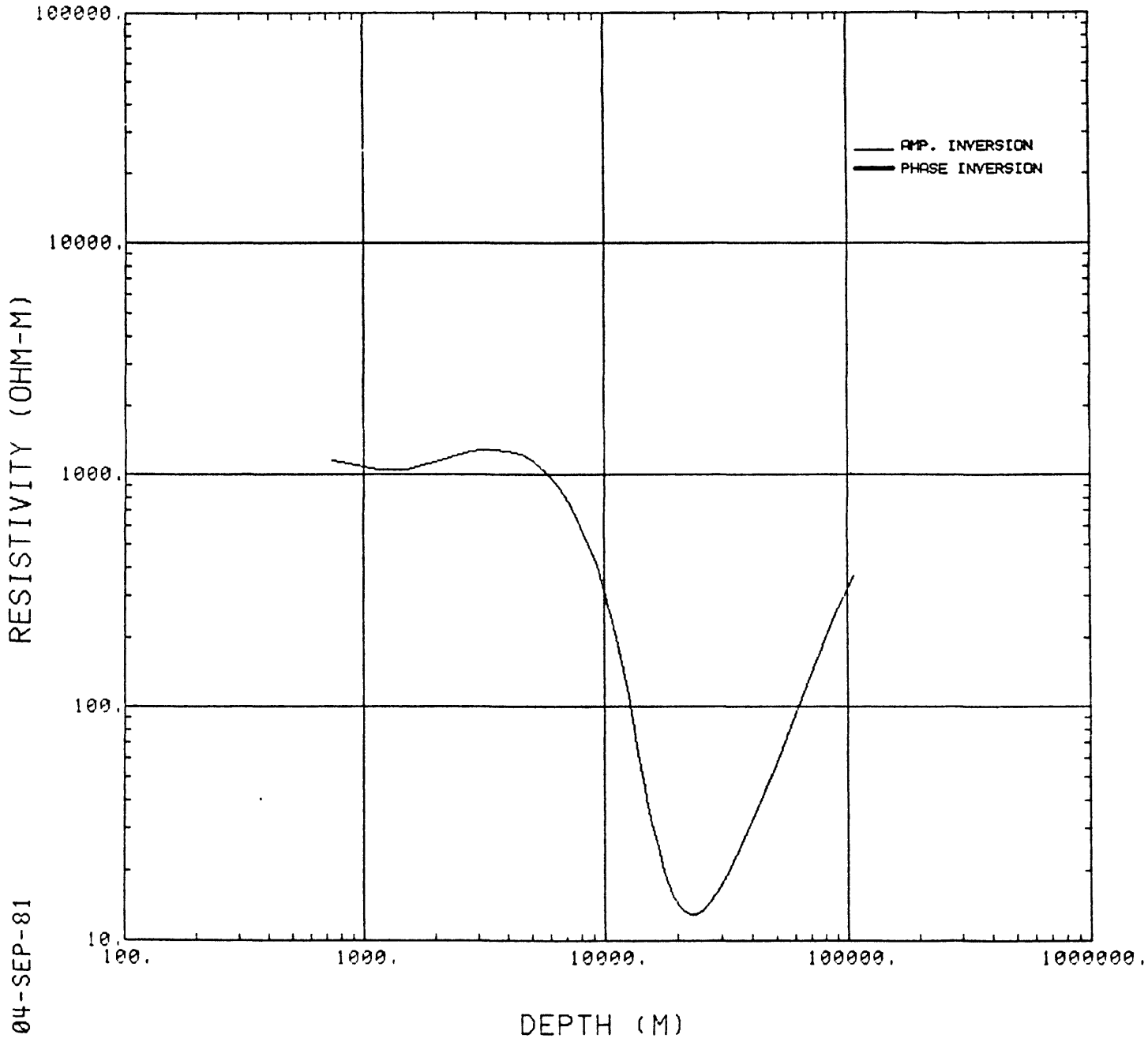
100000.
10000.
1000.
100.
10.
RESISTIVITY (OHM-M)
AMP. INVERSION
PHASE INVERSION
100.
1000.
10000.
100000.
1000000.
DEPTH (M)
04-SEP-81
U002Y1

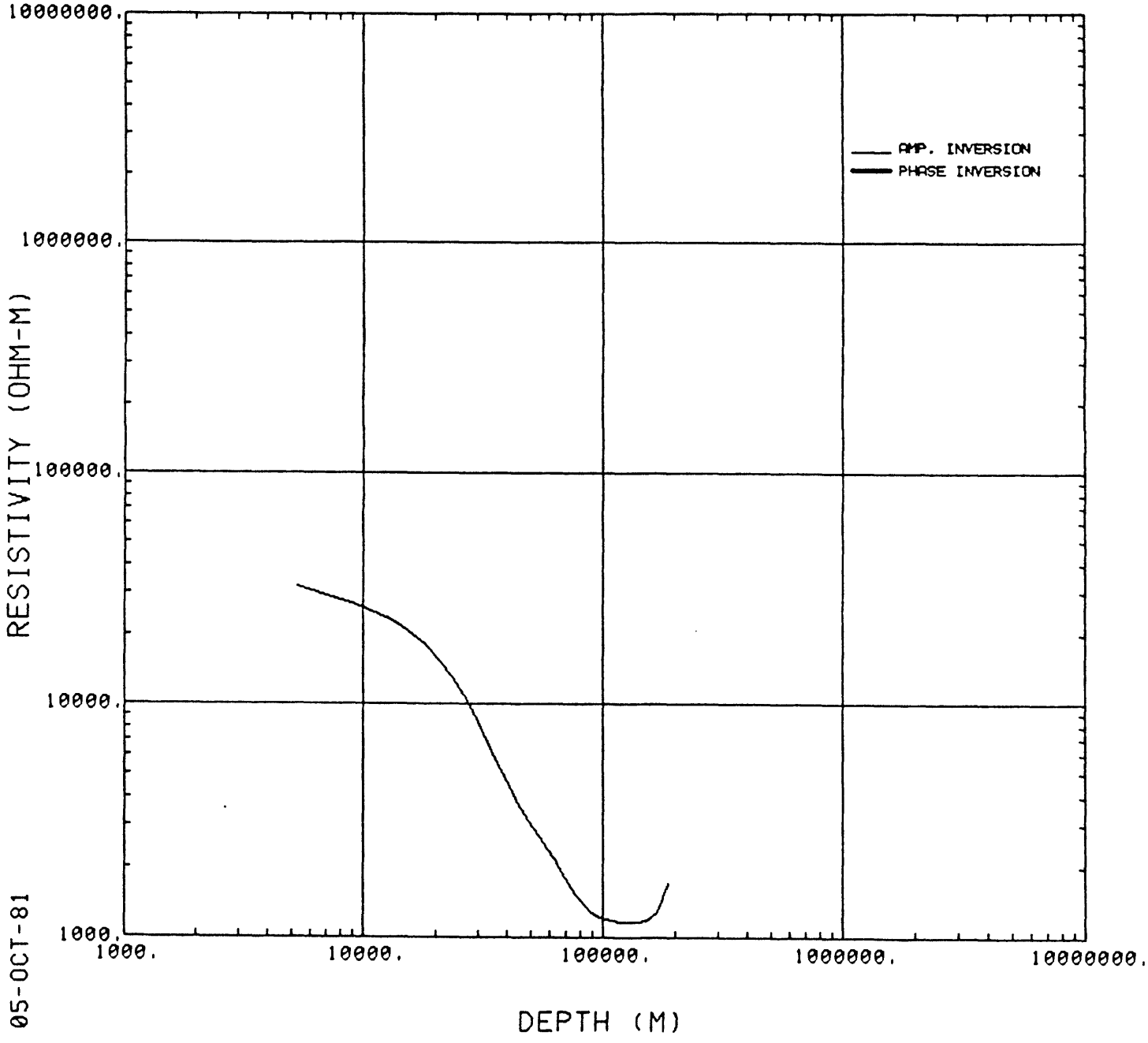
10000000.
1000000.
100000.
10000.
1000.
1000.
10000.
100000.
1000000.
10000000.
RESISTIVITY (OHM-M)
DEPTH (M)
AMP. INVERSION
PHASE INVERSION
05-OCT-81
U003X1

001

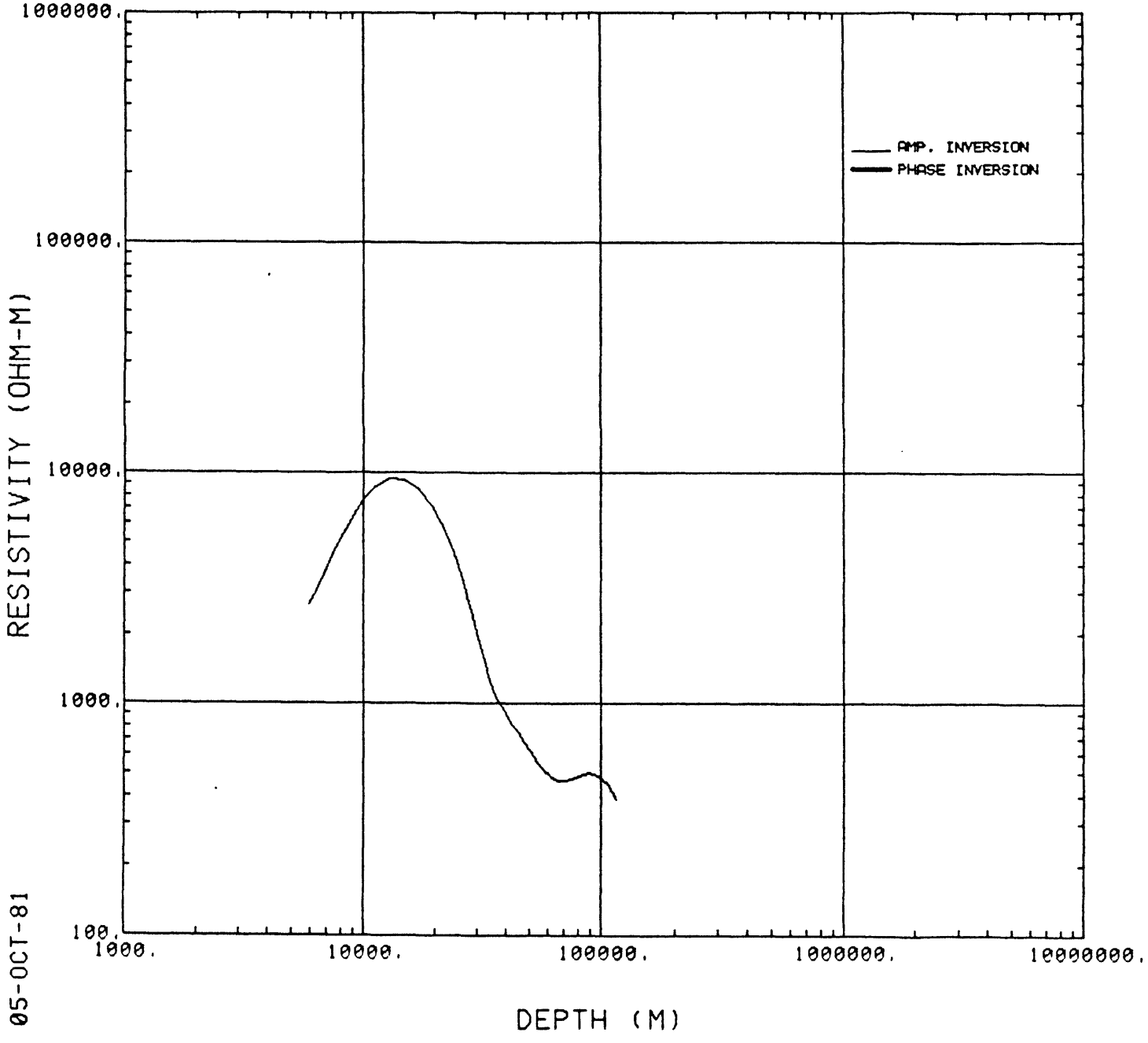
1000000.
100000.
10000.
1000.
100.
RESISTIVITY (OHM-M)
AMP. INVERSION
PHASE INVERSION
1000.
10000.
100000.
1000000.
10000000.
DEPTH (M)
05-OCT-81
U003Y1

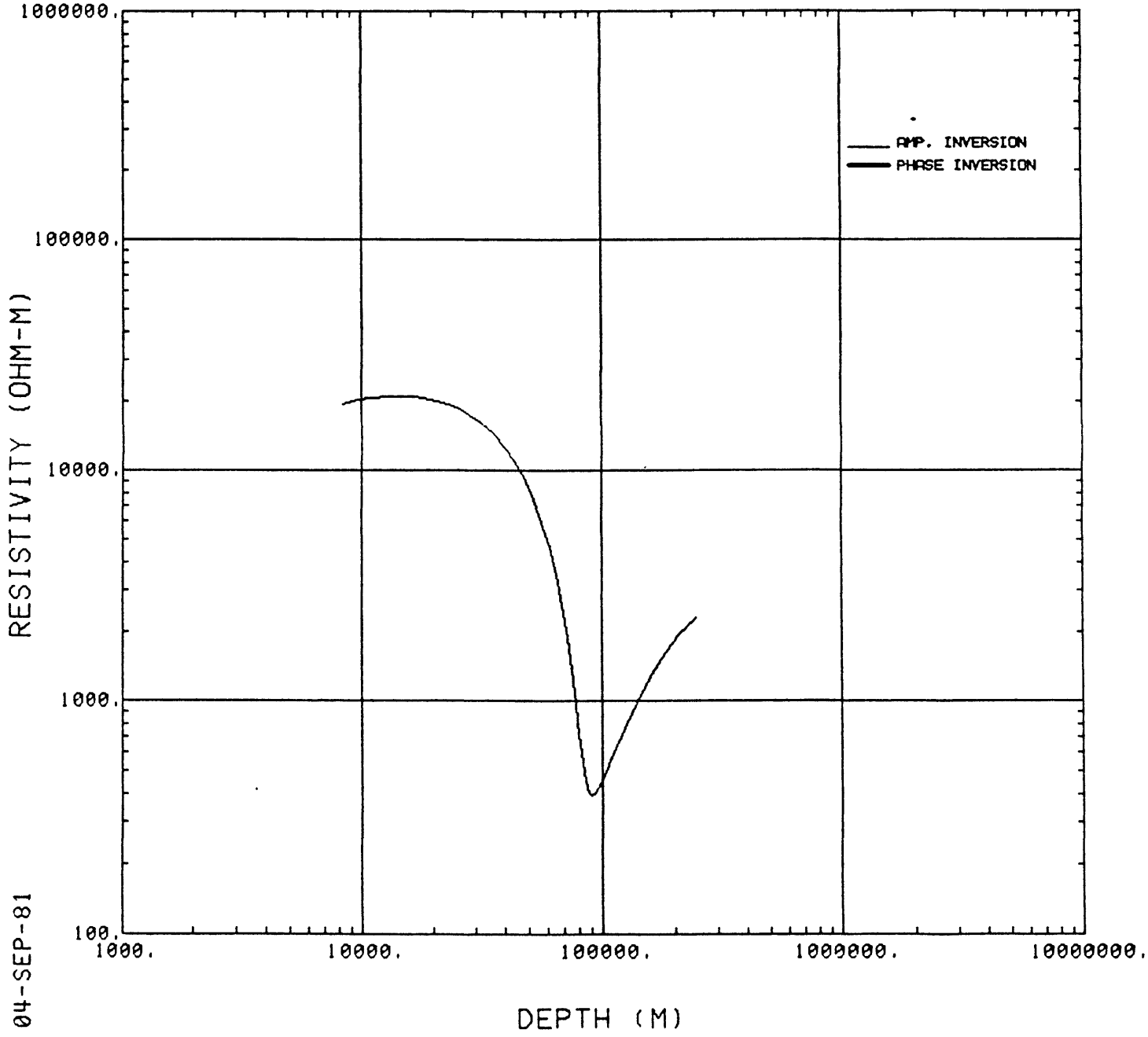
1000000.
100000.
10000.
1000.
100.
RESISTIVITY (OHM-M)
AMP. INVERSION
PHASE INVERSION
1000.
10000.
100000.
1000000.
10000000.
DEPTH (M)
04-SEP-81
U004X1

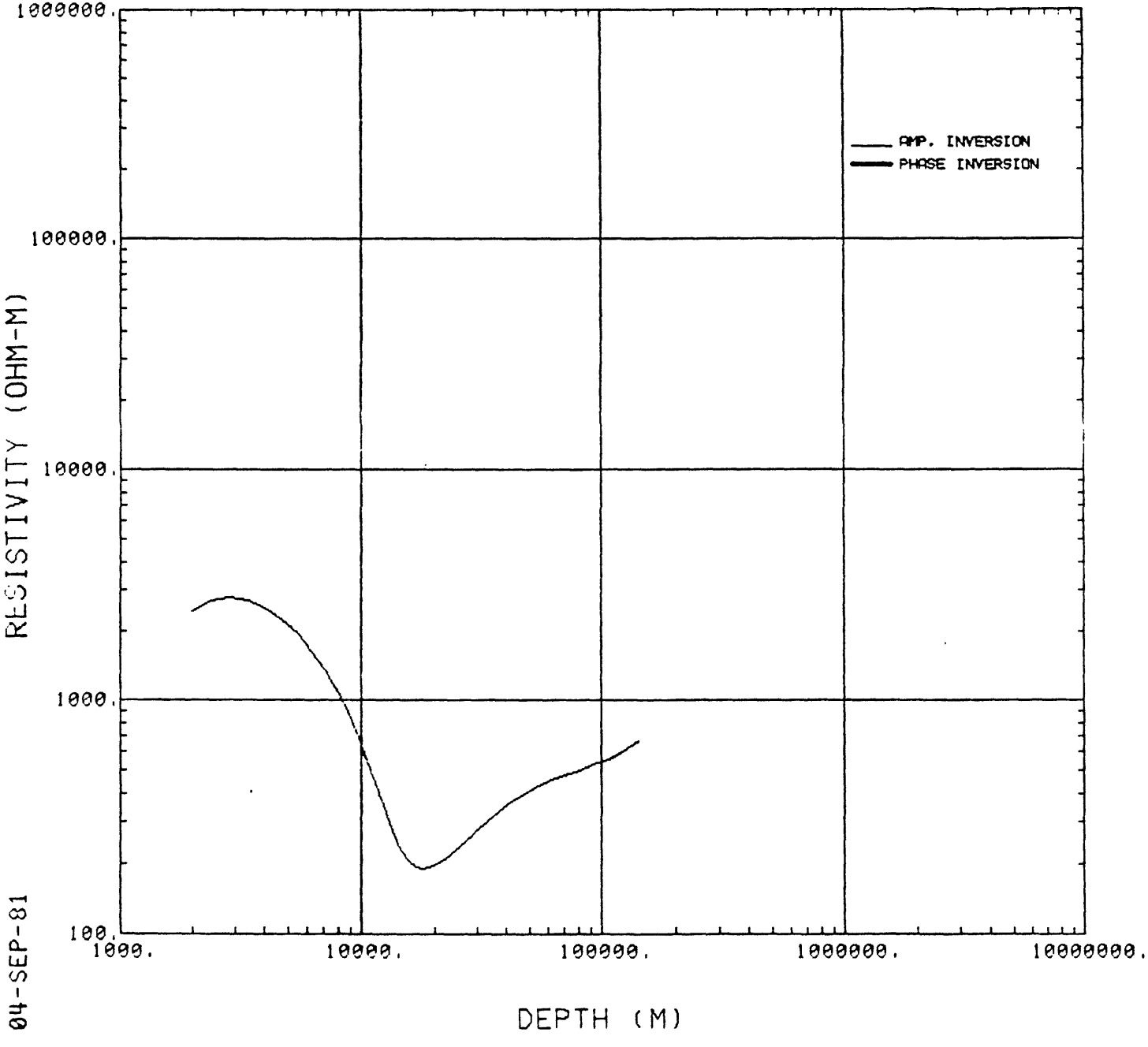
1000000.
100000.
10000.
1000.
100.
RESISTIVITY (OHM-M)
AMP. INVERSION
PHASE INVERSION
1000.
10000.
100000.
1000000.
10000000.
DEPTH (M)
04-SEP-81
U004Y1

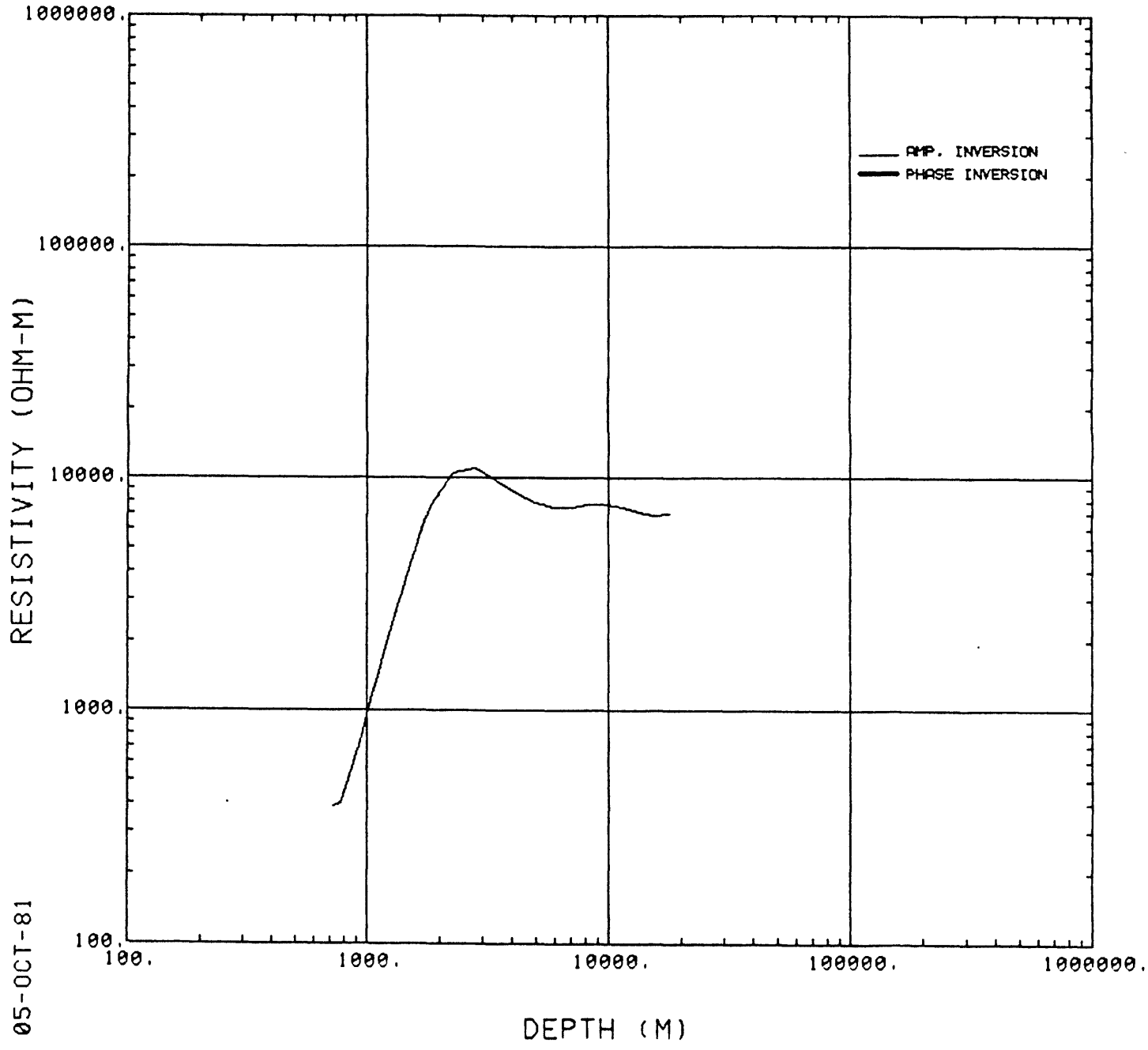
1000000.
100000.
10000.
1000.
100.
RESISTIVITY (OHM-M)
AMP. INVERSION
PHASE INVERSION
100.
1000.
10000.
100000.
1000000.
DEPTH (M)
05-OCT-81
U005X1

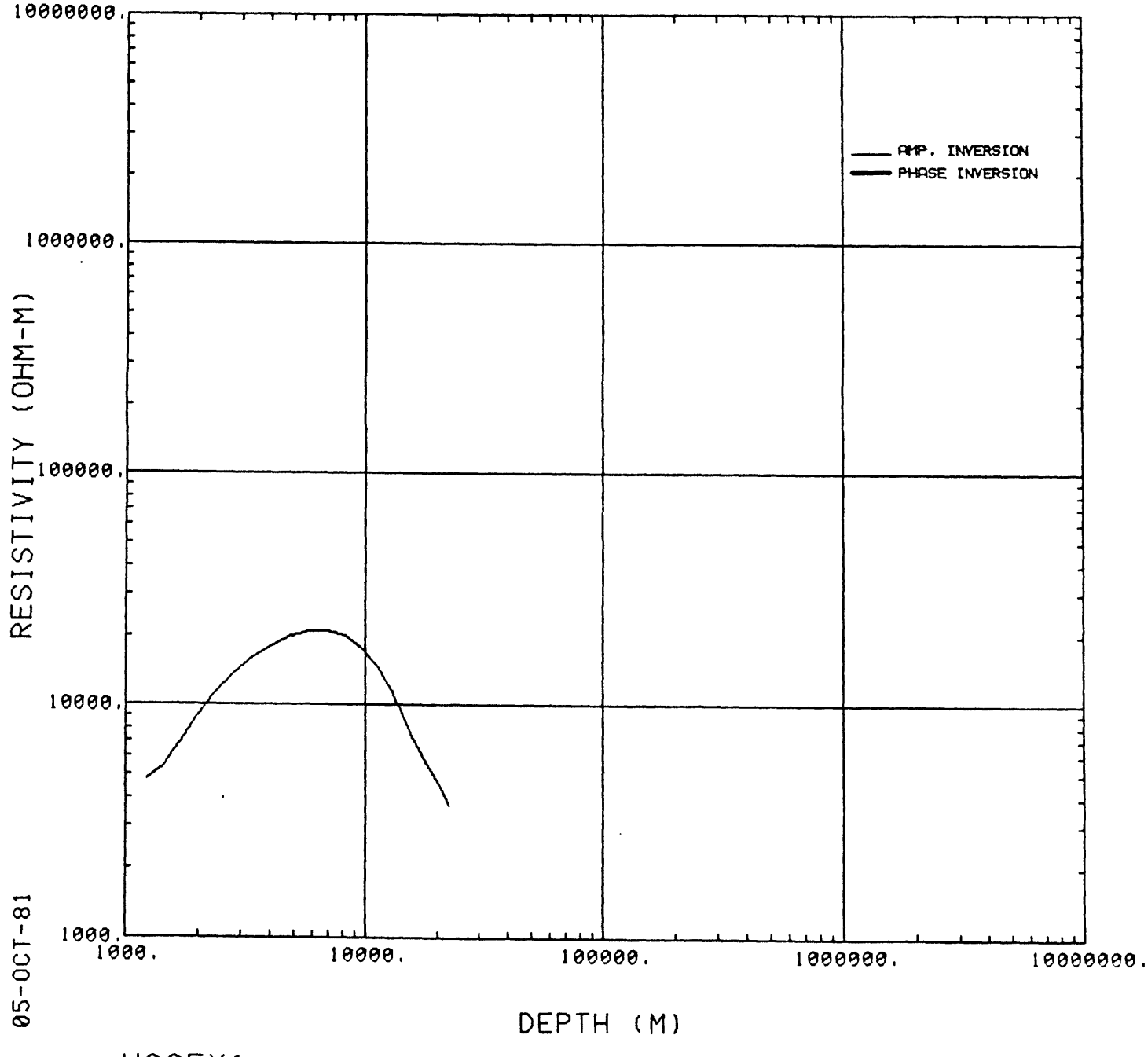
10000000.
1000000.
100000.
10000.
1000.
RESISTIVITY (OHM-M)
AMP. INVERSION
PHASE INVERSION
1000.
10000.
100000.
1000000.
10000000.
DEPTH (M)
05-OCT-81
U005Y1

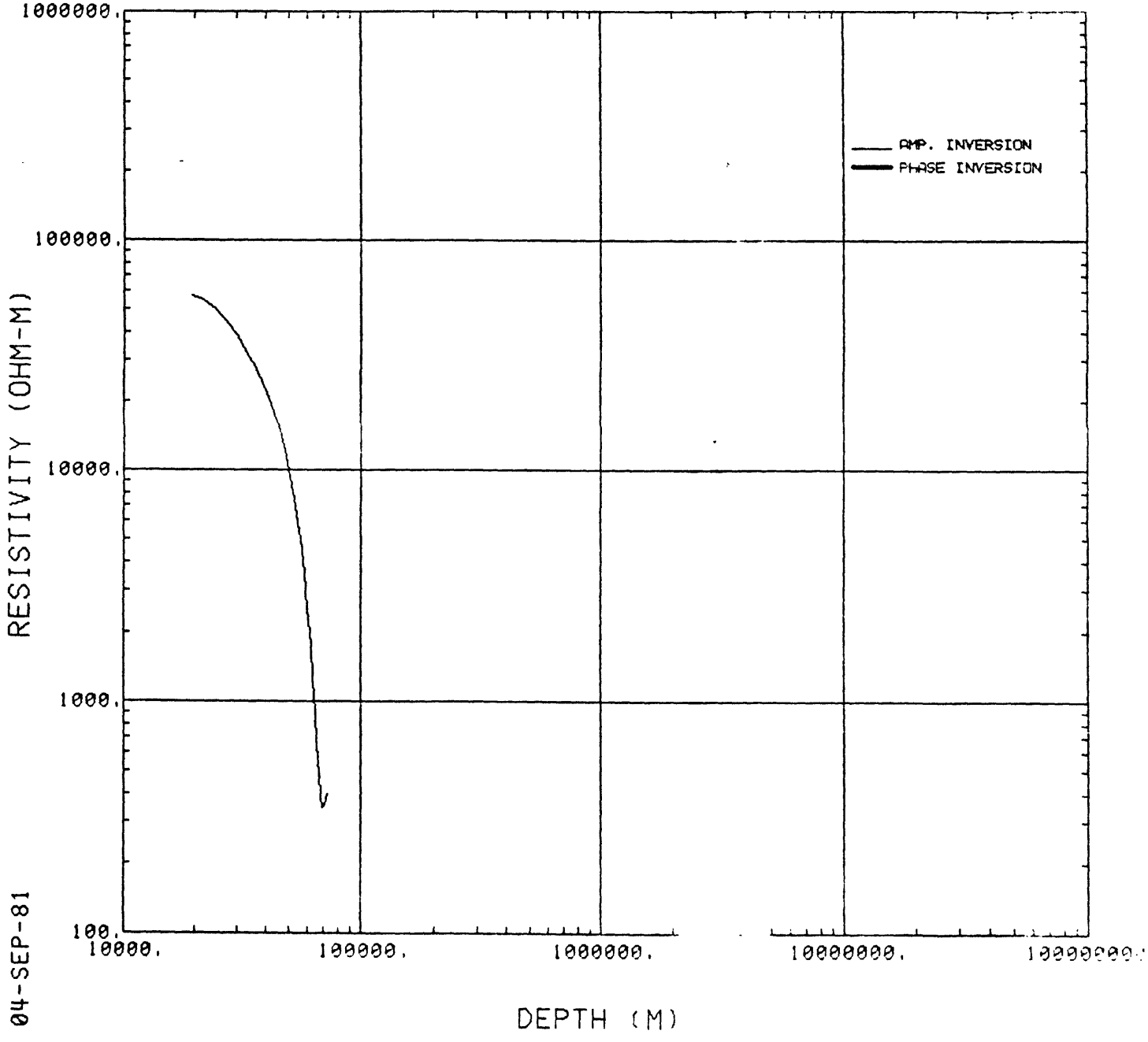
1000000.
100000.
10000.
1000.
100.
RESISTIVITY (OHM-M)
AMP. INVERSION
PHASE INVERSION
10000.
100000.
1000000.
10000000.
DEPTH (M)
04-SEP-81
U006X1

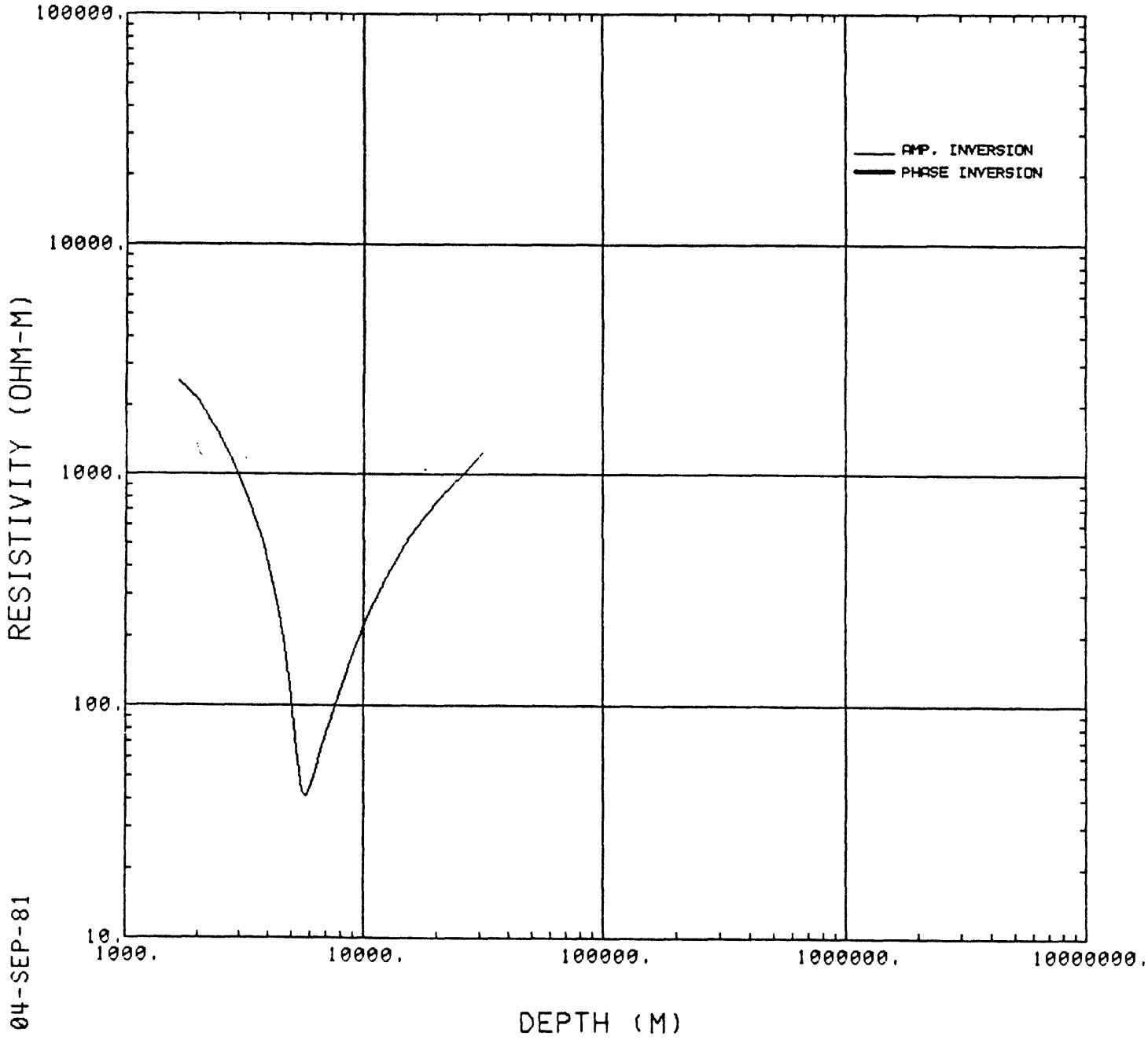
100000.
10000.
1000.
100.
10.
RESISTIVITY (OHM-M)
AMP. INVERSION
PHASE INVERSION
1000.
10000.
100000.
1000000.
10000000.
DEPTH (M)
04-SEP-81
U006Y1

L01

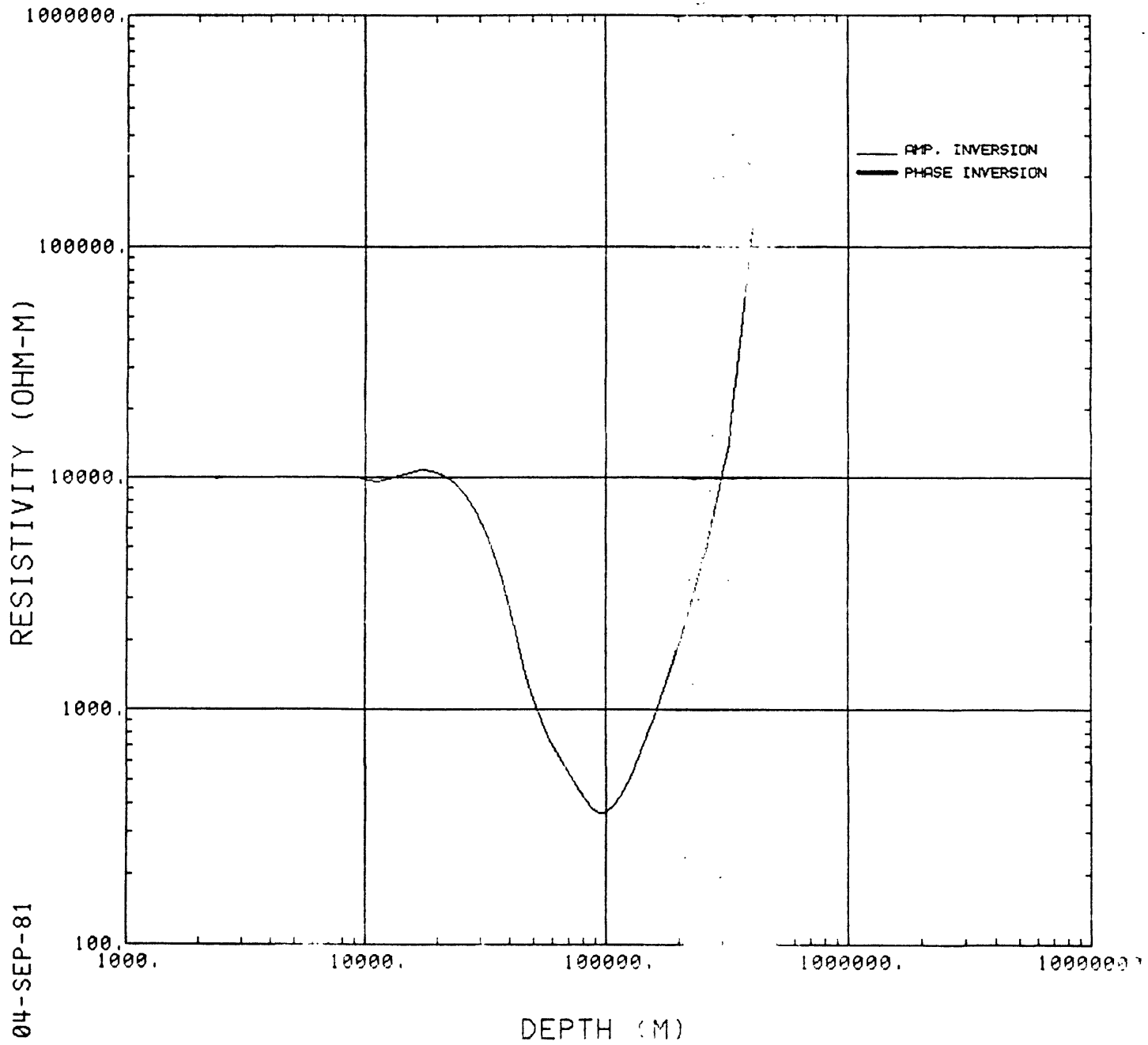
1000000.
100000.
10000.
1000.
100.
RESISTIVITY (OHM-M)
1000.
10000.
100000.
1000000.
DEPTH (M)
AMP. INVERSION
PHASE INVERSION
04-SEP-81

U007X1

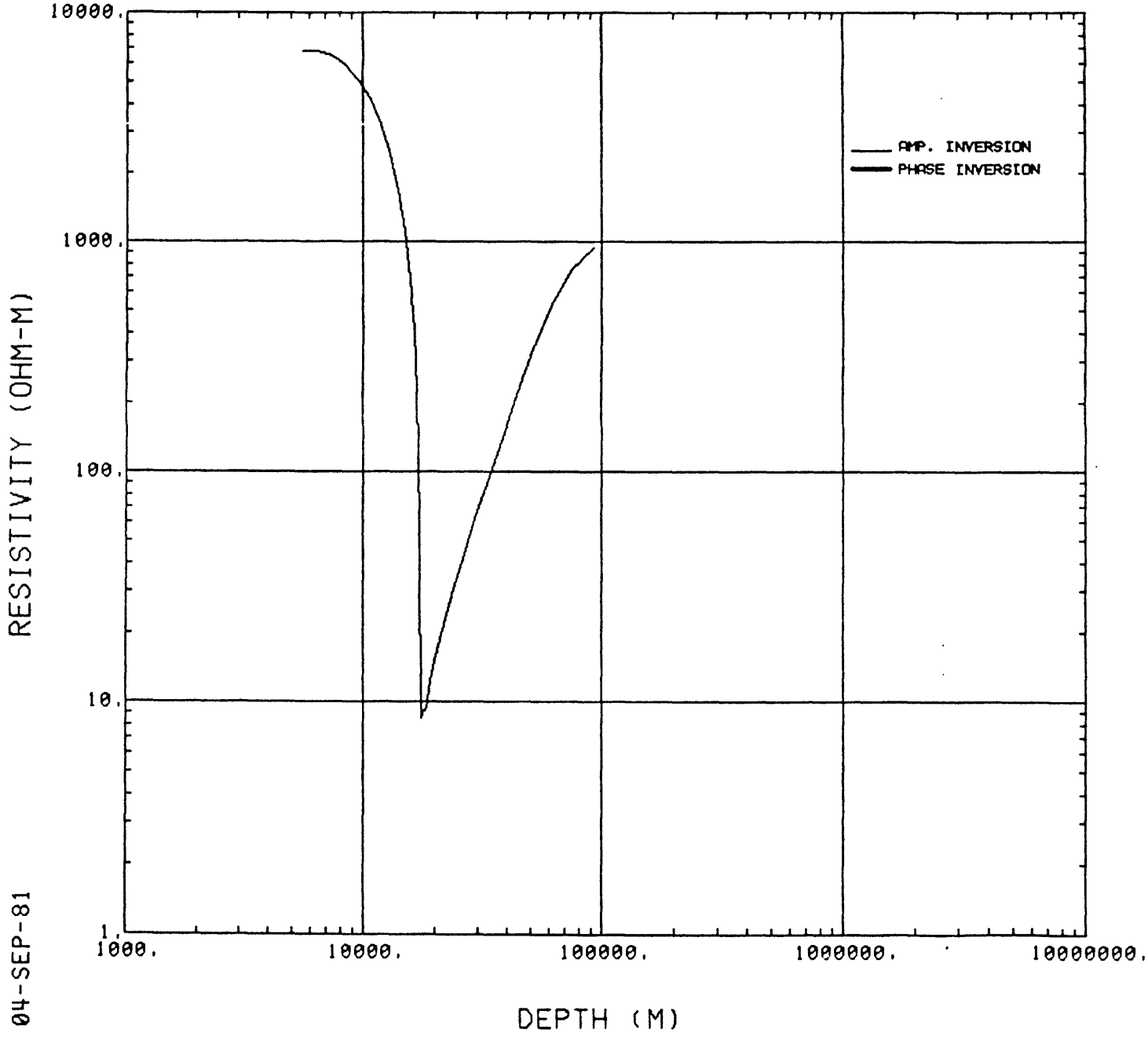
10000.
1000.
100.
10.
1.
RESISTIVITY (OHM-M)
AMP. INVERSION
PHASE INVERSION
1000.
10000.
100000.
1000000.
10000000.
DEPTH (M)
04-SEP-81
U007Y1

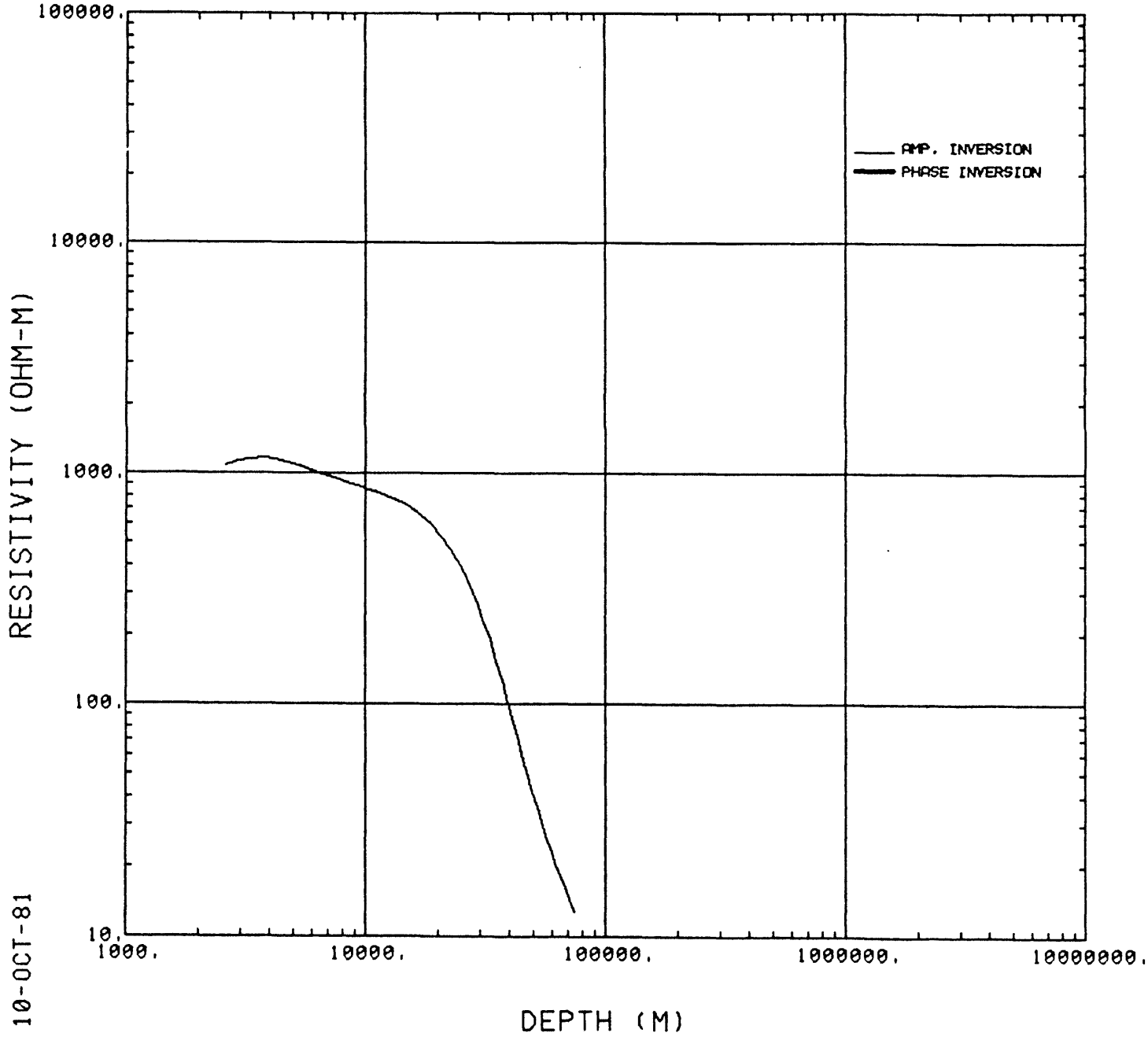
100000.
10000.
1000.
100.
10.
RESISTIVITY (OHM-M)
AMP. INVERSION
PHASE INVERSION
1000.
10000.
100000.
1000000.
10000000.
DEPTH (M)
10-OCT-81
U008X3

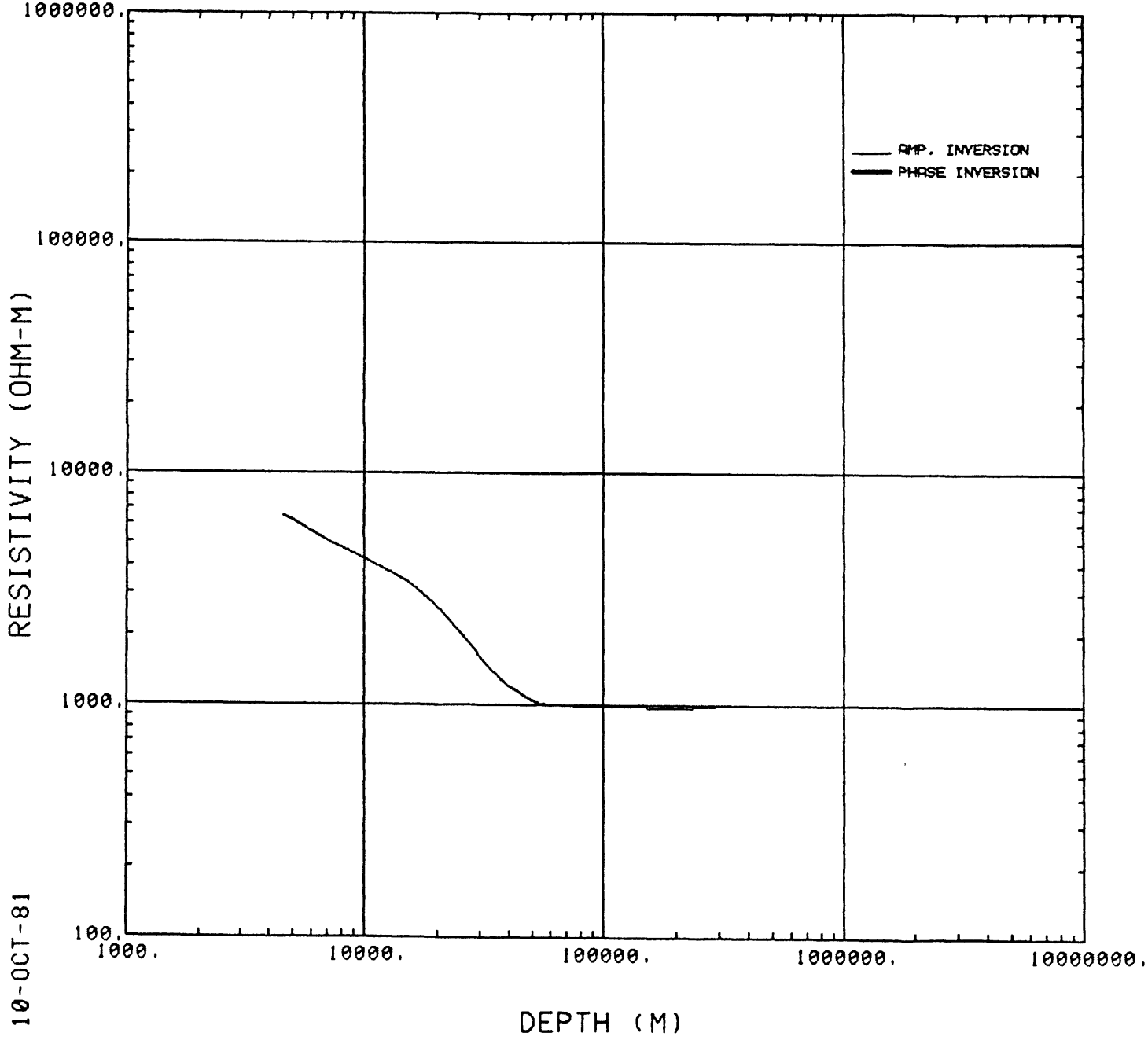
1000000.
100000.
10000.
1000.
100.
RESISTIVITY (OHM-M)
AMP. INVERSION
PHASE INVERSION
1000.
10000.
100000.
1000000.
10000000.
DEPTH (M)
10-OCT-81

U008Y3

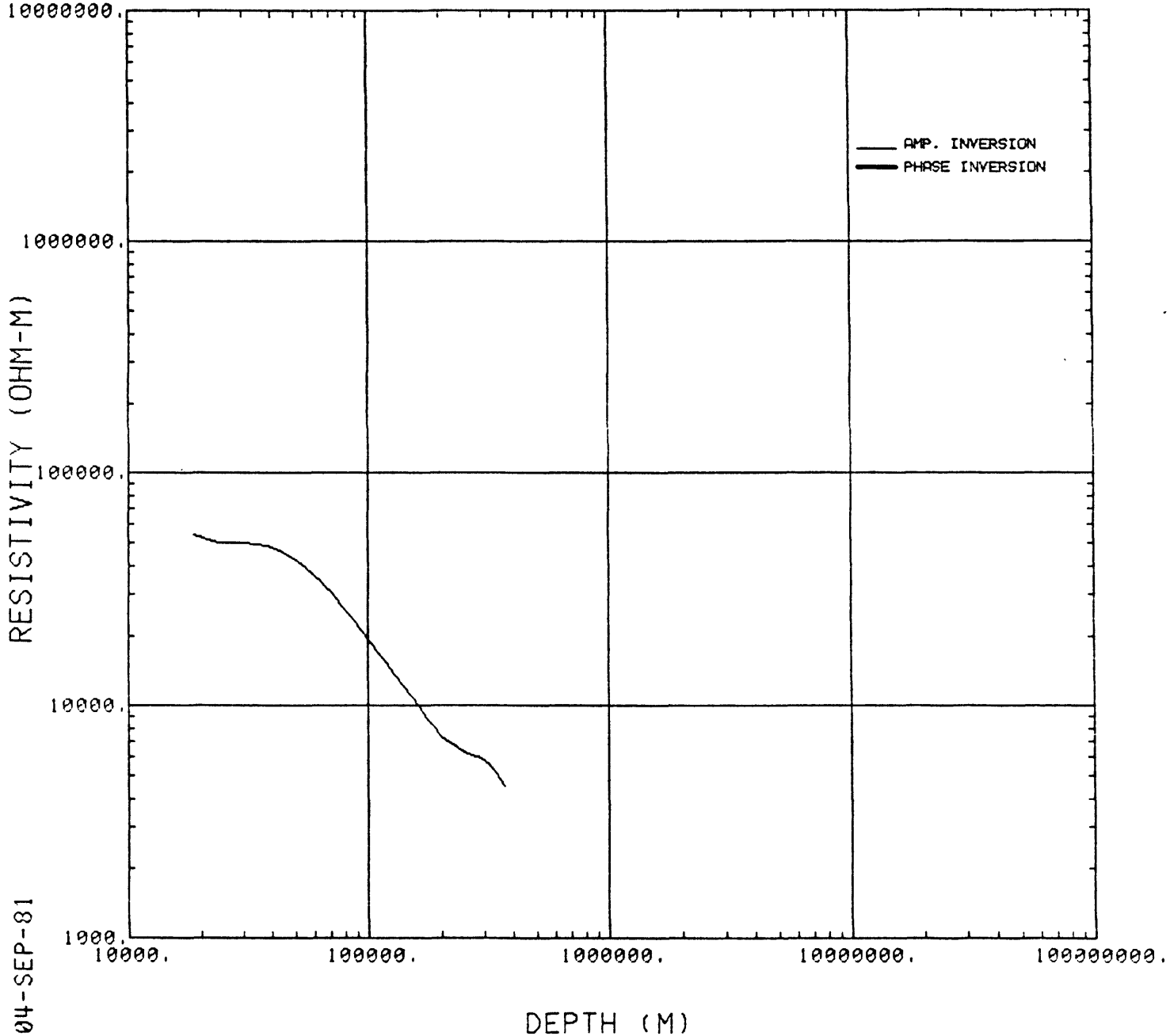
10000000.
1000000.
100000.
10000.
1000.
RESISTIVITY (OHM-M)
AMP. INVERSION
PHASE INVERSION
10000.
100000.
1000000.
10000000.
100000000.
DEPTH (M)
04-SEP-81
U009X1

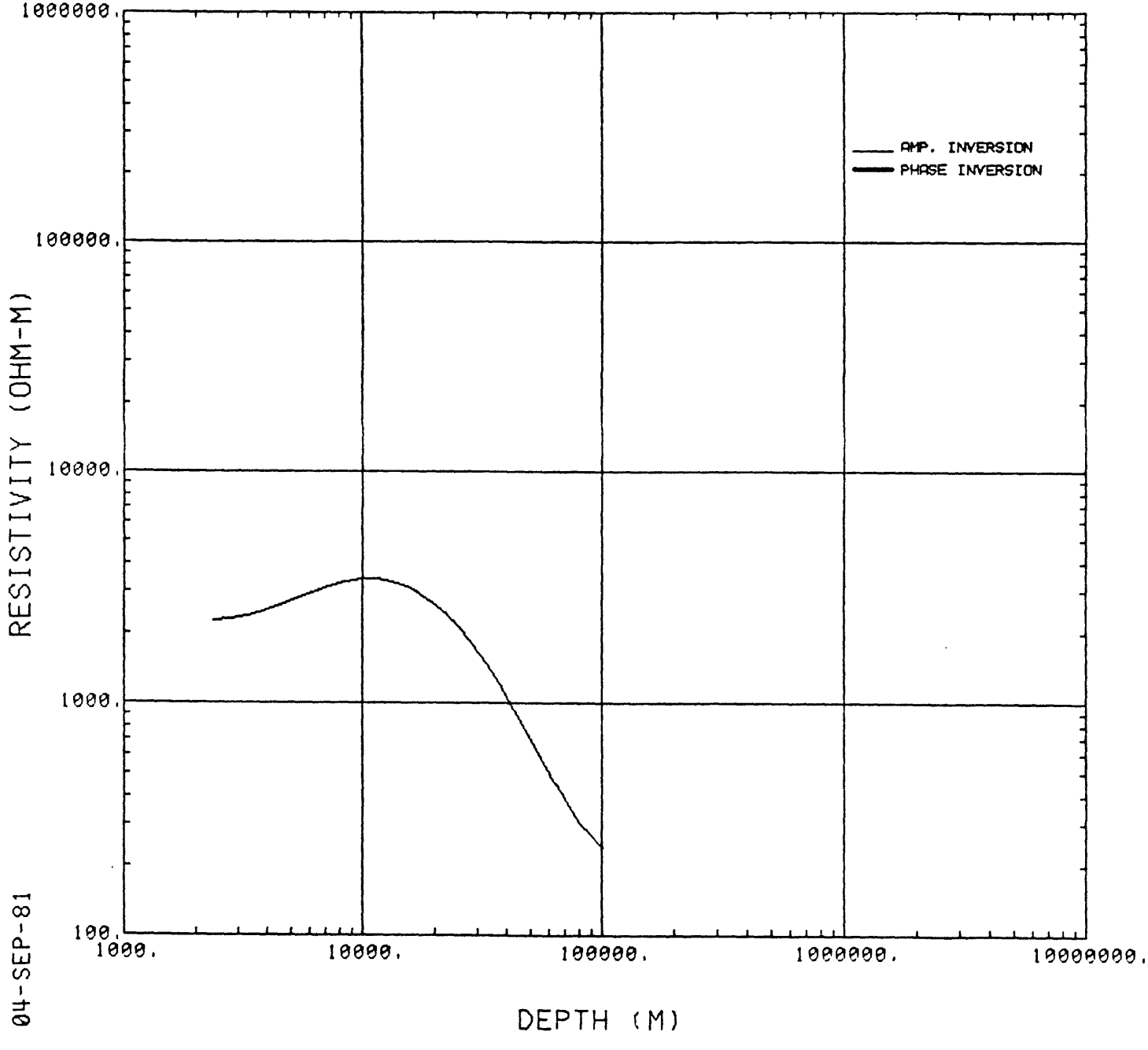
1000000.
100000.
10000.
1000.
100.
RESISTIVITY (OHM-M)
AMP. INVERSION
PHASE INVERSION
1000.
10000.
100000.
1000000.
10000000.
DEPTH (M)
04-SEP-81

U009Y1

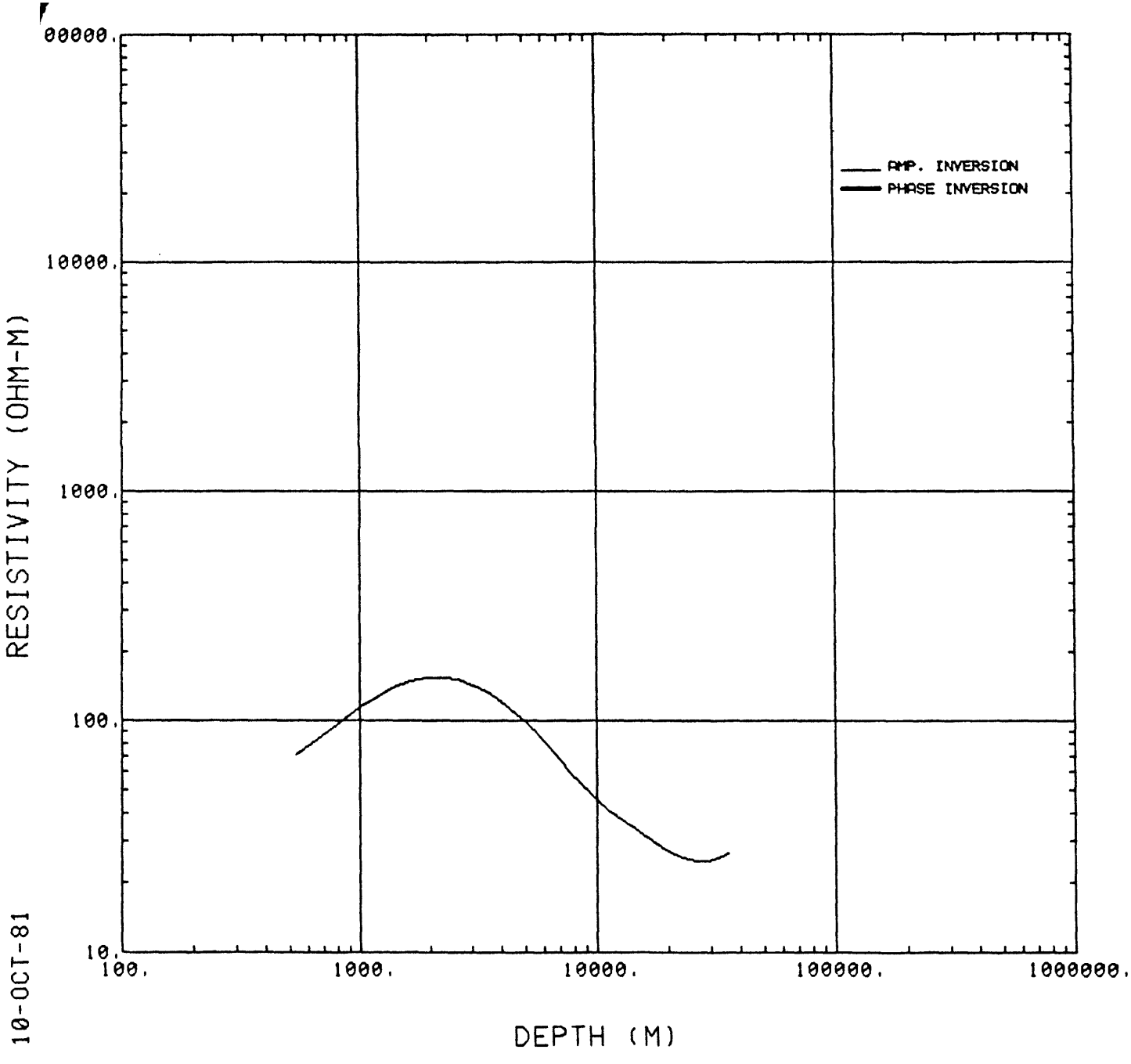
00000.
10000.
1000.
100.
10.
RESISTIVITY (OHM-M)
AMP. INVERSION
PHASE INVERSION
100.
1000.
10000.
100000.
1000000.
DEPTH (M)
10-OCT-81
U010X3

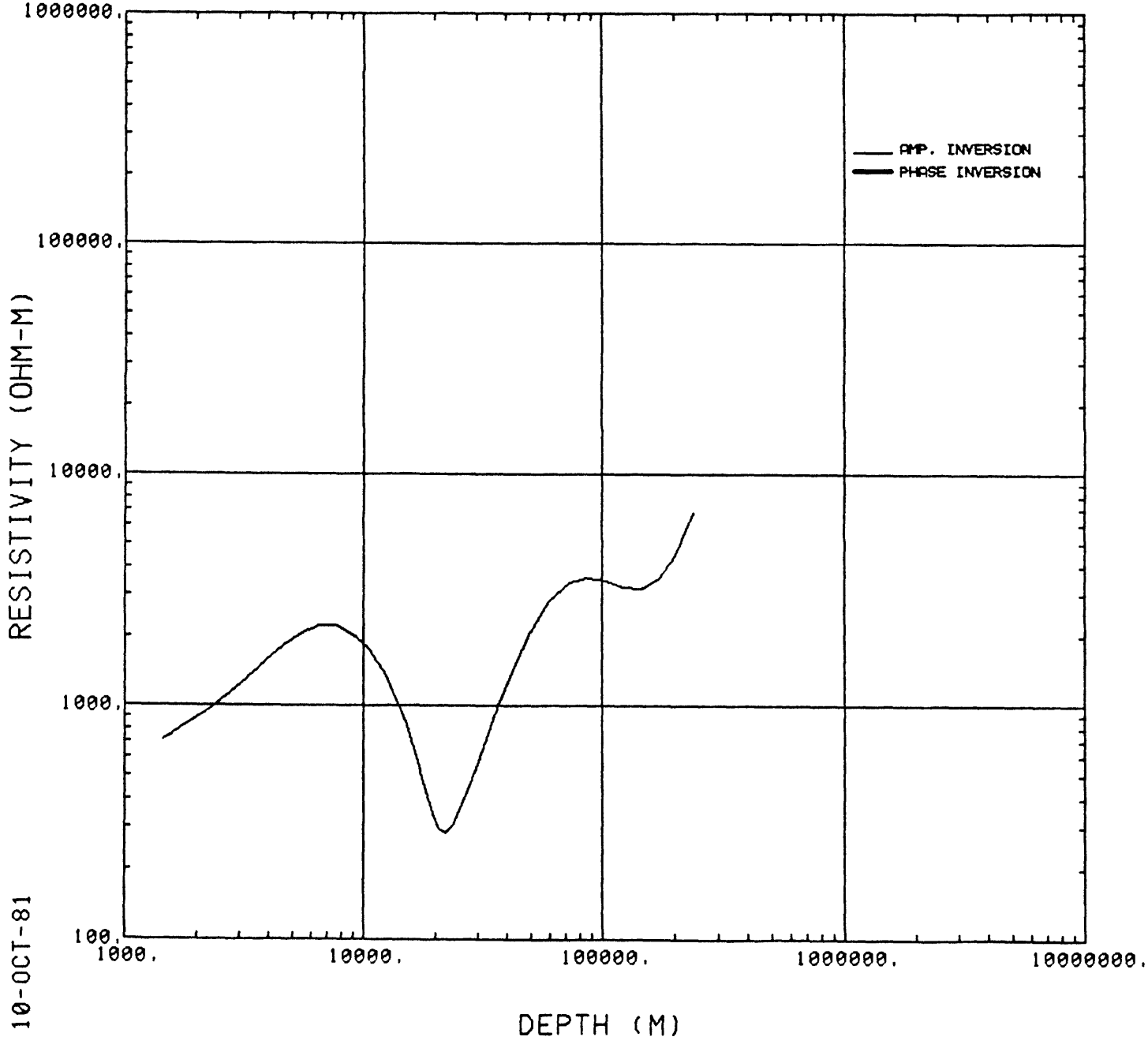
1000000.
100000.
10000.
1000.
100.
RESISTIVITY (OHM-M)
AMP. INVERSION
PHASE INVERSION
1000.
10000.
100000.
1000000.
10000000.
DEPTH (M)
10-OCT-81

U010Y3

APPENDIX E

NOTES ON THE INTERPRETATION OF MAGNETOTELLURIC DATA IN COMPLEX AREAS

by

Arnold Orange
Emerald Exploration Consultants
8108 Mesa, Suite A-215
Austin, Texas 78759

Revised and Expanded April 1981

APPENDIX C

TABLE OF CONTENTS

I. Introduction

These notes are intended to provide guidance as to the interpretation and understanding of magnetotelluric data obtained in geologically complex areas. The discussion will be non-mathematical, relying heavily on the use of computed models and analogies to other geophysical methods to explain interpretive concepts. The information will be presented in two parts; first a general tutorial discussion, which will be followed by examples applicable to the report to which these notes are an appendix.

In the context of these notes, complexity is defined as any geologic situation where the MT data differs markedly from that which would be obtained over a homogeneous or plane-layered earth. Obviously this encompasses a great many if not most prospects of current interest to explorationists. Therefore, MT will only be useful if meaningful interpretations can be obtained in these cases. We feel that such interpretations are routinely possible, but only when the effects of complex structure on the data are recognized and understood.

In the section that follows, the basis for MT exploration and a brief description of interpretive procedures will first be reviewed. Then, the MT effect as observed over representative structures will be discussed, with emphasis on potential interpretive "pitfalls" that await the unwary.

II. Interpretive Concepts and Pitfalls

A. Definitions

In order to understand the material that follows, it is necessary to become familiar with the terminology that is used to describe magnetotelluric data. It is assumed that the reader possesses a general familiarity with MT and its utilization as an exploration tool. For a review, the paper by Vozoff (1972)[1] is recommended.

1. Apparent Resistivity - Apparent resistivity is the basic parameter computed from the MT field data. It is a function of the ratio of electric to magnetic field variations, and is computed as a complex function (amplitude and phase) of frequency. While not giving the resistivity-depth relationship directly, the apparent resistivity vs. frequency is related to true resistivity vs. depth in that the electromagnetic field obeys the skin depth relationship; i.e., the lower the frequency the deeper the depth of investigation. (It should be noted that the apparent resistivity is not an interpretated function, but is the result of straightforward computation of the field-recorded data.)

2. True, or Intrinsic, Resistivity - Sometimes termed inverted resistivity, this function is derived from the apparent resistivity (1. above) and is expressed as

---

[1]Vozoff, K., 1972, The Magnetotelluric Method in the Exploration of Sedimentary Basins: Geophysics, Volume 37, No. 1, pp. 98-141.

resistivity vs. depth. True resistivity functions can be obtained by modeling, or thorough analytic inversion of the apparent resistivity-frequency function.

3. TE/TM Modes - In a one-dimensional setting (variation of resistivity with depth only) the apparent resistivity will be the same regardless of the azimuthal direction that the electromagnetic field is measured in. However, in a two-dimensional setting (variation of resistivity vertically with depth and horizontally in the dip direction, but with no variation along strike), due to the "channeling" of the flow of induced currents in the earth by the 2-D structure, the apparent resistivity will vary as a function of measurement direction. Borrowing from electrical engineering terminology, two "modes" are defined; TE (transverse electric), resistivity parallel to structural strike; and TM (transverse magnetic), resistivity perpendicular to structural strike. Note that the actual orientation of the field sensors is arbitrary, "rotation" to a coordinate system parallel and perpendicular to strike is an arithmetic step performed on the data in the computer processing step. Plots of apparent resistivity vs. frequency thus have two curves shown, representing the two modes. In the case of a departure from the assumption of two-dimensionality (towards the normal three-dimensional structure with finite strike dimensions), two modes are still computed but can no

longer be simply defined as parallel or perpendicular to strike.

4. Anisotropy - An anisotropic material is one in which the physical property under consideration is a function of the measurement direction within the material. In MT parlance, anisotropic data is data where the apparent resistivity varies with measurement azimuth, and two orthogonal resistivity functions (the TE and TM modes described in (3.) above) which differ (or are separated when plotted) are computed. Note that the "anisotropic" data may be the result of structure involving intrinsically isotropic materials.

5. Conductivity - Conductivity is the inverse of resistivity; i.e., high resistivity is low conductivity and vice versa. This is important as it is at times confusing when extremely low resistivity materials are referred to as "highly conductive".

6. Resistivity Contrast - The contrast between the resistivities of different materials; i.e., the resistivity contrast between a 100 ohm meter carbonate and 10 ohm meter shale is said to be 10:1. MT responds to contrast, and the ability to resolve an interface between two rock units is a function of the resistivity contrast and thicknesses involved.

7. Electrical Basement - In a vertical geologic section the depth of the deepest low-resistivity over high-resistivity interface which can be resolved, and which occurs

at or above anticipated geologic basement. A point of confusion often arises when, for example, geologic basement (say Precambrian granite) is overlain by Paleozoic carbonates, which are in turn overlain by a marine clastic section. If the carbonates are tight and roughly equivalent to the granite in resistivity so that there is little or no electrical contrast between them, then the electrical basement will be at the high resistivity contrast, clastic-carbonate interface. Thus, electrical basement may be several thousand feet above what is normally considered geologic basement.

B. Rock Resistivity

The interpretation of MT data requires a familiarity with the relationship between rock types and the resistivities inferred from MT data. While there is a correlation between rock resistivities as measured by well logs and those measured by MT, it must be borne in mind that the log investigates properties only in the immediate vicinity of the well bore while MT investigates bulk properties averaged over a considerable volume of rock. The resistivity of most rocks, and virtually all of the rocks of interest to hydrocarbon exploration, is determined by the fluids contained within the rock. This is because the dry rock matrix is a virtual insulator and for even the tightest of crystalline rocks electrical conduction can be considered entirely through the

pore fluids. In sedimentary rocks the conduction is through the fluids which are present in the ordinary pore spaces in the rock. In very tight rocks; the igneous, metamorphic and nonporous carbonate rocks where intrinsic porosity is very low, the fluids in joints, cracks and faulted zones become the primary conductors. Thus the factors affecting resistivity are the porosity (bulk porosity including intergranuler pores as well as micro and macro-joints) and the salinity of the pore fluids. Of lesser importance at oil explorative depths is the temperature of the formation, this becomes a strong factor in locating geothermal anomalies.

As an aid to the interpreter, the following table presents an approximate relationship between rock types and in situ bulk resistivity. As with most phenomena in nature there are important exceptions.

Table 1

Rock Resistivities

Rock Type	Resistivity Range	
Clay	1-5	ohm meters
Shale	2-20	ohm meters
Sandstone	10-80	ohm meters
Carbonate*	50-500	ohm meters
Volcanics (flow)*	200-4000	ohm meters
Igneous*	1000-10,000	ohm meters

*Unfractured; jointing and fracturing especially if fault-related can drop resistivities in excess of an order of magnitude.

C. Interpretive Procedures

The interpretation of MT data as currently practiced by most geophysicists active in the field relies heavily on one-dimensional inversions of the parallel to strike (TE) component of apparent resistivity. Two-dimensional models are used as an aid to interpretation but final resistivity and geologic sections are most frequently seen as contoured or "picked" sections with the one-dimensional (TE) inversions as the base. This technique is applicable in many instances, and excellent MT interpretives have been produced as a result. There are, however, important geologic structures where the TE based, one-dimensional inversion interpretation will be seriously in error. To avoid this the interpreter must learn to recognize those situations where the procedure is inappropriate, and to have available alternate procedures to follow in order to arrive at a successful interpretation.

Probably the single most important interpretive step is the systematic examination of the apparent resistivity verses frequency data for the survey area. This step, roughly equivalent to the familiar seismic "brute stack", yields (a) the approximate vertical sequence of resistive and conductive units, (b) approximate location of faults and structural trends, and (c), most important, the structural complexity as evidenced in the data, which will indicate which modeling route to take for the continuation of the interpetation. The above procedures involve examining all of the MT data with an

eye to the interrelation between sites, as impressions gained from an individual site by itself or even a single profile may be misleading. As will be seen from the examples that follow, it is most important to identify evidence of strong two and three-dimensional effects. While one is usually forewarned by preliminary geologic and regional geophysical (gravity, magnetics) studies, frequently the MT data will exhibit unanticipated effects. The qualitative examination step identifies these effects, and leads to the determination of the approriate modeling procedures.

Modeling relies heavily on two-dimensional "case" models, which are used to identify the structural style of a prospect and to provide either a basis for the appropriate use of one-dimensional inversions, correction factors for the inversions, or an indication that the one-dimensional inversions will be inappropriate and that more exact two-dimensional models will be required. In the case of strongly three-dimensional situations, no currently available modeling procedures may be appropriate.

D. Examples and Pitfalls

1. Introduction

It is not possible within the confines of these notes to present an exhaustive compedium of MT data "type" examples. The few cases presented are considered among those most important to practical exploration problems. Attention is

drawn to the summary at the close of the section, where we endeavor to point out the concepts that it is felt are most critical.

The examples, as well as the rest of these notes for that matter, are not offered as an unbiased, academic treatise, but are the results of many years of active MT interpretation, and of watching other interpreters at work.

"Pitfalls" lie in wait of the unwary in each of the cases to be discussed. In many cases there would be no pitfall if perfect, noise-free data were available and if data were recorded at any and all points on the surface. However, noisy data, and more important, a finite sampling of the surface, lead to ambiguities and potential misinterpretations. For the examples the effects of noise and low site density will be pointed out.

NOTE: For each example the model results will be shown as plotted apparent resistivity verses frequency, in a manner identical to the presentation of the apparent resistivity computed from field data. TE is resistivity parallel to strike, TM is resistivity perpendicular to strike.

Each example contains a sketch of the model, and a sketch of the resistivity curve computed at one or more locations on the surface. Curves noted as "1D" are the layered earth, forward model for the sequence of interfaces

vertically beneath the indicated location. The sketch of the model geometry is a sectional view perpendicular to the strike of the structure. As a two-dimensional feature each structure is considered to extend to infinity into and out of the page.

2. Two-Dimensional Model Series - Shallow Feature Test (Figures 1 through 3)

Object: The object of this series of models is to examine the "statics" effect on MT data resulting from shallow resistivity anomalies. Such anomalies might be represented in nature by alluvial-filled depressions, stream beds, narrow valleys bounded by outcrop, etc. These shallow resistivity anomalies have the effect of shifting the MT apparent resistivity verses frequency and intrinsic resistivity verses depth sections in a manner completely analagous to the effect of shallow velocity anomalies on seismic data of shifting the time and depth sections. Hence the term "statics correction" is used in an identical sense in both cases.

Description of Models: These models consist of a thin tabular layer on the surface in an otherwise plane-layered earth. The only two-dimensional complexity is the surface layer termination. Resistivity data is plotted for measurement locations on both the resistive and conductive sides of the boundary. The different models have been

computed with various resistivity values to illustrate varying degrees of the statics effect.

Description of Results: The model for Figure 1 contains a low contrast (2:1) shallow resistive body. The tabular body may be thought of as a thin, discontinuous resistive volcanic or carbonate layer. The effect in the immediate vicinity of the contact is a shift of the TM curve over the full frequency range, a conductive shift on the conductive side, a resistive shift on the resistive side. The TE curves for the two cases are nearly identical except for the highest frequencies. The 1-D curve is virtually identical with the TE curve, thus inversion of the TE curve will give the best interpreted subsurface resistivity. The inversion of the TM mode curve on the conductive (left) side will result in a computed depth to the electrical basement interface (actually at 6500 feet) as erroneously shallow, while on the resistive side the error will be towards a too deep pick. At a distance of 1000 feet from the boundary the effect has virtually disappeared, with TE and TM curves almost coincident.

The model of Figure 2 is the same geometry as that of Figure 1, but with a higher, 8:1, contrast. The conductive, 5 ohm meter unit may be a saturated clay or alluvial unit. The effect again is a shift of the TM curves. The 1-D solution is not identical to the TE curve, but is close enough to make

the TE solution a good approximation if the error at the high frequencies is corrected.

Discussion: The problem presented to the interpreter by this class of models is to insure that the mode selection is correct, since obviously it is the TE curve one wants to chose to invert. Mode selection is simple with closely spaced sites, but since the effect dies out significantly in a mile or less, if sites are two or more miles apart as in a normal reconnaissance survey then site-to-site correlation becomes difficult. The vertical field relationship, which one would like to utilize for mode selection, presents problems in two ways: First, the vertical field for these features is relatively weak, the effect is easily dominated by a deep, major geologic structure which can be at some distance. Second, because the vertical fields are weak, noise presents a real problem. It is often difficult to record good vertical field data, especially at the higher frequencies which are needed here. Thus, in the case of simple, parallel curves such as shown in the examples, the interpreter must often rely heavily on topographic and surficial geologic maps to decide which curve to utilize. If all else fails an alternative is to minimize the possible error by drawing an "average" curve between the two plotted curves.

A potentially more serious problem exists in the case of data exhibiting complexity due to deep, significant structures

with the effects of a shallow feature superimposed. Consider the examples shown on Figure 3. Assume that the interpreter wishes to rely heavily on the curve identified as TE in Figure 3A. The separation of the curves at 100 Hz indicates that the curves are affected by a near surface feature, in addition to the deeper feature causing the further split below 10 Hz. If the curve marked "TE" is TE also with respect to the near surface feature, then it can be safely inverted and interpreted "as is". If, on the other hand, the marked TE curve is in reality the TM curve with respect to the near surface feature, then it must be shifted as shown to eliminate the "statics", or near surface feature, effect. In a case such as that illustrated the vertical field is usually of little help, since the effect of the deep feature will tend to dominate that of the shallow feature so that the determination of which curve to adjust must again be based on geologic and topographic evidence.

Of even more concern is the hypothetical case shown in Figure 3B. Here, with the effect more subtle, the interpreter may not know which curve to shift, and in all likelihood will need to test an interpretation using both curves. The shift shown, although of low amplitude, will nevertheless significantly affect the interpretation of a structure of exploration interest. Thus, the examination of each site and a determination of the correct shift can be of crucial importance.

3. Two-dimensional Model Series - Fault and Graben Geology (Figures 4 through 6)

Object: The object of this series of models is to examine the MT effect caused by large scale faulting, especially that which comes near or to the surface. Such features dominate MT data acquired in the basin and range provinces, and are a major factor in the interpretation of many mountainous prospects. The effect on the MT data is a marked anisotropy, or difference between the two MT curves. The anisotropy is not as simple as for the shallow features discussed in the previous section, and can be much more extreme. In the previous section the effect was a "shift" or offset in one or both curves. In the models to be presented here often the two curves bear little or no similarity to one another, or to the one dimensional solution at the location in question.

Description of Models: The models consist of simple fault or graben situation, with the faults or bounding faults brought to or near the surface. A high 100:1 resistivity contrast is used to illustrate the effects, with the conductive clastics and/or recent fill modeled by 10 ohm meter materials and the resistive carbonate and crystalline rocks modeled by 1000 ohm meters. The extremely deep, hot lower crust is modeled by 10 ohm meters.

For each model the computed MT data is shown for two cases, one on either side of the fault or bounding fault. Both

TE and TM curves are shown, as well as the one-dimensional, layered earth solutions. Note that it is the 1-D solution that, if it could be measured or computed would, when inverted, lead to the most accurate interpretation of the subsurface immediately beneath that one site alone.

Description of Results: The model of Figure 4 contains a fault to the surface with a throw of 6560 feet, with a 10 ohm meter conductive section terminating against the fault. The computed apparent resistivity is shown for "sites" 6560 feet on either side of the fault. Note the vertical scale difference between the two plots.

The data illustrates the important features of this class of models. On the conductive (right) side of the fault the TE curve is of the same form as the 1-D solution, but exhibits a shift to the right. The TM curve, on the other hand, bears no relationship to the 1-D solution, showing a strong "undershoot" at the frequency where the resistive electrical basement becomes evident on the TE.

On the resistive (left) side of the fault neither curve is a good approximation to the 1-D solution, although the TM curve is probably least misleading. The TE curve is strongly affected by the 10 ohm meter material across the fault, a phenomenon similar to the "side shot" in seismic data. If the TE curve were inverted and used alone as the base for an interpretation, a non-existent conductor would be the result.

Clearly both sites together are needed to arrive at a correct solution since, except for the resistivity shift crossing the fault, certain similarities in curve character exist when comparing the two. This would be expected to be even more of a problem with field data where noise and more complicated geology combine to make the data less clear cut. If the geology is clearly two-dimensional, the vertical field can be used to good advantage to arrive at the strike direction, and then the resistivity magnitude used to determine which is the upthrown, resistive side of the fault.

The model of Figure 5 is a 10 ohm meter material filled graben with the bounding faults brought to the surface. The results are similar to the previous model, except that the TM curve on the graben shows an even more extreme undershoot than for the simple fault model of Figure 4. Also note that on the upthrown (resistive) side, the TM curve is clearly a better approximation to the 1-D solution than the TE.

The model of Figure 6 is the same structure of Figure 5, but with the graben bounding faults terminating 820 feet below the surface, and the 10 ohm meter graben materials acting as a cover over the shallow 1000 ohm meter electrical basement off of the graben. Examination of the resistivity curves shows that there is a substantial change

in curve shape, in particular the extent of anisotropy, when the resistive contact does not reach the surface. The TE mode remains the best approximation to the 1-D solution on the graben, while the TM is marginally better on the resistive side.

4. Two-dimensional Model Series - Horst and Unrooted Block Geology (Figures 7 through 9)

Object: The object of this series of models is to examine the difference in MT response between rooted horst and unrooted "horst-like" structures. The question is frequently posed as to whether an outcrop, often Precambrian, is autochthonous (rooted) or allochthonous (unrooted, or thrust from elsewhere). MT, with its capability to detect conductive rocks beneath surface crystalline masses, is a natural tool to provide the answer.

Description of Models: The models consist of a simple horst block with vertical bounding faults brought to the surface. The horst is 12.4 mile wide and electrical basement on the downthrown sides is at 6560 feet. Material bounding the horst is 10 ohm meters while the horst and basement is 1000 ohm meters. A 10 ohm meter conductive lower crust is placed at 100,000 feet.

The model of Figure 7 is the simple horst, with the 1000 ohm meter material extending to depth. For the models of Figure 8 and 9, the surface 1000 ohm meter block is 4920

feet thick and rests on conductive material of 100 and 10 ohm meters respectively. In both of these cases electrical basement beneath the block is at 6560 feet.

Description of Results: For the rooted horst, Figure 7, the results are similar in form to those of the graben, Figure 5. On the resistive side, on the horst, the TM curve "overshoots" while the TE curve is strongly influenced by the conductive material across the fault. Off of the horst to the left the non-familiar extreme anisotropy is seen, with the TM curve undershooting and the TE component most faithful to the 1-D solution.

The effect of conductive material beneath the horst is to depress both TE and TM components on the horst, and off of the horst to soften the effect on the TM component by bringing it close to the TE component. With 10 ohm meter materials beneath, Figure 9, the effect is less extreme, but unmistakable.

To continue with the discussion of the rooted horst structure, Figure 10 illustrates an extremely important interpretive point. Two models are shown, both of a horst. The left hand horst involves a resistivity contrast of 10 to 1, with the 1000 ohm meter material possibly representing crystaline rock and the 100 ohm meter material a carbonate or very tight sand. The right hand horst also involves a resistivity contrast of 10 to 1, with the 100 ohm materials possibly as above and the 10 ohm meter materials a porous

sand or shale. Data is plotted for a site on the 100 ohm meter material for both models, which is the off-horst material on the left hand model and the horst material to the right. The scales for the two plots are identical. The form of the data including both curves is very similar for the two cases, and in the presence of noise they would be virtually indistinguishable. The consequences inferred by this model are as follows:

a. Closely spaced sites on either side of the bounding fault will clearly and unambiguously identify the structure.

b. Reliable vertical magnetic field data will identify the TM mode, and also lead to an unambiguous solution <u>if the area is truly two-dimensional</u>. It cannot be overemphasized that the vertical field data, either through noise or the presence of three-dimensional structural features, is frequently ambiguous or misleading. Bear in mind that a vertical magnetic field null occurs at the center of the horst, so that any structural complications along horst strike may easily result in mode misidentification if the vertical field is relied upon. (The vertical field will point or "tip" towards or away from the along-strike structure rather than to the horst-bounding faults, since the effects of the latter cancel in the center of the horst.)

c. The data at adjacent sites are interrelated, more so as complexity increases. No data may be "taken for granted" but must be examined in light of all available information.

5. Three-dimensional Considerations

While it has long been realized that three-dimensional structure will have an affect on MT data, it is only recently that modeling results have become available to provide quantitative analysis and insight into exploration problems. The data discussed here are the results of studies conducted at the University of Utah Department of Geology and Geophysics and reported recently by P. E. Wannamaker, S. H. Ward, G. W. Hohmann, W. R. Sill[2], Sam C. Ting and G. W. Hohmann.[3]

The principal conclusion resulting from the model studies is that, for three-dimensional structures, interpretations based on one-dimensional inversions do not apply. Further, in many cases the TM two-dimensional interpretation will provide an acceptable interpretation.

Consider the example in Figure 11, which has been taken from the referenced report. The model geometry shown on Figure 11 (designed around the constraints of the modeling program) consists of a 14 km wide by 1 km thick low resistivity (2 ohm meter) body buried 1 km in 400 ohm meter country rocks. The feature is shown in section on the figure, and extends for 36 km along strike perpendicular to the plane of the section, as shown on the plan view. Apparent resistivities

---

[2]"Magnetotelluric Models of the Roosevelt Hot Springs Thermal Area, Utah", Report N. DOE/ET/27002-8, University of Utah, September, 1980.

[3]"Integral Equation Modeling of Three-dimensional Magnetotelluric Response", Geophysics, Vol. 46, No. 2, February 1981; p. 182-197.

were computed for only three frequencies due to the lengthy calculation (20 hours per frequency) required.

Computed apparent resistivity curves are shown on Figure 12 for positions on and off the slab. Also shown are the "TE" and "TM" curves for a hypothetical two-dimensional model calculation assuming the slab to be infinitely long (in the 36 km direction). The similarity of the 3-D "TM" curves to the 2-D TM curve is apparent. It is also apparent that the 3-D "TE" curve does not agree with the 2-D TE curve, especially for site B on the conductive slab.

The utility of the TM 2-D solution in 3-D situations is a mixed blessing. On the one hand it allows the interpreter to relate field data to models that can be computed economically (three-dimensional MT models currently consume hours of large computer CPU time). On the other hand, the TM solution can be extremely insensitive to structure. For the example of Figure 12, on the slab the TM (and 3-D) solution do not reflect the underlying 400 ohm meter basement, and structure on the basement surface or intrabasement will be very difficult to locate.

As the three-dimensional structure elongates and begins to approximate the two-dimensional case, the "TE" component (electric field parallel to strike) begins to approximate the 2-D model TE component. This is a frequency dependent effect, with the higher frequencies reacting first as the along-strike dimension increases. To turn the previous

statement around, the lower frequencies will continue to reflect the 3-D phenomena as the structure elongates long after the high frequencies approach the 2-D model curves. Thus, extra caution is required at all times in interpreting the deeper events, especially where structural complexity is known to exist.

The severe effect of three-dimensional structures places additional constraints on the interpreter. Not only must the resistivity components be identified correctly, but the presence and nature of three-dimensional structure must be evaluated. Since an MT grid of sites capable of this evaluation will rarely be economically possible, then geologic studies and gravity and magnetic data will have to play a large part in the interpretation.

E. Summary

This section has touched on a variety of potential problems facing the MT interpreter. The individual interpreter is encouraged to build a "case book" of two-dimensional models in order to be able to recognize gross structure through matching field data with "type" model curves. In the case of three-dimensional structure, the MT data can be strongly affected, and recognition of these effects should be the first chore for the interpreter.

The necessity for a grid of closely spaced recording stations in complex areas should be apparent. The resolution

of the "statics" problem and the recognition of two and three-dimensional effects all require data acquired more than just widely spaced along a single profile. Site density will be a function of economics and of the availability of other reconnaissance exploration data. The most economical site layout results from survey planning based on all available information and guided by reference to computed "case" models.

The models presented provide an insight into the MT interpretation process. In the case of simple "statics", the MT curves are separated but parallel and the interpretive problem is one of choosing the right curve to correct. The problem becomes more difficult when additional structural complexity is present on top of the statics shift, and selecting the curve or curves to correct will in most cases involve study of data in addition to the MT.

It has been shown that faults at or near the surface can result in extreme anisotropy, as do the related horsts and grabens. Interpretation in these cases is a two-dimensional process and relies heavily on mode identification. When approximating the true resistivity section by use of one-dimensional inversions, a good rule of thumb is "TE mode on the conductive side, TM on the resistive".

Three-dimensional effects can be severe, in many 3-D cases the TE mode as defined for the 2-D case does not

exist and interpretations relying on TE inversions will be seriously in error. With 3-D modeling in its infancy and extremely expensive, the interpreter in 3-D situations must rely on proper use of a TM-mode based interpretation and as high a site density as possible, aided by all of the ancillary geologic geophysical data available.

TWO DIMENSIONAL MT MODEL

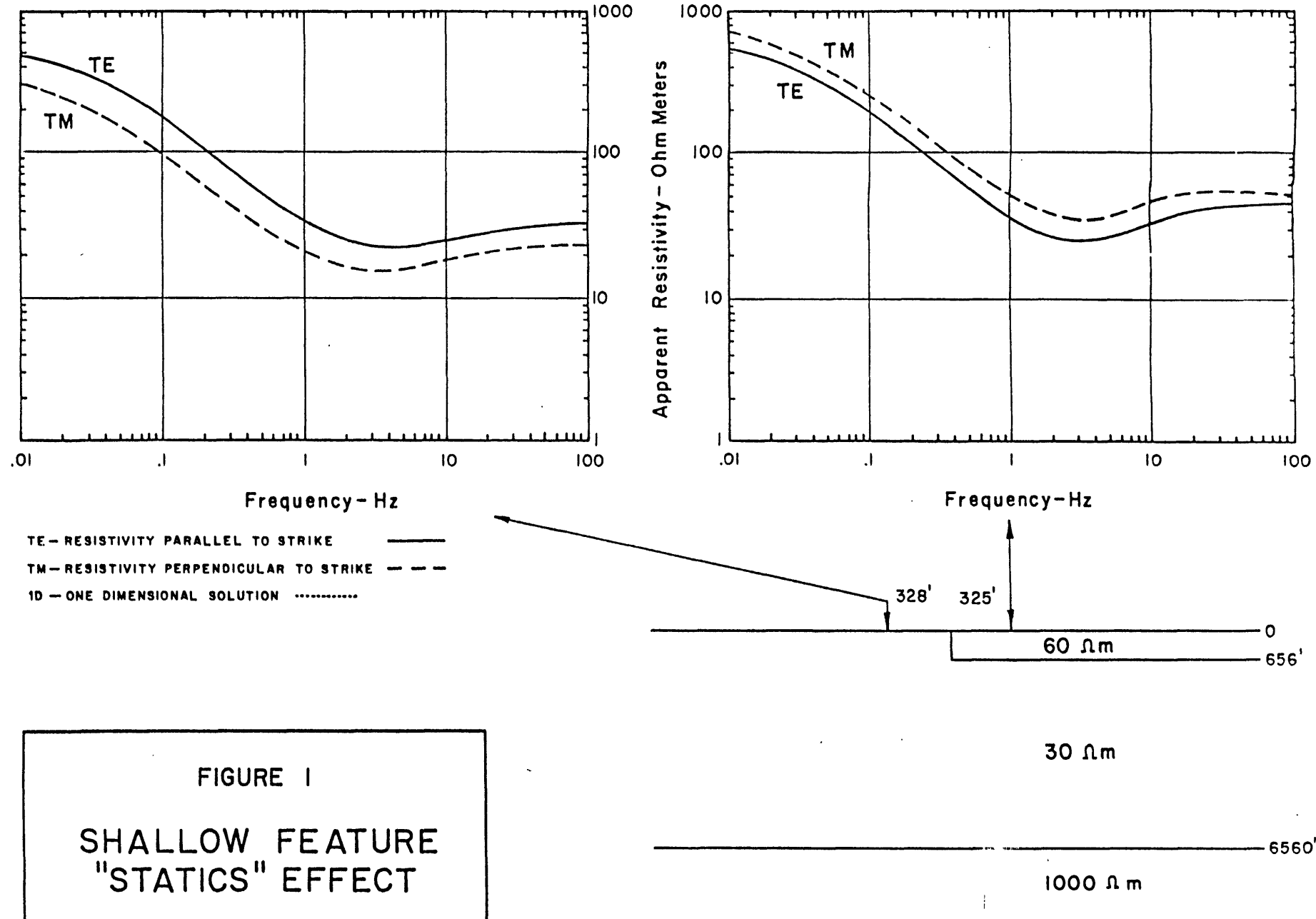

FIGURE 1

SHALLOW FEATURE
"STATICS" EFFECT

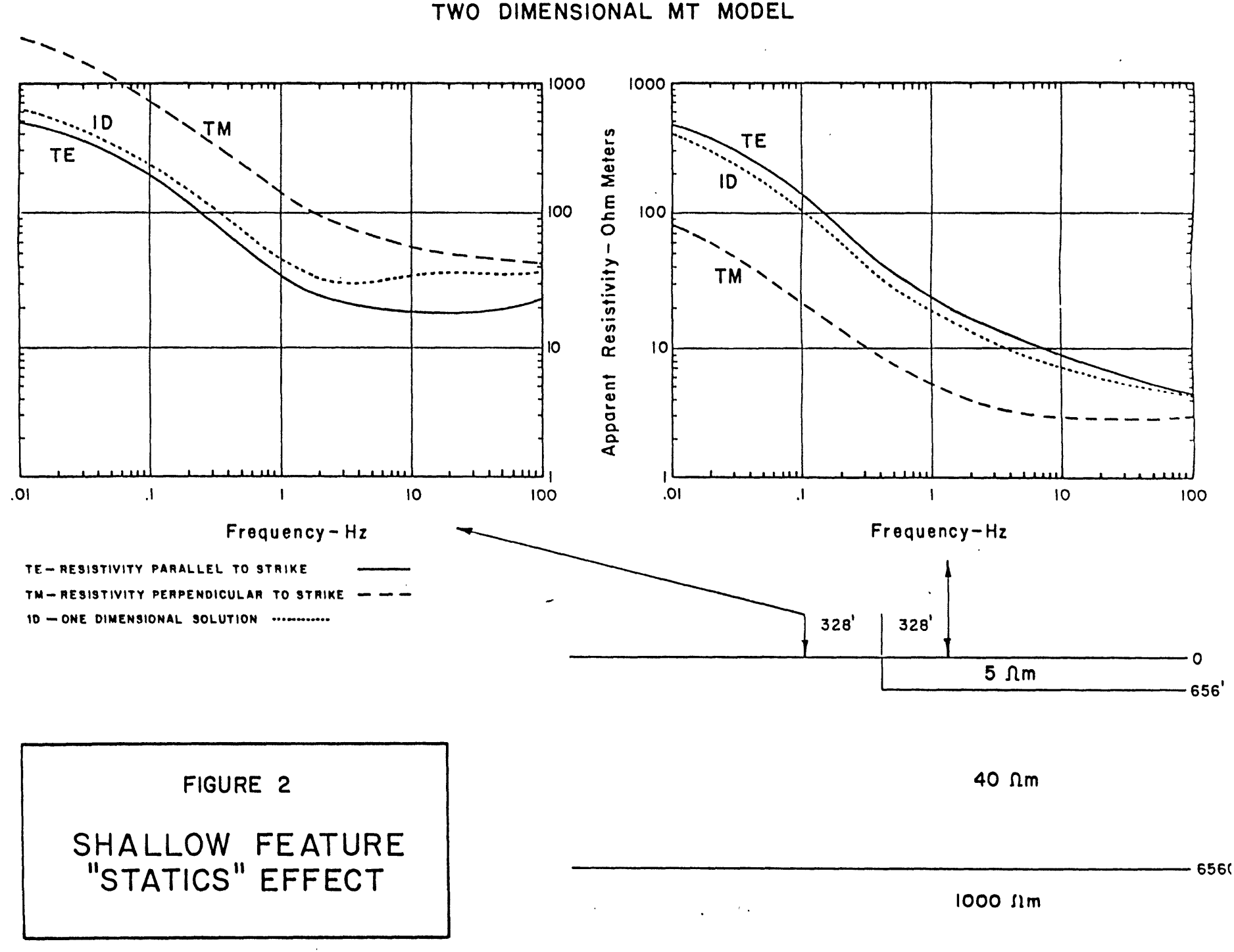

FIGURE 2

SHALLOW FEATURE
"STATICS" EFFECT

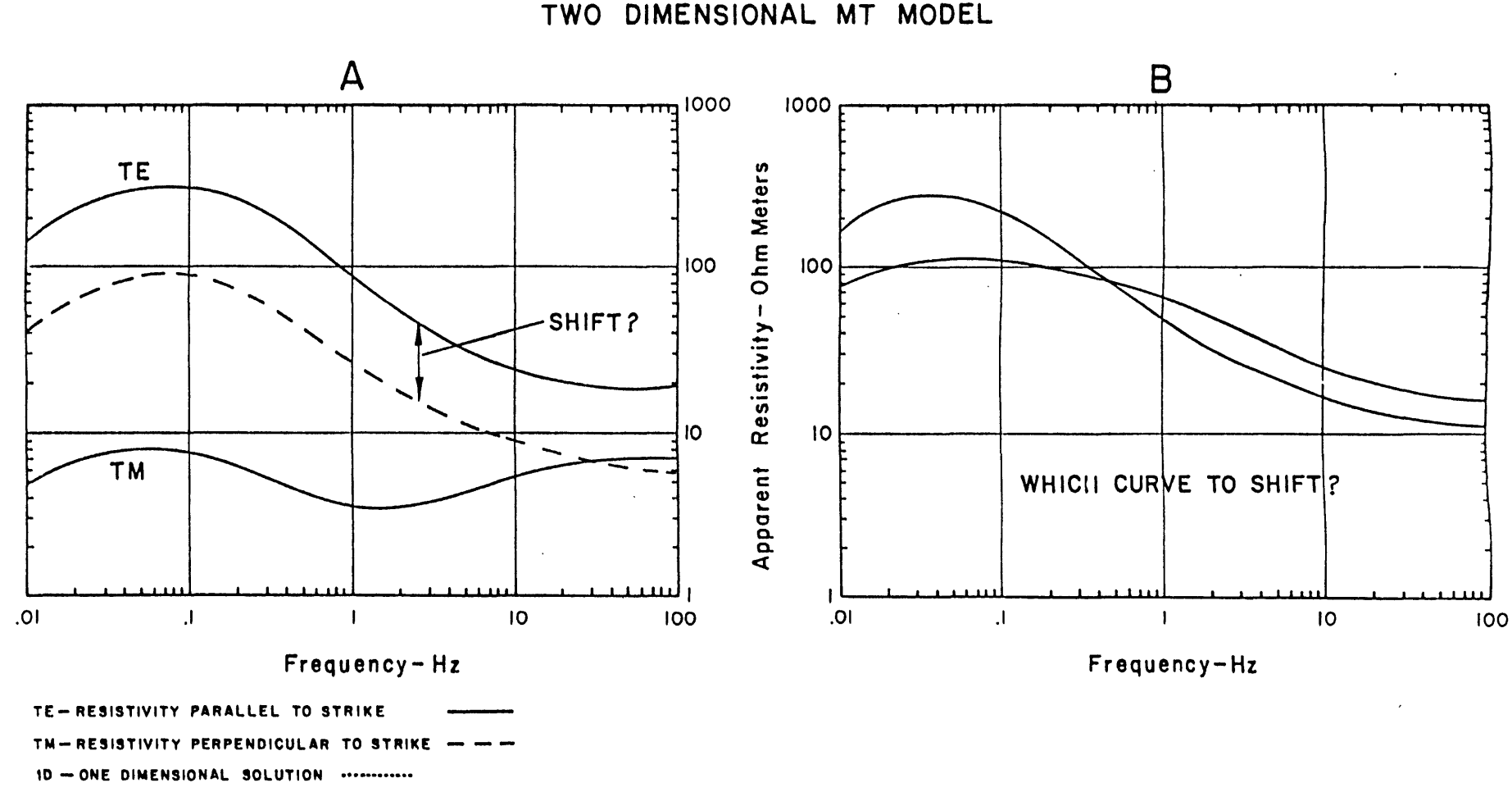

FIGURE 3

COMPLEX DATA WITH SURFACE EFFECT

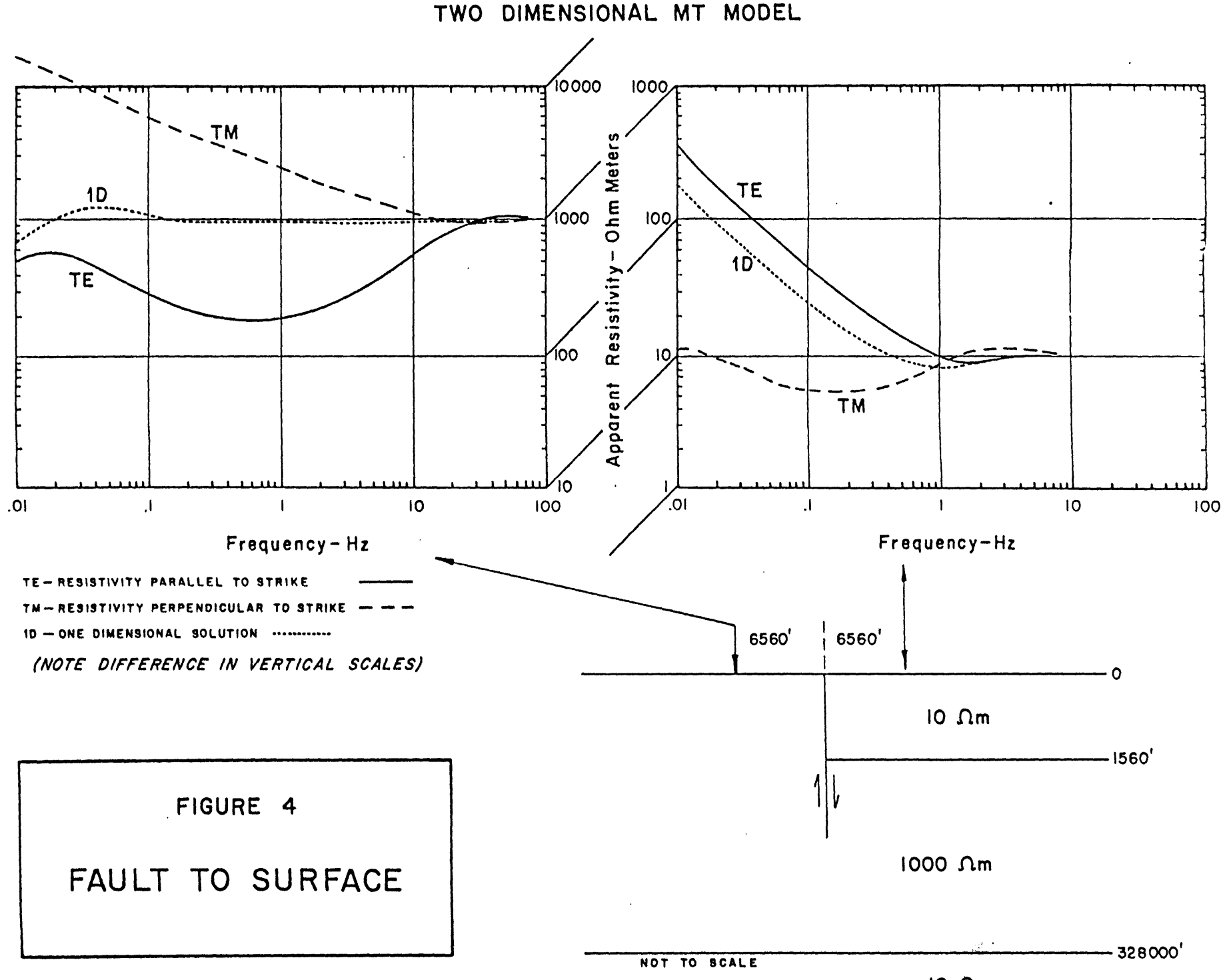

FIGURE 4

FAULT TO SURFACE

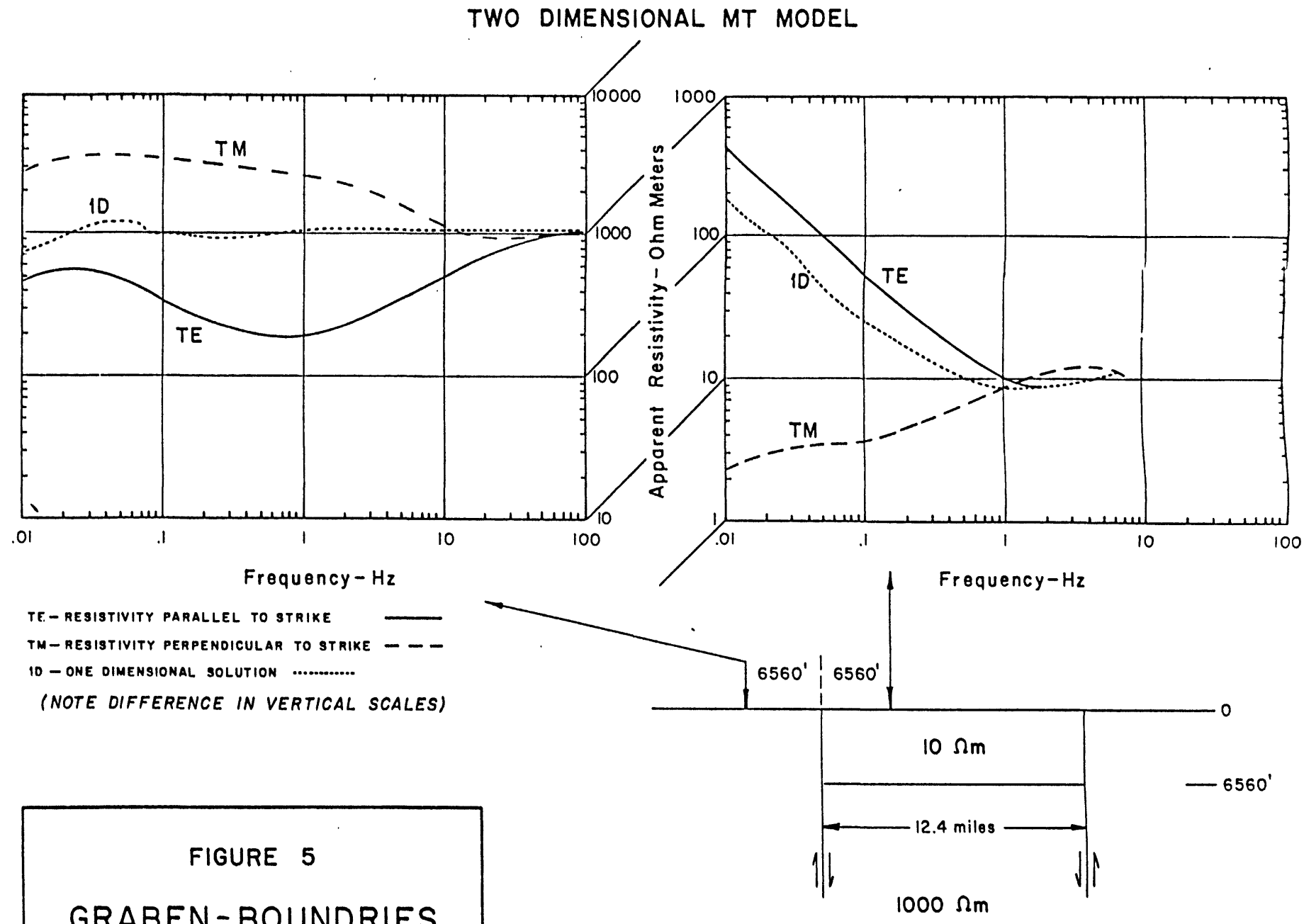

FIGURE 5

GRABEN - BOUNDRIES TO SURFACE

TWO DIMENSIONAL MT MODEL

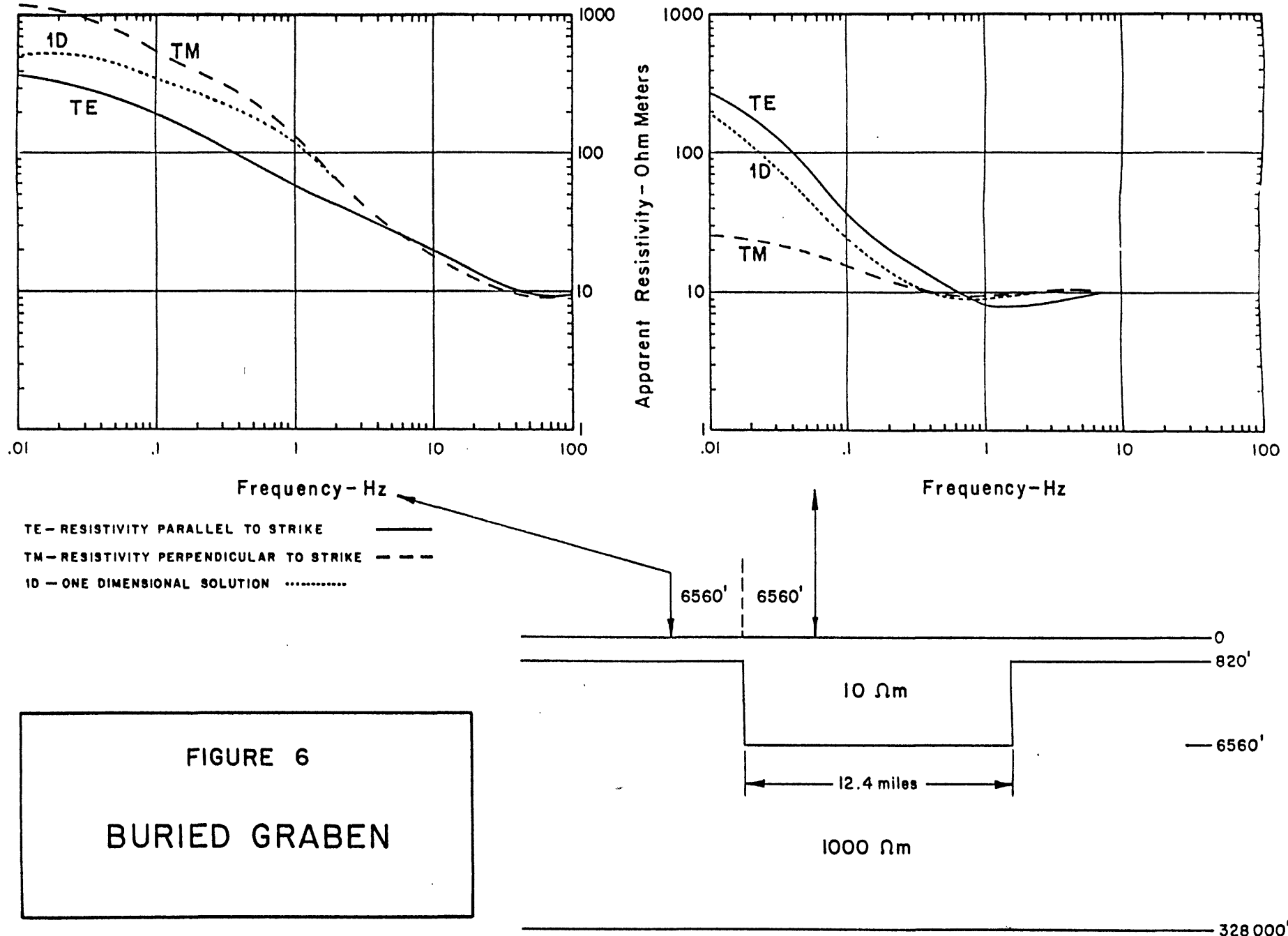

FIGURE 6

BURIED GRABEN

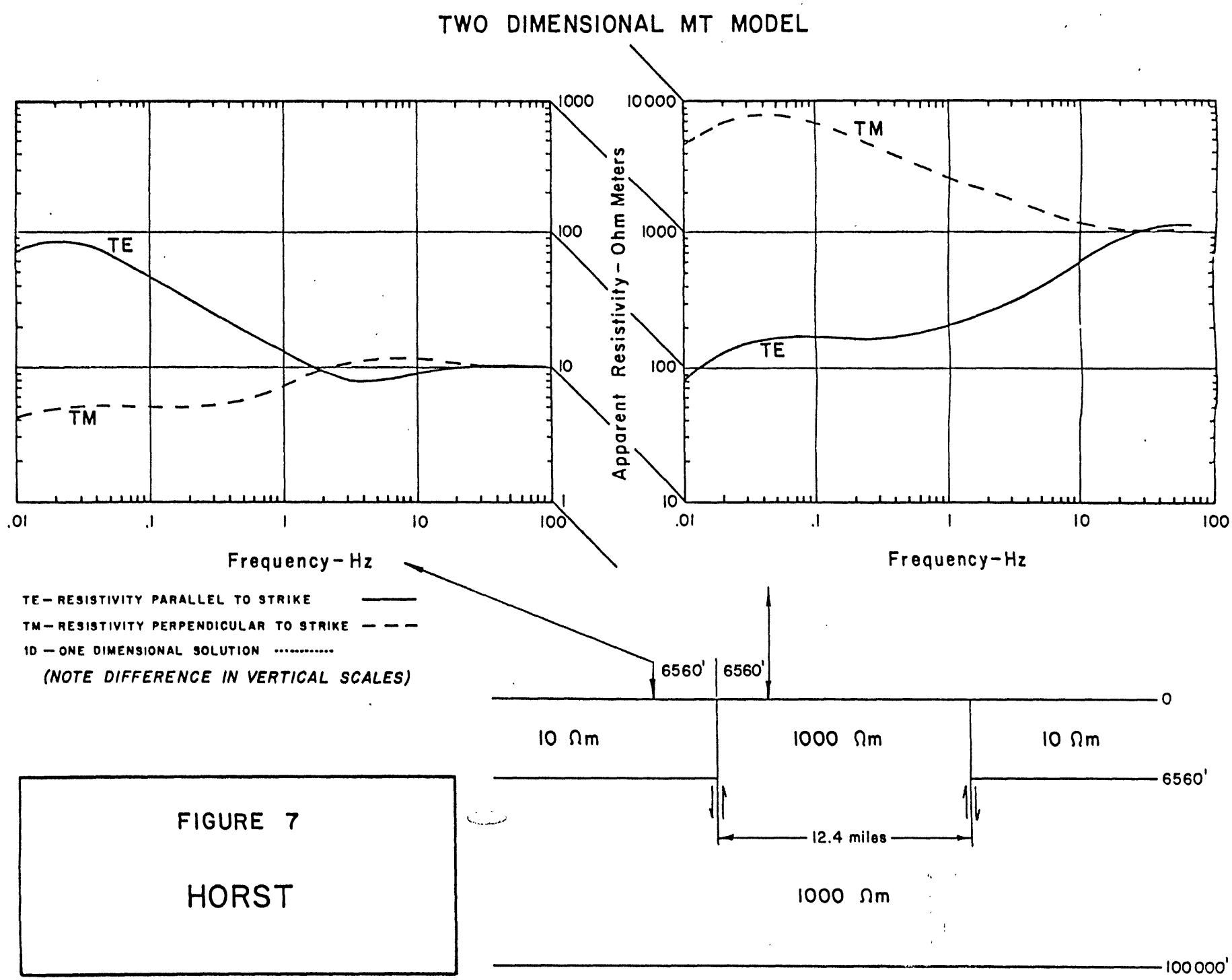

FIGURE 7

HORST

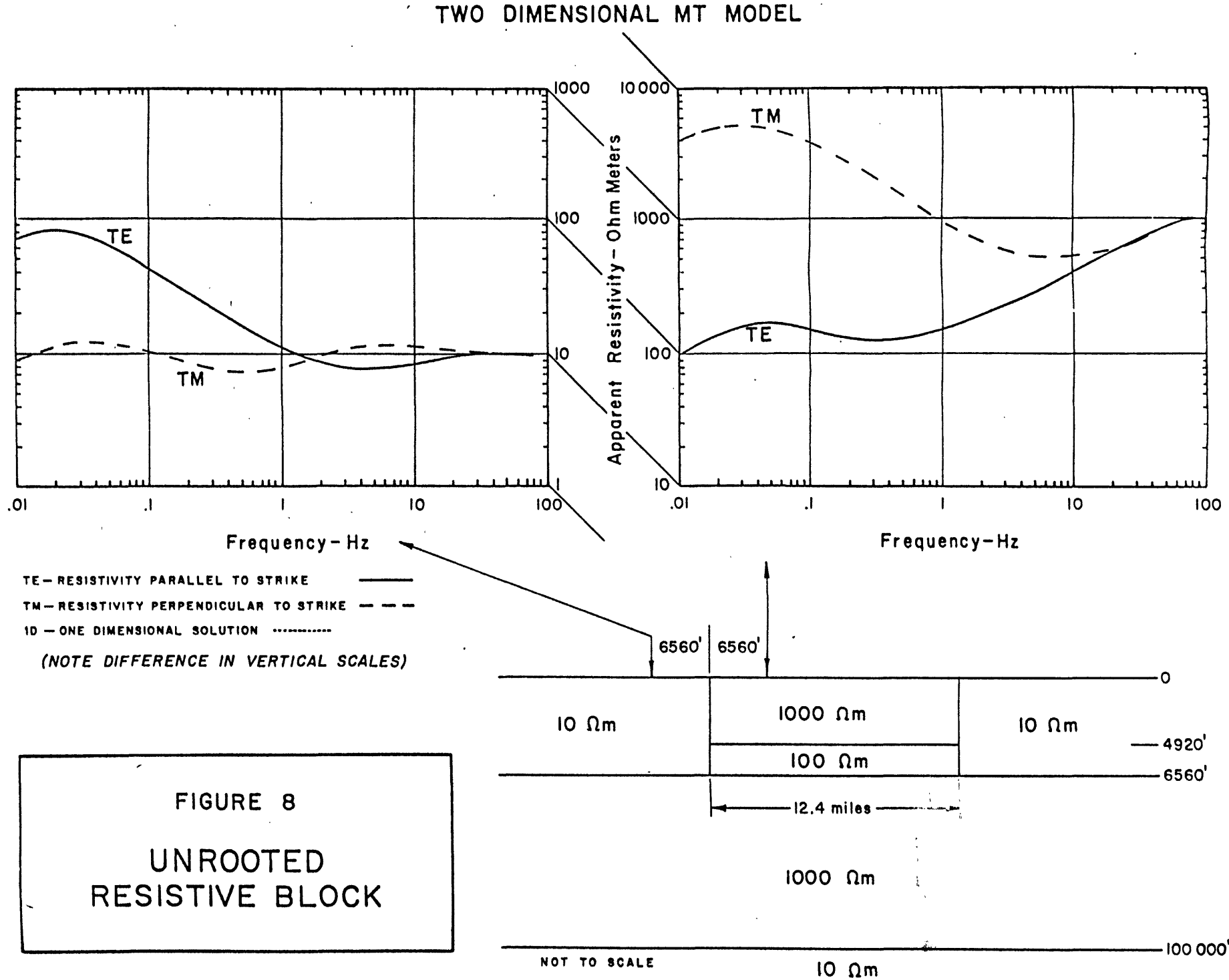

FIGURE 8

UNROOTED
RESISTIVE BLOCK

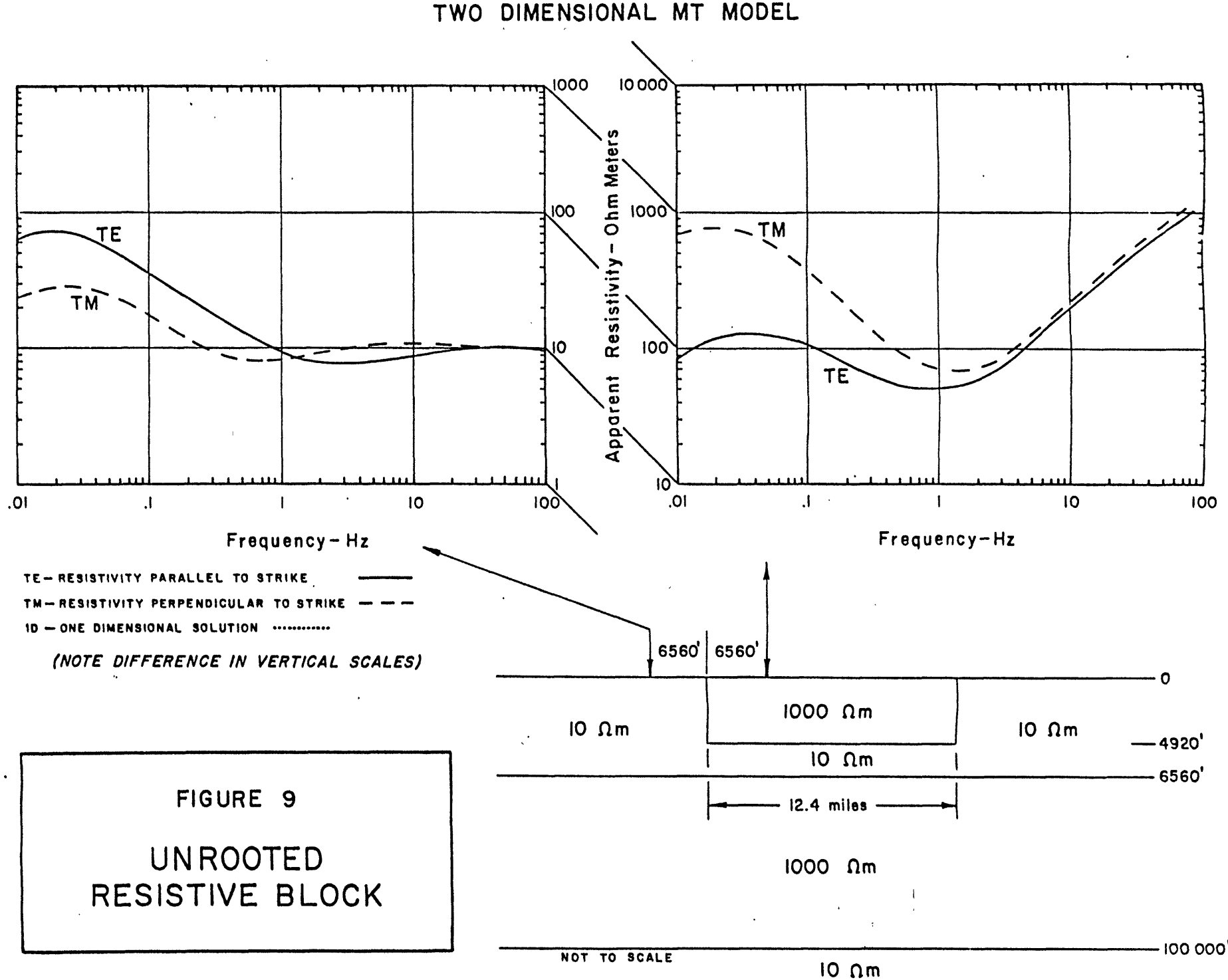

FIGURE 9

UNROOTED RESISTIVE BLOCK

TWO DIMENSIONAL MT MODEL

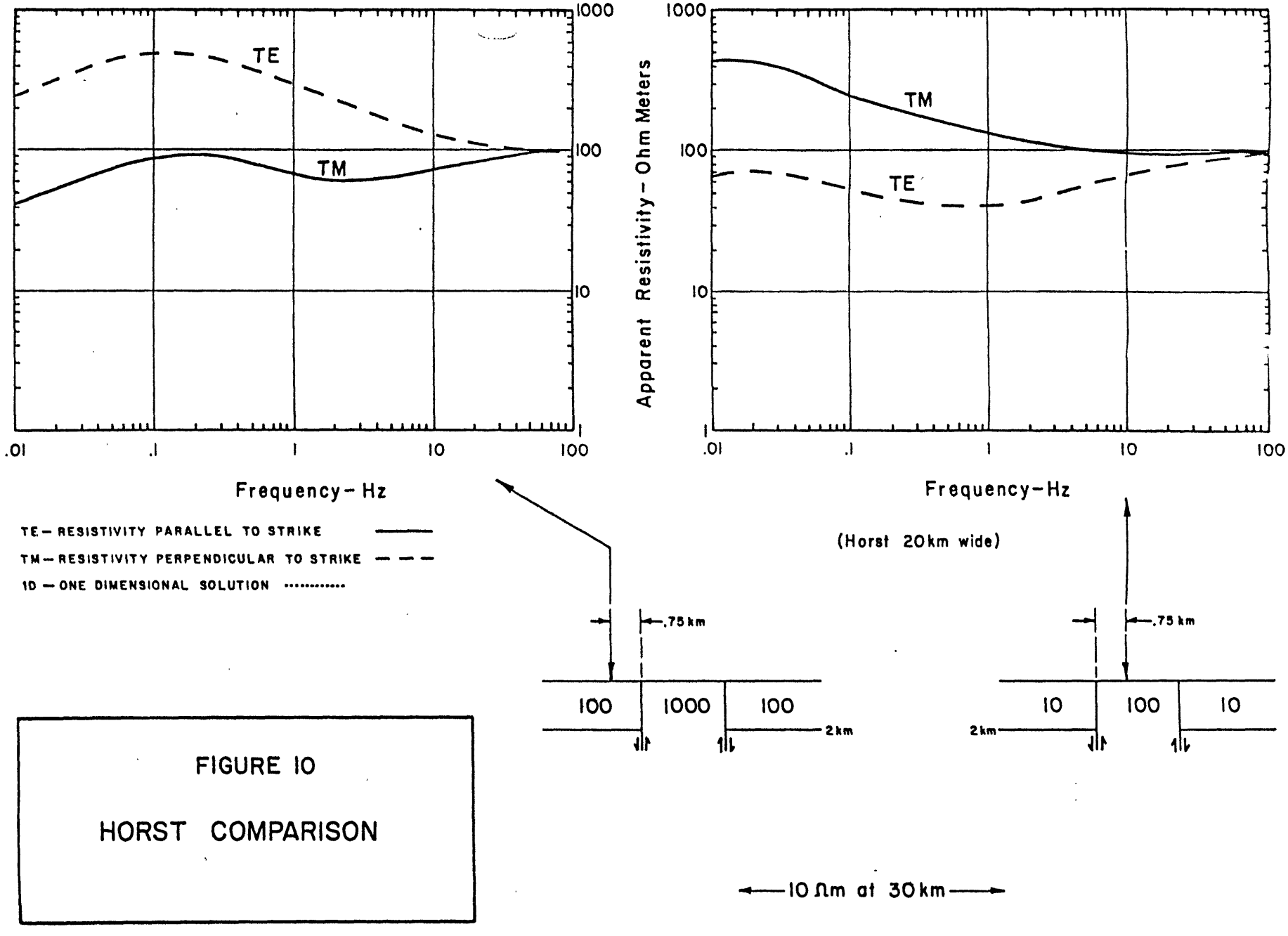

FIGURE 10

HORST COMPARISON

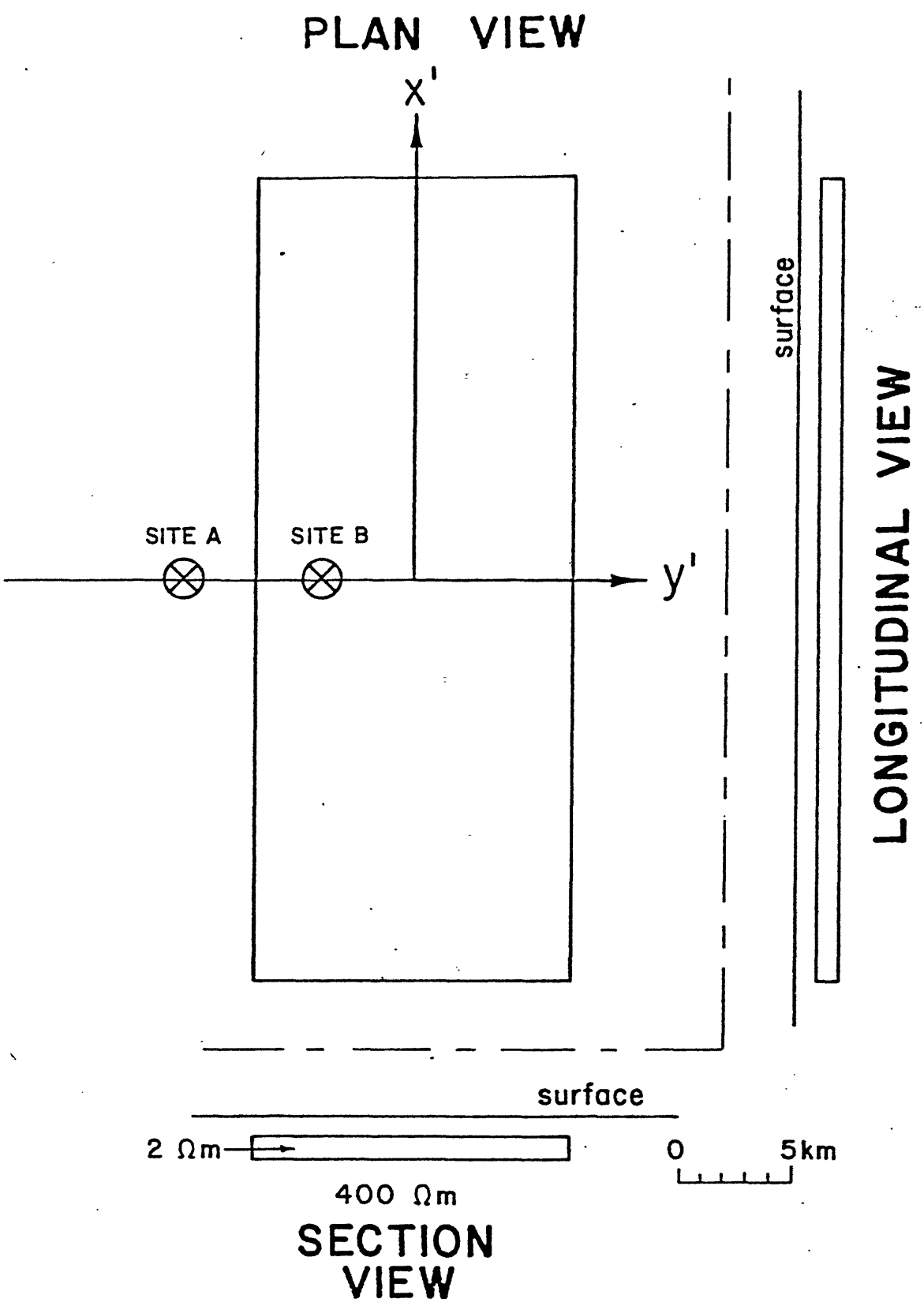

FIGURE 11 — PLATE-LIKE CONDUCTIVE PRISM IN A CONDUCTING HALF-SPACE USED TO REPRESENT THE MILFORD VALLEY SEDIMENTARY FILL. DIMENSIONS MAY BE INFERRED FROM THE SCALE PROVIDED OR TAKEN FROM MAIN TEXT.

(FROM: "MT MODELS OF THE ROOSEVELT HOT SPRINGS THERMAL AREA, UTAH", Univ. OF UTAH REPORT No. DOE/ET/27002-8)

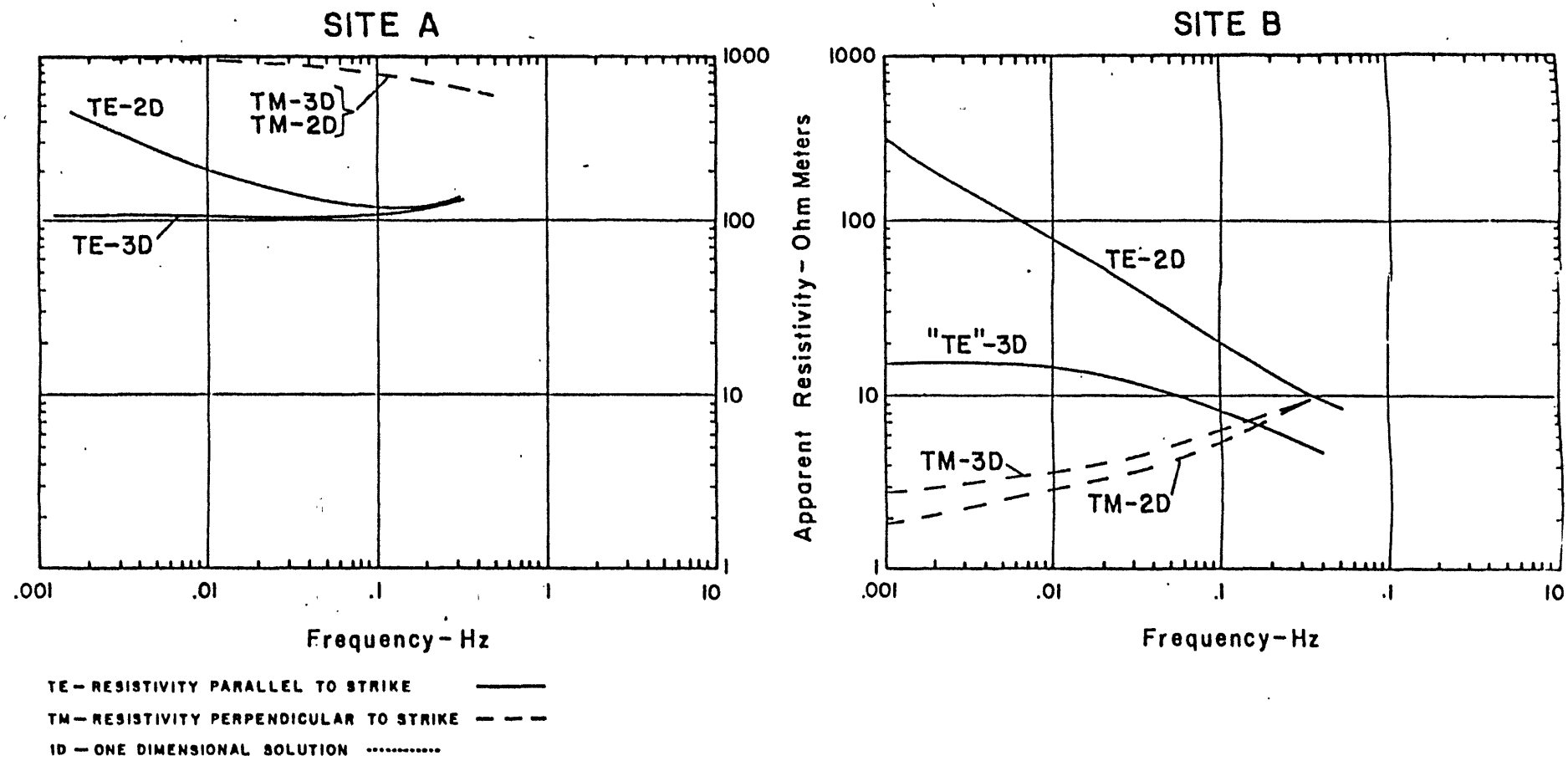

(SEE FIGURE 10 FOR MODEL SKETCH)

FIGURE 12

THREE DIMENSIONAL MODEL